

Analysis of kinetic reaction mechanisms

Version of 20 November, 2025



Tamás Turányi

Chemical Kinetics Laboratory

Institute of Chemistry, Eötvös University (ELTE), Budapest. Hungary

1

Analysis of kinetic reaction mechanisms – the book

Tamás Turányi and Alison S. Tomlin:

Analysis of Kinetic Reaction Mechanisms

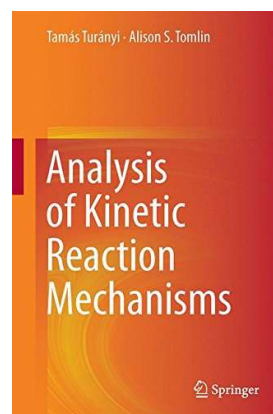
Springer, 2014

(with 1025 references)

Web page:

<http://garfield.chem.elte.hu/Turanyi/KineticReactionMechanisms.html>

- [table of contents](#)
- [download the chapters](#)
- [references](#)
- [typos found](#)



2

Topic 1: Reaction kinetics basics

stoichiometric equation, reaction mechanism,
parameterization of temperature dependence,

stoichiometric matrix, calculation of **J** and **F** matrices, general
characteristics of the system of kinetic differential equations,

trajectories, conserved properties.

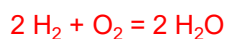
reaction kinetic simplifying principles:
rate determining step,
quasi steady state approximation (QSSA),
fast pre-equilibrium approximation,
pool component approximation;

applications of reaction kinetics models

Reaction kinetics basics

**Characterization of chemical changes with
a stoichiometric (overall) equation:**

- properly indicates the ratio of reactants and products
- usually there is no such a real chemical process



$$0 = \sum_j \nu_j A_j$$

$$\nu_1 = -2$$

$$\nu_2 = -1$$

$$\nu_3 = +2$$

$$A_1 = \text{„H}_2\text{“}$$

$$A_2 = \text{„O}_2\text{“}$$

$$A_3 = \text{„H}_2\text{O“}$$

ν_j stoichiometric coefficient
(negative for reactants, positive for products)

Features:

- the order of the species is arbitrary
- the stoichiometric coefficients can be multiplied with the same real number



4

Reaction rate

production rate of a species: $\frac{dY_j}{dt}$

reaction rate: $r = \frac{1}{\nu_j} \frac{dY_j}{dt}$

Y_j is the molar concentration of species A_j e.g. [mole dm⁻³]

in a small domain of concentrations always applicable: $r = k \prod_j Y_j^{\alpha_j}$,

k rate coefficient

α_j reaction order with respect species j

$\alpha = \sum_j \alpha_j$ overall reaction order

5

Complex reaction mechanisms

Almost always there are many simultaneous reaction steps:

$$\sum_j \nu_{ij}^L A_j = \sum_j \nu_{ij}^R A_j$$

A reaction step

can be an elementary reaction (physically occurs this way) or

can be a non-elementary reaction lumped from elementary reactions

ν_{ij}^L matrix of left hand side stoichiometric coefficients
 elementary: sum is not more than 2; zero or positive integer
 non-elementary: zero or positive integer

ν_{ij}^R matrix of right hand side stoichiometric coefficients
 elementary: sum is not more than 2; zero or positive integer
 non-elementary: any real number (can be zero, negative, fraction)

$\Delta \nu_{ij} = \nu_{ij}^R - \nu_{ij}^L$ calculation of the (previous) stoichiometric matrix

6

Kinetic system of differential equations

law of mass action (Guldberg and Waage, 1865):

$$r_i = k_i \prod_j Y_j^{\nu_{ij}^r}$$

k_i rate coefficient of reaction step i

r_i rate of reaction step i

Definition of the kinetic system of differential equations:

$$\frac{dY_j}{dt} = \sum_i \Delta \nu_{ij} r_i; \quad j = 1, 2, \dots, n$$

The kinetic system of differential equations in matrix-vector form:

$$\frac{d\mathbf{Y}}{dt} = \mathbf{v}\mathbf{r}$$

7

Matrices to be mentioned frequently

Initial value problem in reaction kinetics:

$$\frac{d\mathbf{Y}}{dt} = \mathbf{f}(\mathbf{Y}, \mathbf{k}), \quad \mathbf{Y}(t_0) = \mathbf{Y}_0$$

Jacobian: $\mathbf{J} = \left\{ \frac{\partial f_i}{\partial y_j} \right\}$

The Jacobian usually changes with changing concentrations

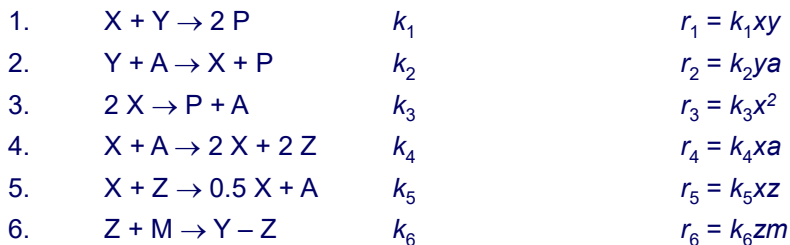
matrix \mathbf{F} : $\mathbf{F} = \left\{ \frac{\partial f_i}{\partial k_j} \right\}$

also depends on the concentrations

8

Kinetic system of differential equations: an example

The Oregonator model of the Belousov-Zhabotinskii oscillating reaction:



$X = \text{HBrO}_2$

$Y = \text{Br}^-$

$Z = \text{Ce}^{4+}$

$A = \text{BrO}_3^-$

$P = \text{HOBr}$

$M = \text{malonic acid}$

The detailed 80-step reaction mechanism could be reduced to this 6 reaction step.

Note, that negative and fractional stoichiometric coefficients are present on the right hand side!

9

Kinetic system of differential equations: an example 2

$X = \text{HBrO}_2$

$Y = \text{Br}^-$

$Z = \text{Ce}^{4+}$

$A = \text{BrO}_3^-$

$P = \text{HOBr}$

$M = \text{malonic acid}$

variable of a diff. equation

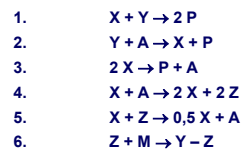
variable of a diff. equation

variable of a diff. equation

constant concentration

product only

constant concentration



$$\frac{dx}{dt} = -1r_1 + 1r_2 - 2r_3 + 1r_4 - 0.5r_5 \quad \Rightarrow \quad \frac{dx}{dt} = -k_1xy + k_2ya - 2k_3x^2 + k_4xa - 0.5k_5xz$$

$$\frac{dy}{dt} = -1r_1 - 1r_2 + 1r_6 \quad \Rightarrow \quad \frac{dy}{dt} = -k_1xy - k_2ya + k_6zm$$

$$\frac{dz}{dt} = +2r_4 - 1r_5 - 2r_6 \quad \Rightarrow \quad \frac{dz}{dt} = 2k_4xa - k_5xz - 2k_6zm$$

10

| | | | | | |
|--|--|---|---|--|--|
| $\frac{dx}{dt} = -k_1xy + k_2ya - 2k_3x^2 + k_4xa - 0.5k_5xz$ $\frac{dy}{dt} = -k_1xy - k_2ya + k_6zm$ $\frac{dz}{dt} = 2k_4xa - k_5xz - 2k_6zm$ | | | calculation of the Jacobian | | |
| | | | $\mathbf{J} = \left\{ \frac{\partial f_i}{\partial y_j} \right\}$ | | |
| $\frac{\partial \frac{dx}{dt}}{\partial x} = -k_1y - 4k_3x + k_4a - 0.5k_5z$ | $\frac{\partial \frac{dx}{dt}}{\partial y} = -k_1x + k_2a$ | $\frac{\partial \frac{dx}{dt}}{\partial z} = -0.5k_5x$ | | | |
| $\frac{\partial \frac{dy}{dt}}{\partial x} = -k_1y$ | $\frac{\partial \frac{dy}{dt}}{\partial y} = -k_1x - k_2a$ | $\frac{\partial \frac{dy}{dt}}{\partial z} = +k_6m$ | | | |
| $\frac{\partial \frac{dz}{dt}}{\partial x} = 2k_4a - k_5z$ | $\frac{\partial \frac{dz}{dt}}{\partial y} = 0$ | $\frac{\partial \frac{dz}{dt}}{\partial z} = -k_5x - 2k_6m$ | | | |
| | | | 11 | | |

| | | | | | | | | | | | |
|--|---|---|---|--|--|---|--|--|--|--|--|
| $\frac{dx}{dt} = -k_1xy + k_2ya - 2k_3x^2 + k_4xa - 0.5k_5xz$ $\frac{dy}{dt} = -k_1xy - k_2ya + k_6zm$ $\frac{dz}{dt} = 2k_4xa - k_5xz - 2k_6zm$ | | | | | | calculation of matrix F | | | | | |
| | | | | | | $\mathbf{F} = \left\{ \frac{\partial f_i}{\partial k_j} \right\}$ | | | | | |
| $\frac{\partial \frac{dx}{dt}}{\partial k_1} = -xy$ | $\frac{\partial \frac{dx}{dt}}{\partial k_2} = ya$ | $\frac{\partial \frac{dx}{dt}}{\partial k_3} = -2x^2$ | $\frac{\partial \frac{dx}{dt}}{\partial k_4} = xa$ | $\frac{\partial \frac{dx}{dt}}{\partial k_5} = -0.5xz$ | $\frac{\partial \frac{dx}{dt}}{\partial k_6} = 0$ | | | | | | |
| $\frac{\partial \frac{dy}{dt}}{\partial k_1} = -xy$ | $\frac{\partial \frac{dy}{dt}}{\partial k_2} = -ya$ | $\frac{\partial \frac{dy}{dt}}{\partial k_3} = 0$ | $\frac{\partial \frac{dy}{dt}}{\partial k_4} = 0$ | $\frac{\partial \frac{dy}{dt}}{\partial k_5} = 0$ | $\frac{\partial \frac{dy}{dt}}{\partial k_6} = zm$ | | | | | | |
| $\frac{\partial \frac{dz}{dt}}{\partial k_1} = 0$ | $\frac{\partial \frac{dz}{dt}}{\partial k_2} = 0$ | $\frac{\partial \frac{dz}{dt}}{\partial k_3} = 0$ | $\frac{\partial \frac{dz}{dt}}{\partial k_4} = 2xa$ | $\frac{\partial \frac{dz}{dt}}{\partial k_5} = -xz$ | $\frac{\partial \frac{dz}{dt}}{\partial k_6} = -2zm$ | | | | | | |
| | | | | | | 12 | | | | | |

Properties of kinetic differential equations

- The system of differential equations contains only first order derivatives (dc / dt), which are usually nonlinear functions of the concentrations.
⇒ **first order nonlinear system of differential equations**
- In general, several other concentrations influence the production rate of each species.
⇒ **coupled differential equations**
- The reaction rates differ several orders of magnitude
⇒ **stiff differential equations**
- Simulation results of laboratory experiments do not depend on the wall clock time, **BUT** the results of atmospheric chemical models depend on the actual pressure, temperature and solar radiation ⇒ depend on the physical time.
⇒ **autonomous OR non-autonomous differential equations**
- Some laboratory reactions can be (approximately) spatially homogeneous, but outside the laboratories most chemical reactions are spatially inhomogeneous. In most cases the transport of species and heat have to be taken into account.
⇒ **partial system of differential equations, with chemical source term**

13

Conserved properties

Isolated system:

The total internal energy is constant

Constant volume closed system:

the sum of the concentrations is constant,
if each the change of the number of moles in each reaction step is zero.
e.g. for reaction $\text{H}_2 + \text{Cl}_2 = 2 \text{HCl}$

Closed system, elementary reactions only:

the number of moles of the elements is constant.

The moles of moieties (e.g. benzene ring) can remain constant

Example for conserved properties in a $\text{C}_2\text{H}_4, \text{CH}_4, \text{C}_6\text{H}_6$ mixture:

C-atom $\rightarrow 2 [\text{C}_2\text{H}_4] + 1 [\text{CH}_4] + 6 [\text{C}_6\text{H}_6] = \text{constant}$

H-atom $\rightarrow 4 [\text{C}_2\text{H}_4] + 4 [\text{CH}_4] + 6 [\text{C}_6\text{H}_6] = \text{constant}$

Some linear combinations of the concentrations are constant.

N conserved property:

⇒ the rank of the stoichiometric matrix is lower by N

⇒ the system can be simulated **exactly** with $(n-N)$ variables

14

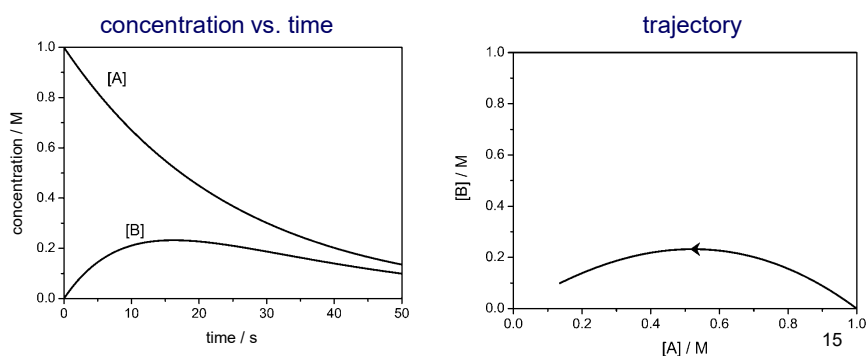
Trajectory

Actual state of the system: a point in the phase space

History of events: trace of this point in the phase space (a solid line)

In chemical kinetics this phase space can be the space of concentrations.
This figure does not show time, but can be more interesting than the usual concentration vs. time curves.

Example: reaction $A \rightarrow B \rightarrow$



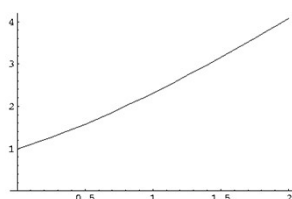
Trajectories 2

closed systems:

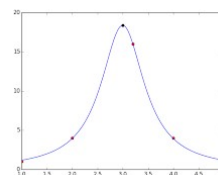
The concentrations are continuously changing from the initial state to an equilibrium point

Possible variations:

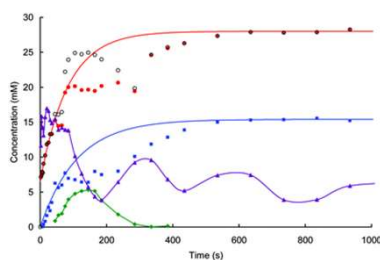
monotonic



maximum / minimum



oligo oscillation



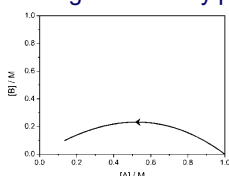
16

Trajectories 3

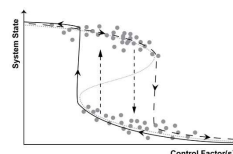
open systems:

The concentrations are continuously changing from the initial state to a ...

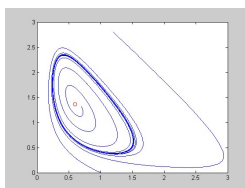
single stationary point



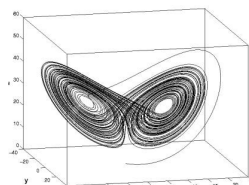
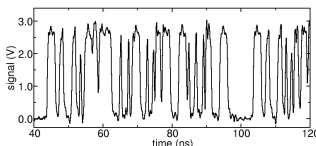
bistable behaviour



closed loop (limit cycle)



strange attractor



17

Temperature dependence of rate coefficient k

Described by the Arrhenius equation:

$$k = A \exp\left(-\frac{E_a}{RT}\right) \quad \ln k = \ln A - \frac{E_a}{RT}$$

A preexponential factor
 E_a activation energy

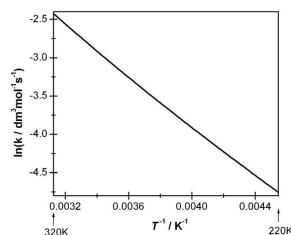
If the rate coefficient k is measured at several T temperatures and

$\ln k$ is plotted as a function of $1/T$

the data fit to a line, if the (original) Arrhenius equation is valid

slope is $m = -E_a/R \Rightarrow$ determination of E_a

Arrhenius plot:

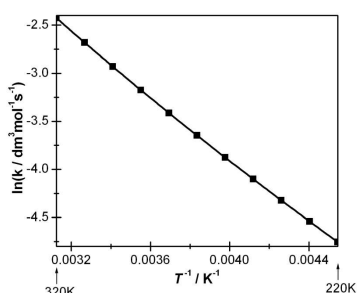


18

Example: reaction $\text{CH}_4 + \text{OH} \rightarrow \text{CH}_3 + \text{H}_2\text{O}$

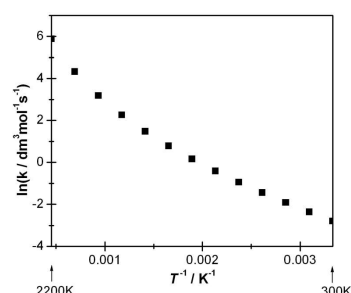
- the most important methane consuming reaction step in the troposphere
- one of the most important steps at methane combustion

Arrhenius plot between 220 K (– 53 °C)
and 320 K (+ 47 °C)



the Arrhenius equation is usually
very accurate in a small
(few times 10 K) temperature range.
(solution phase and atmospheric chemistry)

Arrhenius plot between 300 K (27 °C)
and 2200 K (≈1930 °C)

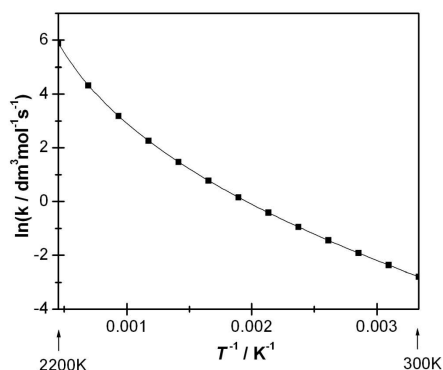


the original Arrhenius equation
is usually not applicable in a wide
temperature range
(combustion and pyrolytic systems)

Temperature dependence of the rate coefficient 2

$$k = BT^n e^{-\frac{C}{RT}}$$

extended Arrhenius equation



Important!

If $n \neq 0$. then $A \neq B$ and $E_a \neq C$

General definition of
activation energy:

$$E_a = -R \frac{\partial \ln k}{\partial (1/T)}$$

20

Reaction kinetics simplifying principles

Reaction kinetics simplifying principles: can be used for the simplification of a reaction mechanism (kinetic system of differential equations) in such a way that the obtained reaction mechanism (or system of differential equations) provides an almost identical (say within 1%) solution.

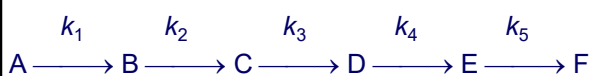
Reaction kinetic simplifying principles:

- rate determining step
- quasi steady state approximation (QSSA)
- fast pre-equilibrium approximation
- pool component approximation

Rate determining step

The case of consecutive first order reactions

Reaction step having the smallest rate coefficient is the rate determining. The rate of production of the end product is equal to the rate coefficient of the rate determining step times the concentration of its reactant.



$$k_2 \ll k_1, k_3, k_4, k_5 \Rightarrow \quad d[F]/d t = k_2 [B]$$

In the case of any reaction mechanism: small increase of the rate coefficient of the rate determining step results in a large increase of the rate of production of the end product.

In general, the reaction step having the smallest rate coefficient is not the rate determining step!

Quasi steady-state approximation (QSSA)

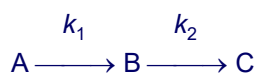
Highly reactive and low-concentration species in a mechanism are selected. These species (usually very reactive radicals) are called the QSSA species. The left-hand-sides of the kinetic differential equations are zeroed, converting these differential equations to algebraic equations. The obtained set of algebraic equations describe the dependence of the concentrations of the QSSA species on the concentrations of the non-QSSA species. Solving together the sets of differential and algebraic equations provides a solution that is in good accordance with the solution of the original kinetic system of differential equations.

In most cases the system of algebraic equations can be solved analytically, the concentrations of the QSSA species can be given explicitly and this solution can be inserted to the remaining system of differential equations for the non-QSSA species.

⇒ smaller system of differential equations

The QSSA species are usually highly reactive and therefore low concentration species (e.g. radicals).

Application of the QSSA



if $k_1 \ll k_2$ B "QSSA species" A and C "non-QSSA species"

$$d[B]/dt = k_1 [A] - k_2 [B]$$

$$0 = k_1 [A] - k_2 [B]$$

$$[B] = k_1/k_2 [A]$$

[B] can be calculated from [A]

Pre-equilibrium approximation

If the reactants of a fast equilibrium reaction is consumed by much slower reactions, then the concentrations of the species participating in the fast equilibrium can be calculated from the equilibrium equations only and the effects of other reactions should not be taken into account.



if $k_3 \ll k_2$ and $d[B]/dt \approx 0$ (state of equilibrium)

$$\Rightarrow k_1 [A] = k_2 [B]$$

$$\Rightarrow [B] = k_1/k_2 [A] = K [A]$$

$$\Rightarrow d[C]/dt = k_3 [B] = k_3 K [A]$$

Pool component approximation

If the concentration of one of the reactants is much higher than those of the others, then this concentration will not change significantly during the reaction.

This way a second order reaction can be converted to an equivalent first order reaction by merging the rate coefficient and the concentration of the pool component.

$$\frac{d[C]}{dt} = k[A][B] = k'[A]$$

where $k' = k[B]$ is constant. \Rightarrow „pseudo first order reaction“

Example: „inversion of sucrose“

Hydrolysis of sucrose in an acidic solution. The products formed are optically active and their optical rotation can be determined by using a polarimeter. The decomposition of sucrose can be described by a first order decay reaction.

Applications of reaction kinetics models

- **modelling atmospheric chemical processes**
 - forecast of air pollution (weather forecast is needed!)
 - determination of emission limits
- **modelling of ignition and combustion**
 - modelling power stations, furnaces, engines
 - improving efficiency
 - elaboration of methods for the decrease of pollutant emission
- **process engineering; modelling of chemical engineering processes**
 - considering efficiency and the aspects of environment protection
- **systems biology: modelling biochemical processes within living organisms**
 - metabolic networks (e.g. medical drug decomposition in the body)
 - molecular signal transfer
 - modelling the cell cycle
- **non-chemical models using reaction kinetic formalism**
 - predator-prey models
 - description of ecological systems

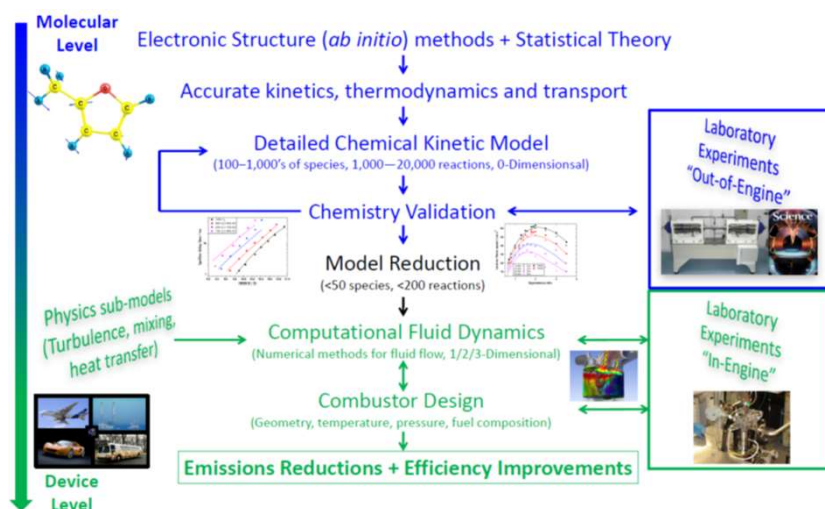
27

Topic 2: Construction of detailed reaction mechanisms and the reaction pathways

data sources,
traditional construction of reaction mechanisms,
automatic mechanism generation;

pathway analysis:
species conversion pathways, element following pathways,
pathways leading to the production of a given species

Hierarchy of combustion models



Henry J. Curran: Developing detailed chemical kinetic mechanisms for fuel combustion
Proc. Combust. Inst., in press (2019)

29

Source of chemical kinetic data

measured and calculated
chemical kinetic data

→ journal publications

data compilation

→ books, data bases.
e.g. **NIST database**
www.nist.gov

data evaluation
reevaluation and comparison
of several articles

→ review articles

evaluated/recommended data ₃₀

NIST databases

www.nist.gov

⇒ Databases ⇒ Chemical Kinetics

⇒ NIST Chemical Kinetics Online (<http://kinetics.nist.gov/kinetics/>)

NIST Scientific and Technical Databases

NIST
National Institute of Standards and Technology

SEARCH OUR WEBSITE

Chemical Kinetics

The NIST Program on Chemical Kinetics has long years, data provided by the program have been in combustion chemistry, atmospheric changes related to global warming, and other areas.

The new web version of the database has completed its development and is now available online.

NIST has made available an excellent online comp. Kinetics Database. This database is derived from the University of Notre Dame.

CKMech is an online system for chemical kinetic calculations.

The codes in the list below have the following meanings:

| | |
|--------|--|
| PC | PC product, most available for purchase. |
| Online | Free online system. |
| Inc | Inclusion in the NIST Data Gateway - a paid service. |

Kinetics Database

Chemical Kinetics Database on the Web

Standard Reference Database 17, Version 7.0 (Web Version), Release 1.3

A compilation of kinetics data on gas-phase reactions

Reaction Database Quick Search Form

Enter the reactant(s) and/or product(s) in the fields below. Fields may be left blank.

+ →

If you would like more searching options, try...
advanced reaction search form
bibliographic search form

Welcome
About the database
Getting Started
A quick introduction to the database
Credits and History
Who created the present version and the earlier versions?

31

NIST Databases 2

Author(s): Gierczak. T.; Talukdar. R.K.; Herndon. S.C.; Vaghjiani. G.L.

Ravishankara. A.R.

Title: Rate coefficients for the reactions of hydroxyl radicals with methane and deuterated methanes

Journal: J. Phys. Chem. A:

Volume: 101

Page(s): 3125 - 3134

Year: 1997

Reference type: Journal article

Squib: 1997GIE/TAL3125-3134

Reaction: $\text{CH}_4 + \cdot\text{OH} \rightarrow \cdot\text{CH}_3 + \text{H}_2\text{O}$

Reaction order: 2

Temperature: 196 - 420 K

Pressure: 0.13 Bar

Rate expression: $1.76 \times 10^{-13} (\text{cm}^3/\text{molecule s}) (T/298 \text{ K})^{2.82} e^{-1.96 (\pm 0.02 \text{ kcal/mole})/RT}$

Bath gas: He

Data type: Absolute value measured directly

Excitation technique: Flash photolysis (laser or conventional)

Analytical technique: Laser induced fluorescence

32

Computer generation of mechanisms

General ideas:

- 1 starting from some reactants (for example: fuel molecule + O₂)
- 2 elementary reactions are generated according to reaction types
(e.g. H-abstraction, additions, fission of radicals)
- 3 unrealistic elementary reactions are not considered
(based on various filtering principles)
- 4 getting rate and thermodynamic parameters from databases
- 5 approximate automatic calculation of the missing parameters
- 6 new list of intermediates **GOTO 2**

Stopping of mechanism generation at some complexity/number of reactions.

Investigation of the computer generated mechanism by

- comparison with human generated mechanisms
- testing against experimental data.

35

Codes for mechanism generation – some examples

EXGAS (Nancy)

includes mechanism generator, kinetic data base and estimation of thermochemical parameters

wider classes of fuels: heavy alkanes, oxygenated species, biomass fuels

F. Battin-Leclerc, P. A. Glaude, V. Warth, R. Fournet, G. Scacchi, G. M. Côme: Computer tools for modelling the chemical phenomena related to combustion. *Chem. Eng. Sci.* **55**, 2883-2893 (2000)

MAMOX (Milano)

- automatic generation of mechanisms
- considering isomers with similar kinetic behaviour as a single lumped
- species lumping parallel reaction pathways for similar isomers
- fitting lumped reaction rates to predictions from the full scheme

Ranzi, E., Faravelli, T., Gaffuri, P., Sogaro, A.: Low-temperature combustion: Automatic generation of primary oxidation reactions and lumping procedures. *Combust. Flame* **102**, 179-192 (1995)

RMG - Reaction Mechanism Generator (MIT) <http://rmg.sourceforge.net/>

„RMG is an automatic chemical reaction mechanism generator that constructs kinetic models composed of elementary chemical reaction steps using a general understanding of how molecules react.”

W. H. Green, P. I. Barton, B. Bhattacharjee, D. M. Matheu, D. A. Schwer, J. Song, R. Sumathi, H. H. Carstensen, A. M. Dean, J. M. Grenda: Computer construction of detailed chemical kinetic models for gas-phase reactors. *Ind. Eng. Chem. Res.* **40**, 5362–5370 (2001)

Pathway analysis

species conversion pathways

pathways leading to the production of a given species

37

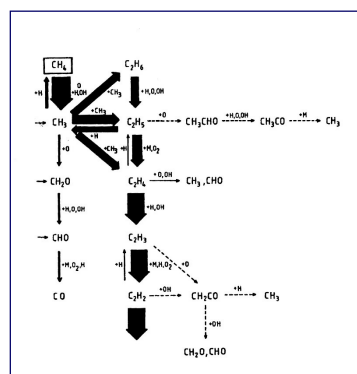
Reaction pathways

Conversion of one species to another

Reaction fluxes:

The width of the arrows is proportional to the interconversion rate

Several textbooks contain pathway figures,
But usually the exact calculation of
The width of the arrows is not revealed.



pathways in a rich methane-air flame

Warnatz J., Maas U., Dibble R. W.
*Combustion. Physical and chemical fundamentals,
modeling and simulation, experiments, pollutant formation*
Springer, New York, 1996

38

Reaction fluxes

S.R. Turns:
An introduction to combustion.
Concepts and applications.
 second edition,
 Boston, McGraw-Hill, 2000.

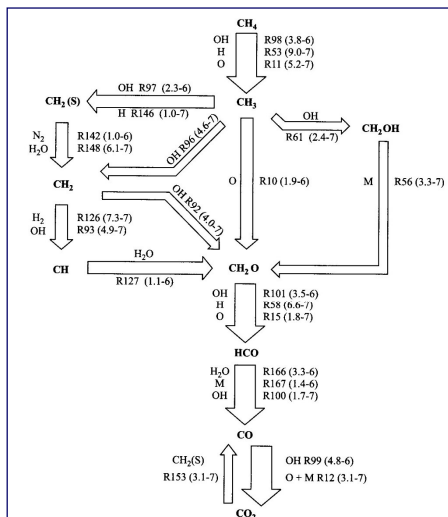
„each arrow indicates a reaction step”

„the width of the arrows is proportional
 to the consumption rate of the reactant”

Not a good idea, since consecutive arrows
 having different width may belong to identical
 fluxes.

⇒ **Flux of a conserved property
 Has to be plotted!!!**

⇒ Fluxes of elements (Revel *et al.*, 1994)



Calculation of element fluxes using KINALC

c **ATOMFLOW** Fluxes of elements from species to species are investigated
c The name(s) of element(s) are listed after the keyword.
c Usage: **ATOMFLOW** <element1> <element2> ...

ATOMFLOW C H

```
===== ATOMFLOW =====
```

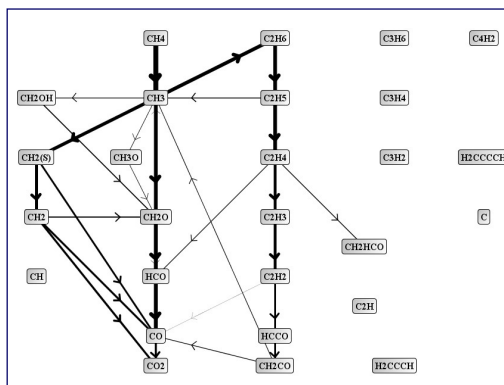
Fluxes of elements from species to species

| Net fluxes of element H | | | absolute | rel. |
|-------------------------|------|---------|--------------------------|--------|
| 1 | H2 | => H2O | 6.843E-02 mole/(cm3 sec) | 1.0000 |
| 2 | H2 | => H | 4.584E-02 mole/(cm3 sec) | .6699 |
| 3 | OH | => H2O | 4.034E-02 mole/(cm3 sec) | .5895 |
| 4 | H | => OH | 3.360E-02 mole/(cm3 sec) | .4910 |
| 5 | H | => HO2 | 2.370E-02 mole/(cm3 sec) | .3463 |
| 6 | OH | => H | 2.302E-02 mole/(cm3 sec) | .3364 |
| 7 | HO2 | => OH | 1.797E-02 mole/(cm3 sec) | .2626 |
| 8 | H2 | => OH | 1.162E-02 mole/(cm3 sec) | .1699 |
| 9 | H | => H2 | 6.346E-03 mole/(cm3 sec) | .0927 |
| 10 | H | => H2O | 4.084E-03 mole/(cm3 sec) | .0597 |
| 11 | HO2 | => H2 | 3.334E-03 mole/(cm3 sec) | .0487 |
| 12 | HO2 | => H2O | 2.689E-03 mole/(cm3 sec) | .0393 |
| 13 | OH | => H2 | 1.049E-03 mole/(cm3 sec) | .0153 |
| 14 | H2O | => OH | 7.891E-04 mole/(cm3 sec) | .0115 |
| 15 | OH | => H2O2 | 7.617E-04 mole/(cm3 sec) | .0111 |
| 16 | H2O | => H2 | 7.010E-04 mole/(cm3 sec) | .0102 |
| 17 | H2O2 | => H2O | 5.367E-04 mole/(cm3 sec) | .0078 |
| 18 | H2O2 | => OH | 2.131E-04 mole/(cm3 sec) | .0031 |

KINALC → FluxViewer

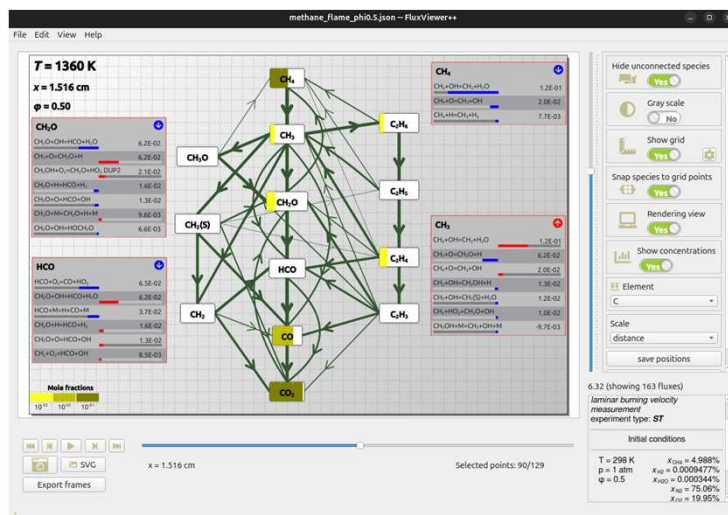
FluxViewer: JAVA code for the visualization of the element fluxes

- the labels of the species can be moved („drag-and-drop“)
- the width of the arrows is proportional to the log of the element fluxes
- the width of the arrows can be hanged
- creation of drawings or movie films



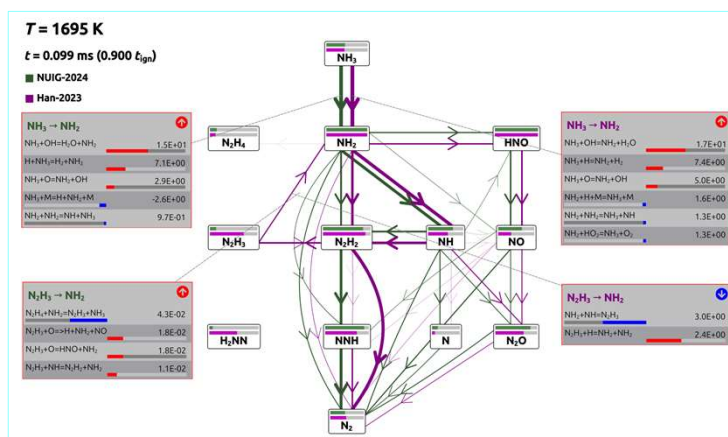
I. Gy. Zsély, I. Virág, T. Turányi:
Investigation of a methane oxidation mechanism via the visualization of element fluxes
Paper IX.4 in: Proceedings of the 4th Mediterranean Combustion Symposium,
Lisbon, Portugal, 5-10 October, 2005. Eds: F. Beretta, N. Selçuk, M.S. Mansour

Fluxviewer++



43

Fluxviewer++



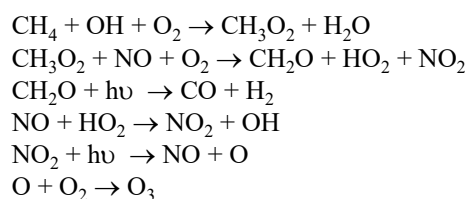
44

Pathways for the consumption/production of a given species

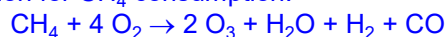
Problem: What is the sequence of reactions that leads to the consumption (or production) of a given species? The detailed reaction mechanism is known.

Example: What is the sequence of reactions that leads to the consumption of methane in the stratosphere?

Answer:



The global reaction for CH_4 consumption:



R. Lehmann: An algorithm for the determination of all significant pathways in chemical reaction systems. *J. Atm. Chem.* **47**, 45-78 (2004)

45

Topic 3: Local sensitivity analysis 1

Local sensitivity coefficient and its interpretation,

system of differential equations
for local sensitivity coefficients,

initial concentration sensitivity coefficients,

calculation of sensitivity coefficients with
finite difference approximation,

calculation of sensitivity coefficients with
the Direct Method and the Decoupled Direct Method

automatic differentiation

Local sensitivity analysis

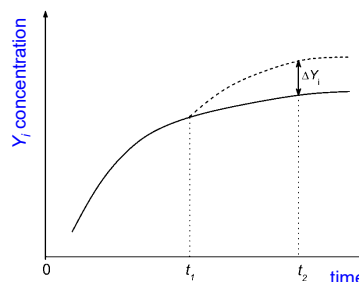
Sensitivity analysis is a family of mathematical methods. It investigates the dependence of the model results on the values of the parameters

Local sensitivity analysis: investigates the effect of the small change of parameters

Local sensitivity coefficients can be investigated by a finite difference approximation:

$$\frac{\partial Y_i}{\partial p_j}(t_1, t_2) \approx \frac{\Delta Y_i(t_2)}{\Delta p_j} = \frac{Y_i(t_2) - Y_i(t_2)}{\Delta p_j}$$

parameter is changed at time t_1
the result is observed at time t_2



T. Turányi: Sensitivity analysis of complex kinetic systems: Tools and applications, *J. Math. Chem.*, **5**, 203-248(1990)

47

Local sensitivity analysis 2

Another approach: Taylor series expansion

$$Y_i(t, \mathbf{p} + \Delta \mathbf{p}) = Y_i(t, \mathbf{p}) + \sum_{j=1}^m \frac{\partial Y_i}{\partial p_j} \Delta p_j + \frac{1}{2} \sum_{k=1}^m \sum_{j=1}^m \frac{\partial^2 Y_i}{\partial p_k \partial p_j} \Delta p_k \Delta p_j + \dots$$

Local sensitivity coefficient: $s_{ik} = \frac{\partial Y_i}{\partial p_k}$

Local sensitivity matrix: $\mathbf{S} = \left\{ \frac{\partial Y_i}{\partial p_k} \right\}$

The effect of parameter changes can be estimated using local sensitivities:

Changing a single parameter: $Y_i'(t_2) = Y_i(t_2) + \frac{\partial Y_i}{\partial p_j} \Delta p_j$

Changing several parameters: $\mathbf{Y}'(t_2) = \mathbf{Y}(t_2) + \mathbf{S}(t_2) \Delta \mathbf{p}(t_1)$

48

Local sensitivity analysis 3

$$\frac{d\mathbf{Y}}{dt} = \mathbf{f}(\mathbf{Y}, \mathbf{p})$$

$$\mathbf{Y}(t_0) = \mathbf{Y}_0$$

Differentiation with respect p_j

$$\frac{d}{dt} \frac{\partial \mathbf{Y}}{\partial p_j} = \mathbf{J} \frac{\partial \mathbf{Y}}{\partial p_j} + \frac{\partial \mathbf{f}}{\partial p_j} \quad \frac{\partial \mathbf{Y}}{\partial p_j}(t_0) = 0 \quad j = 1, 2, \dots, m$$

The same equation with matrix-vector notation:

$$\dot{\mathbf{S}} = \mathbf{J} \mathbf{S} + \mathbf{F}, \quad \mathbf{S}(0) = \mathbf{0} \quad \text{where} \quad \mathbf{J} = \left\{ \frac{\partial f_i}{\partial Y_j} \right\} \quad \mathbf{F} = \left\{ \frac{\partial f_i}{\partial p_k} \right\}$$

indirect effect

direct effect

49

Initial concentration sensitivities

initial concentration sensitivities: the consequence of changing the initial conc. can be calculated with finite differences:

$$\frac{\partial Y_i}{\partial Y_j}(t_2) \approx \frac{\Delta Y_i(t_2)}{\Delta Y_j(t_1)} = \frac{Y_i(t_2) - Y_i(t_1)}{\Delta Y_j(t_1)}$$

$$\text{kinetic system of ODEs:} \quad \frac{d\mathbf{Y}}{dt} = \mathbf{f}(\mathbf{Y}, \mathbf{p}) \quad \mathbf{Y}(t_0) = \mathbf{Y}_0$$

Differentiating it with respect to $Y_j(t_1)$:

$$\frac{d}{dt} \frac{\partial \mathbf{g}}{\partial Y_j^0(t_1)} = \mathbf{J} \frac{\partial \mathbf{g}}{\partial Y_j^0(t_1)} \quad \frac{\partial \mathbf{Y}}{\partial Y_j^0(t_1)}(t_1) = \delta_j \quad j = 1, 2, \dots, n$$

$$\frac{d}{dt} \mathbf{G}(t, t_1) = \frac{\partial \mathbf{f}}{\partial \mathbf{Y}}(t) \mathbf{G}(t, t_1) \quad \mathbf{G}(t_1, t_1) = \mathbf{I}$$

at time t_1 the initial value of variable j is changed and the effect is read at time t_2

$$g_{ij}(t, t_1) = \frac{\partial Y_i(t)}{\partial Y_j^0(t_1)} \quad \mathbf{g}_j(t, t_1) = \frac{\partial \mathbf{Y}(t)}{\partial Y_j^0(t_1)} \quad \text{Green function matrix } \mathbf{G}$$

50

Calculation of local sensitivity coefficients

1 Brute force method (finite difference approximation)

$$\frac{\partial Y_i}{\partial p_j}(t_1) \approx \frac{\Delta Y_i(t_2)}{\Delta p_j(t_1)} = \frac{Y_i(t_2) - Y_i(t_1)}{\Delta p_j(t_1)}$$

Δp_j small: large error due to the representation of numbers
 Δp_j large: large error due to nonlinearity

2 Direct method

2a. Coupled Direct Method:

coupled solution of the kinetic and sensitivity differential equations:

$$\begin{aligned} \frac{d\mathbf{Y}}{dt} &= \mathbf{f}(\mathbf{Y}, \mathbf{p}) & \mathbf{Y}(t_0) &= \mathbf{Y}_0 \\ \frac{d}{dt} \frac{\partial \mathbf{Y}}{\partial p_j} &= \mathbf{J} \frac{\partial \mathbf{Y}}{\partial p_j} + \frac{\partial \mathbf{f}}{\partial p_j} & \frac{\partial \mathbf{Y}}{\partial p_j}(t_0) &= 0 \end{aligned}$$

The coupled solution is repeated for each parameter: $j = 1, 2, \dots, m$

Lots of unnecessary calculations.

51

Calculation of local sensitivity coefficients 2

2b. Decoupled Direct Method (DDM):

joint solution of the kinetic and sensitivity diff. equations in each step:

$$\begin{aligned} \frac{d\mathbf{Y}}{dt} &= \mathbf{f}(\mathbf{Y}, \mathbf{p}) & \mathbf{Y}(t_0) &= \mathbf{Y}_0 \\ \frac{d}{dt} \frac{\partial \mathbf{Y}}{\partial p_j} &= \mathbf{J} \frac{\partial \mathbf{Y}}{\partial p_j} + \frac{\partial \mathbf{f}}{\partial p_j} & \frac{\partial \mathbf{Y}}{\partial p_j}(t_0) &= 0 \end{aligned} \quad j = 1, 2, \dots, m$$

The Jacobian of these equations are identical, therefore in each step

- ⇒ transformation of the Jacobian to a triangle matrix
- ⇒ selection of stepsize Δt based on the Jacobian
- ⇒ solution of the stiff ODE: calculation of new \mathbf{Y}
- ⇒ calculation of the new sensitivity vector for parameter $j=1$ using the same triangle matrix
- ⇒ ⇒ ⇒ ⇒ repeating for all parameters $j = 1, 2, \dots, m$
- ⇒ ⇒ repeating for new time steps from the transformation of \mathbf{J}

features:

- very fast method; the computer time only slightly increases with the number of parameters m (because the transformation of \mathbf{J} is the most time consuming)
- the accuracy of solution can be controlled

52

Automatic differentiation

The simulation result calculated on a computer is obtained by a sequence of simple operations such as additions, multiplications, and elementary functions such as sines and cosines.

By applying the chain rule over and over again to these simple operations it is possible to calculate the derivatives to machine precision in an automatic way.

ADIFOR: a Fortran simulation code is converted by a program to a modified code for the calculation of the local sensitivity coefficients

Bischof, C., Carle, A., Khademi, P., Mauer: The ADIFOR 2.0 system for the automatic differentiation of FORTRAN 77 programmes. *IEEE J. Comput. Sci. Eng.* **3**, 18-32. (1996)

ADIC: a C simulation code is converted by a program to a modified code for the calculation of the local sensitivity coefficients

Bischof, C.H., Roh, L., Mauer-Oats, A.J.: ADIC: an extensible automatic differentiation tool for ANSI-C. *Soft. Pract. Exper.* **27**, 1427-1456 (1997)

Topic 4: Local sensitivity analysis 2

original and normalized sensitivities,

principal component analysis of the sensitivity matrix,

local uncertainty analysis,

applications of local sensitivities

Interpretation of local sensitivity coefficients

$$s_{ik} = \frac{\partial Y_i}{\partial p_k}$$

(Original) local sensitivity coefficients:

the parameter is changed by one unit
inspected: the result is changed by how many units
[unit of result / unit of parameter]

Normalized local sensitivity coefficients:

$$\tilde{s}_{ik} = \frac{p_k}{Y_i} \frac{\partial Y_i}{\partial p_k} = \frac{\partial \ln Y_i}{\partial \ln p_k}$$

investigates relative changes

How much % change of the result
due to 1 % change of the parameter?
dimension free

So far: single parameter is changed
effect on a single model result is investigated

Further information can also be extracted from sensitivity matrix **S**
using principal component analysis, like the case when
several parameters are changed simultaneously, and
the effect on multiple model results is investigated.

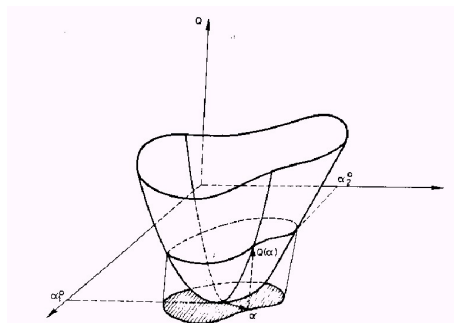
55

PCAS: principal component analysis of the sensitivity matrix S

Several parameters are changed simultaneously and the effect on several model outputs is investigated.

The effect of changing parameters is measured by a
Célfüggvény:

$$e(\mathbf{p}) = \int_{t_1}^{t_2} \sum_{i=1}^m \left(\frac{Y_i^*(t) - Y_i(t)}{Y_i(t)} \right)^2 dt$$



S. Vajda, P. Valkó, T. Turányi: Principal component analysis of kinetic models
Int. J. Chem. Kinet., **17**, 55-81(1985)

56

PCAS: principal component analysis of the sensitivity matrix \mathbf{S}

The objective function can be approximated by:

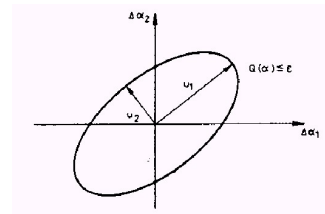
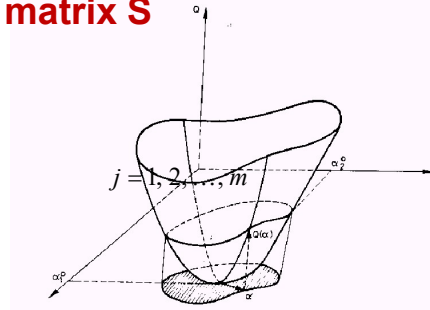
$$e(\boldsymbol{\alpha}) = (\Delta \boldsymbol{\alpha})^T \tilde{\mathbf{S}}^T \tilde{\mathbf{S}} (\Delta \boldsymbol{\alpha})$$

where

$$\Delta \boldsymbol{\alpha} = \Delta \ln \mathbf{p} \quad \tilde{\mathbf{S}} = \begin{bmatrix} \tilde{\mathbf{S}}_1 \\ \tilde{\mathbf{S}}_2 \\ \vdots \\ \tilde{\mathbf{S}}_n \end{bmatrix}$$

And the normed sensitivity matrix belonging to time t_r

$$\tilde{\mathbf{S}}_r = \{(p_k / Y_i) (\partial Y_i(t_r) / \partial p_k)\}$$



57

PCAS: principal component analysis of the sensitivity matrix \mathbf{S}

$$e(\boldsymbol{\alpha}) = (\Delta \boldsymbol{\alpha})^T \tilde{\mathbf{S}}^T \tilde{\mathbf{S}} (\Delta \boldsymbol{\alpha})$$

This quadratic form determines a (hyper) ellipsoid:

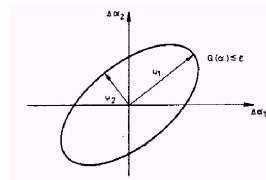
- 2D ellipse
- 3D ellipsoid (rugby ball shape)
- 4D hyper ellipsoid

Another characterization of the hyper ellipsoid:

- length of the axes
- direction of the axes

Eigenvalue-eigenvector decomposition of matrix $\tilde{\mathbf{S}}^T \tilde{\mathbf{S}}$

- λ_i eigenvalue i = length of axis i
if λ_i is small: the objective function increases rapidly to this direction
= parameter group i is highly influential
- \mathbf{u}_i eigenvector i = direction of axis i



58

PCAS: principal component analysis of the sensitivity matrix S

$$e(\mathbf{a}) = (\Delta \mathbf{a})^T \tilde{S}^T \tilde{S} (\Delta \mathbf{a})$$

An alternative form of the objective function:

$$e(\mathbf{a}) = \sum_{i=1}^r \lambda_i (\Delta \Psi_i)^2$$

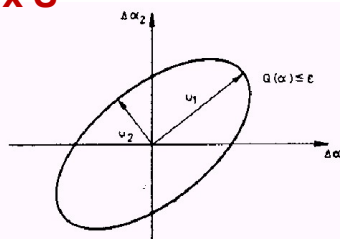
where $\Delta \Psi_i = \mathbf{u}_i \mathbf{a}$ transformed parameters called principal components

In the figure above:

λ_1 small \Rightarrow axis 1 is long; $\mathbf{u}_1 = (0.707, 0.707)$

λ_2 large \Rightarrow axis 2 is short; $\mathbf{u}_2 = (-0.707, 0.707)$

Note: the eigenvectors are unit vectors, therefore $0.707^2 + 0.707^2 = 1$



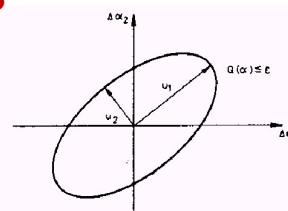
59

PCAS: principal component analysis of the sensitivity matrix S

Example 1:

λ_1 small \Rightarrow axis 1 is long; $\mathbf{u}_1 = (0.707, 0.707)$

λ_2 large \Rightarrow axis 2 is short; $\mathbf{u}_2 = (-0.707, 0.707)$



axis 1 is long \rightarrow changing the parameters to direction \mathbf{u}_1
the objective function changes little

\rightarrow if $\alpha_2 - \alpha_1 = \ln p_2 - \ln p_1 = \ln(p_2/p_1)$ constant, \Rightarrow little change of the objective function

\rightarrow if p_2/p_1 constant, \Rightarrow little change of the objective function

Thus, eigenvector $\mathbf{u} = (0.707, 0.707)$ means that keeping the ratio of the corresponding two parameters constant the inspected result(s) of simulation do not change.

Chemistry: the model results do not change if we keep the equilibrium constant $K = k_1/k_2$ fixed.

60

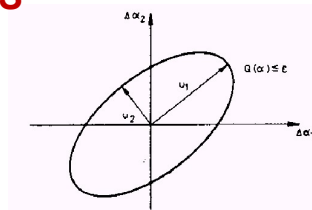
PCAS: principal component analysis of the sensitivity matrix **S**

Example 2:

$\mathbf{u}_1 = (0.707, 0.707, 0)$ large eigenvalue

$\mathbf{u}_2 = (-0.707, 0.707, 0)$ small eigenvalue

$\mathbf{u}_3 = (0, 0, 1)$ large eigenvalue



Interpretation of the eigenvectors:

p_1/p_2 and p_3 can be determined from the experimental data

p_3 can be determined independently

Only the ratio of p_1 and p_2 can be determined.

T. Perger, T. Kovács, T. Turányi, C. Treviño:

Determination of adsorption and desorption parameters from ignition temperature measurements in catalytic combustion systems, *J. Phys. Chem. B*, **107**, 2262-2274 (2003)

61

Local uncertainty analysis

If the parameters are correlated, then using the rule of spread of errors the uncertainty of model results can be calculated from the correlation matrix of parameters:

$$\Sigma_Y = \mathbf{S}^T \Sigma_p \mathbf{S}$$

Here Σ_p is the covariance matrix of parameters, \mathbf{S} is the sensitivity matrix and Σ_Y is the covariance matrix simulation results.

If the parameters are uncorrelated, then variance $\sigma^2(y)$ of model result y can be calculated from the variance of parameters: $\sigma^2(p_k)$

$\sigma_k^2(y)$ is the contribution of parameter k to the variance of model result y

$$\sigma_k^2(y) = \sigma^2(p_k) \left(\frac{\partial y}{\partial p_k} \right)^2 \quad \sigma^2(y) = \sum_k \sigma_k^2(y)$$

T. Turányi, L. Zalotai, S. Dóbbé, T. Bérces: Effect of the uncertainty of kinetic and thermodynamic data on methane flame simulation results *Phys. Chem. Chem. Phys.*, **4**, 2568-2578 (2002)

62

Local uncertainty analysis 2

- Linear approximation of the variance of the model result
- Does not take into account the nonlinear effects
- The result belongs to the nominal set of model parameters
- Realistic results, if the model behaves qualitatively similarly in the whole domain of parameters
- Non-realistic results, if the model is qualitatively different in the various parts of the parameter domain
- Provides separately the contribution of parameters
- Can be calculated fast

63

Applications of local sensitivities

1. **Analysis of models**
 - Estimation of the effect of parameter perturbation
 - Identification of cooperating parameters
2. **Reduction of models**
 - Identification of ineffective parameters;
production of a simpler model with less parameters, but almost identical results
3. **Local uncertainty analysis**
 - May replace global uncertainty analysis:
less accurate, much faster
4. **Parameter estimation**
 - All gradient methods are based on the (hidden) application of local sensitivity coefficients
 - Identification of effective parameters
 - Experimental design

64

Topic 5: Global uncertainty analysis and global sensitivity analysis

local and global uncertainty analysis

Morris' screening method,
Monte Carlo method,
Latin hypercube sampling,
Fourier Amplitude Sensitivity Test (FAST) method,
sensitivity indices,

surface response methods:
polynomial chaos expansion (PCE) method,
high-dimensional model representation (HDMR) method.

What is uncertainty analysis generally good for?

Global uncertainty analysis

Local uncertainty analysis

Provides information at the nominal parameter set

- well applicable, if the model behaves qualitatively similarly in the various regions of parameter space
- exact for linear models

Global uncertainty analysis

the whole physically possible region of parameters is investigated

Global vs. local uncertainty analysis

global methods require much more computer time
acquired information ~ computer time

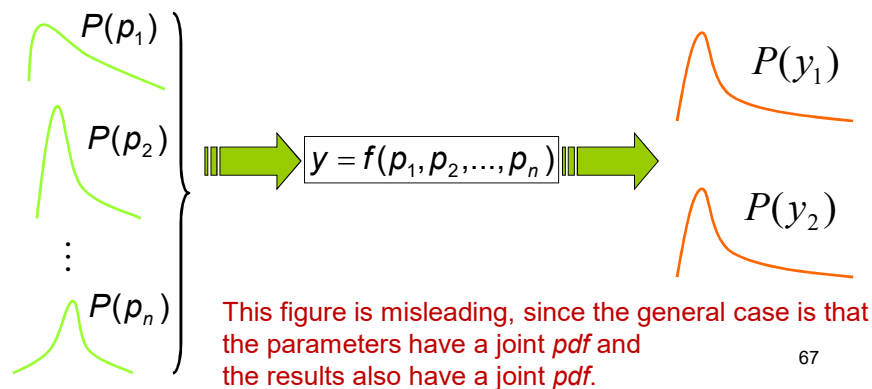
| | |
|-----------------------------|---|
| global uncertainty analysis | calculation of the uncertainty of model results from the uncertainty of model parameters |
| global sensitivity analysis | as above + identification of the individual contribution of the uncertainty of model parameters |

Global uncertainty analysis 2

The uncertainty of parameters can be characterized by their probability density function (*pdf*)

The aims of global uncertainty analysis:

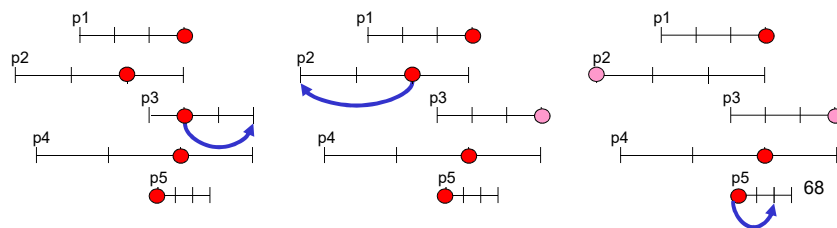
1. Calculation of the *pdf* of the results on the basis of the *pdf* of parameters
2. Determination of the contribution of the individual parameters to the standard deviation of model results



Morris method

Screening methods provide approximate information quickly
The Morris method allows the investigation of the effect of large parameter changes

- lower and upper uncertainty limits are assigned to each parameter.
- the uncertainty interval is divided to n parts for each parameter
- random parameter set is selected
- one parameter is changed at each run
- statistical interpretation of the results
- assumes uniform distribution of the parameters
- does not provide the *pdf* of the results
- intermediate computer time

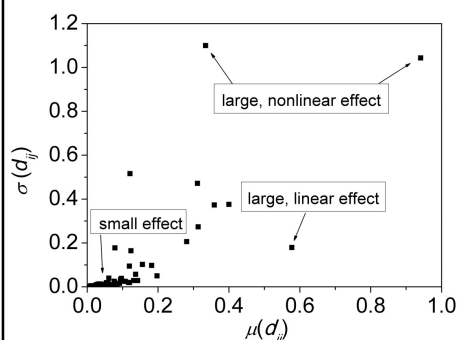


Morris method 2

Value d_{ij} shows the influence of parameter p_j at the random values of all other parameters within their uncertainty interval:

$$d_{ij} = \frac{Y_i(p_1^z, p_2^z, \dots, p_j^z + \Delta, \dots, p_N^z) - Y_i(\mathbf{p}^{z-1})}{|\Delta|}$$

The d_{ij} values are calculated many times in a random calculation and the expected value and standard deviation of d_{ij} is determined.



M. D. Morris:
Factorial sampling plans for preliminary
computational experiments.
Technometrics **33**, 161-174 (1991)

F. Campolongo, J. Cariboni, A. Saltelli:
An effective screening design for
sensitivity analysis of large models.
Env. Model. Softw. **22**, 1509-1518 (2007)

69

Monte Carlo method

Several thousands of random parameter sets are generated in accordance with the joint *pdf* of the parameters.

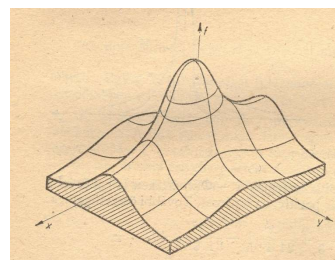
The simulations are carried out at these parameter sets.

Statistical analysis of the simulation results:

- determination of the histogram of a result
- calculation of the expected value and standard deviation

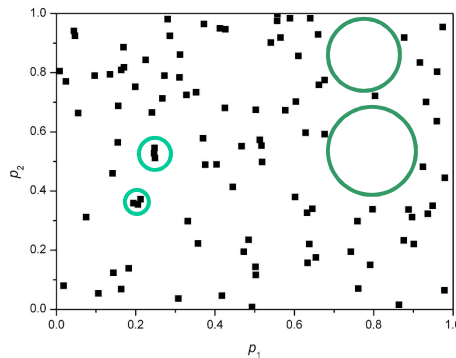
Problems:

- requires much computer time
- it is not easy to trace the effect of individual parameters



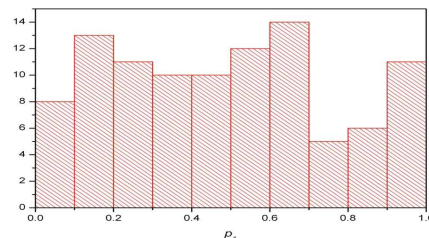
70

Monte Carlo method 2



Generation of 100 (ξ, γ) points
 ξ and γ are random numbers
 with $[0,1]$ even distribution
 \Rightarrow used for the generation of
 parameter values p_1 and p_2 ,
 respectively.

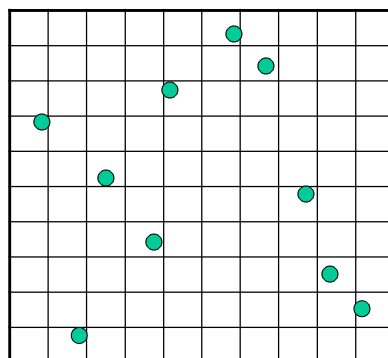
Clogging and empty spots



histogram of p_1

71

Monte Carlo method with Latin hypercube sampling



even distribution

M. D. McKay, R. J. Beckman, W. J. Conover:
 A comparison of three methods for selecting
 values of input variables in the analysis of
 output from a computer code.
Technometrics **42**, 55-61 (2000)

J. C. Helton, F. J. Davis: Latin hypercube
 sampling and the propagation of uncertainty
 in analyses of complex systems.
Reliab. Engng Syst. Safety **81**, 23-69 (2003)

- stripes („strata”) with equal probability are designated
- within each stripe a point is placed randomly
- if a stripe already contains a point, another point is not placed there ⁷²

Monte Carlo method with Latin hypercube sampling



Sir Ronald Aylmer Fisher
(17 February 1890 – 29 July 1962)
British statistician and geneticist.

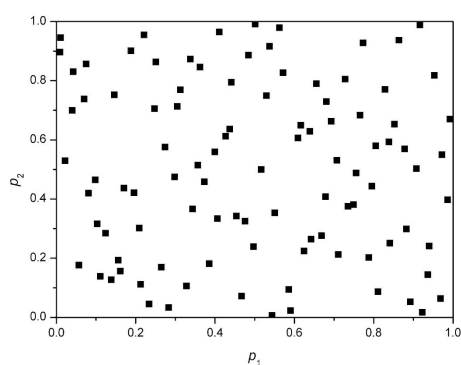
He has been described as
"a genius who almost single-handedly created the
foundations for modern statistical science,,."

His contributions to statistics include the maximum
likelihood, the derivation of various sampling
distributions, founding principles of the design of
experiments, and much more. He developed the
analysis of variance (ANOVA) method.

Stained glass window in the dining hall of
Caius College, in Cambridge, commemorating Ronald
Fisher and representing a Latin square,
discussed by him in *The Design of Experiments*

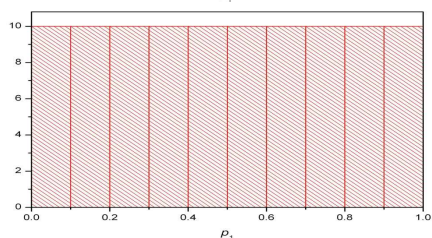
73

Monte Carlo method with Latin hypercube sampling



Generation of 100 (ξ, γ) points
with Latin hypercube sampling

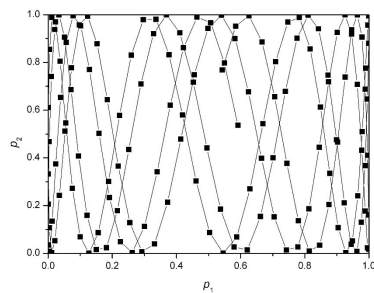
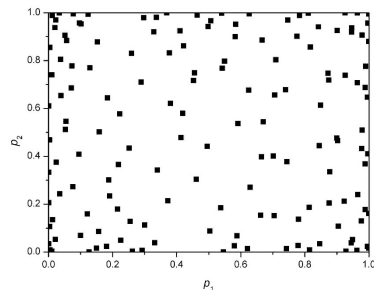
**The distribution is
much more even**



histogram of p_1

74

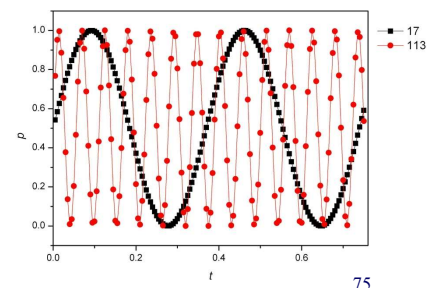
Fourier Amplitude Sensitivity Test (FAST) method



Changing s changing the values of sin functions having incommensurable frequency.

The plotted numerical example shows 150 points and $\Delta s = 0.1$

$x = 0.5 (\sin(17s), \sin(113s)) + 0.5$
 \Rightarrow scaled to a unit square

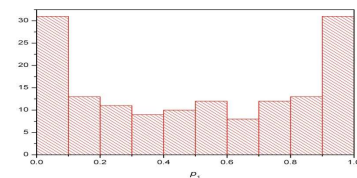
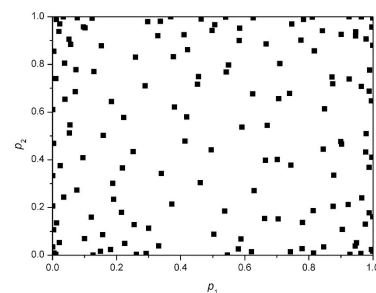
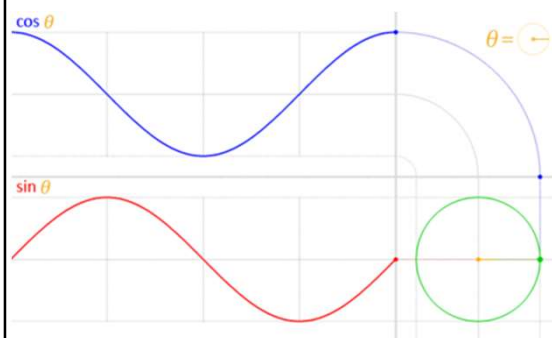


75

Fourier Amplitude Sensitivity Test (FAST) method 2

If the G_j functions are linear, then (due to the nature of the sine function) there are more points at the edges

Using appropriate G_j functions, an *pdf* can be reconstructed (for independent parameters)



76

Fourier Amplitude Sensitivity Test (FAST) method 3

$E(Y_i)$ is the expected value of model result Y_i :

$$E(Y_i) = \iiint \dots \int h_i(p_1, p_2, \dots, p_N) P(p_1, p_2, \dots, p_N) dp_1 dp_2 \dots dp_N$$

Y_i is the value of function h_i ; P is the joint *pdf* of parameters \mathbf{p}

Parameter p_j is changed by changing scalar s

$$p_j(s) = G_j(\sin \omega_j s)$$

Function G_j has to be selected to reproduce the joint probability density of parameters \mathbf{P}

ω_j is the frequency assigned to parameter p_j

The frequencies have to be relative primes.

If $-\pi < s < \pi$ and $\Delta s = 2\pi/N \Rightarrow N$ points are located in the space of parameters; the local density corresponds to the *pdf*

R. I. Cukier, C. M. Fortuin, K. E. Shuler, A. G. Petschek, J. H. Schaibly:
Study of the sensitivity of coupled reaction systems to uncertainties in rate coefficients I. Theory.
J. Chem. Phys. **59**, 3873-3878 (1973)

Fourier Amplitude Sensitivity Test (FAST) method 4

The simulation results are investigated by Fourier analysis:

$$\sigma^2(Y_i) = 2 \sum_{l=1}^{+\infty} (A_{il}^2 + B_{il}^2)$$

Here $\sigma^2(Y_i)$ is the variance of the result; A_{il} and B_{il} are the Fourier coefficients:

$$A_{il} = \frac{1}{2\pi} \int_{-\pi}^{\pi} Y_i(s) \cos(ls) ds, \quad l = 0, 1, \dots$$

$$B_{il} = \frac{1}{2\pi} \int_{-\pi}^{\pi} Y_i(s) \sin(ls) ds, \quad l = 1, 2, \dots$$

When the Fourier coefficients are calculated at frequency ω_j and its overtones, then the partial variance caused by parameter j is obtained:

$$\sigma_j^2(Y_i) = 2 \sum_{r=1}^{+\infty} (A_{i,r\omega_j}^2 + B_{i,r\omega_j}^2)$$

78

Fourier Amplitude Sensitivity Test (FAST) method 5

partial variance:

$$S_{ij} = \frac{\sigma_j^2(Y_i)}{\sigma^2(Y_i)}$$

This is the fraction of the total variance caused by parameter j

FAST is a slow algorithm; the total number of required simulations:
 $N = 1.2 k^{2.5}$

$N = 21000$ simulations are needed for the investigation of a model having $k = 50$ parameters

The source of extra information for the same amount of computer time:
 Unlike in the MC method, the order of simulations is important;
 patterns are identified in the sequence of simulations

A. Saltelli, R. Bolado: An alternative way to compute Fourier Amplitude Sensitivity Test (FAST)
Comput. Stat. Data Anal. **26**, 445-460 (1998)

79

Sensitivity indices

May be considered as a further developed version of FAST:

The expected value of Y_i :

$$E(Y_i) = \int \int \dots \int f_i(p_1, p_2, \dots, p_N) P(p_1, p_2, \dots, p_N) \, dp_1 \, dp_2 \dots dp_N$$

The variance of Y_i :

$$\begin{aligned} V(Y_i) &= \int \int \dots \int (f_i(p_1, p_2, \dots, p_N) - E(Y_i))^2 P(p_1, p_2, \dots, p_N) \, dp_1 \, dp_2 \dots dp_N = \\ &= \int \int \dots \int f_i^2(p_1, p_2, \dots, p_N) P(p_1, p_2, \dots, p_N) \, dp_1 \, dp_2 \dots dp_N - E^2(Y_i) \end{aligned}$$

Variance of Y_i , if parameter p_j is fixed:

$$V(Y_i|p_j)$$

Its expected value:

$$E(V(Y_i|p_j))$$

Variance of Y_i caused by p_j :

$$V(E(Y_i|p_j)) = V(Y_i) - E(V(Y_i|p_j))$$

First order uncertainty index (similar to FAST partial variance):

$$S_{j(i)} = \frac{V(E(Y_i|p_j))}{V(Y_i)}$$

A. Saltelli: Making best use of model evaluations to compute sensitivity indices, *Comput. Phys Commun.*, **145**, 280-297 (2002)

80

Sensitivity indices 2

Variance of Y_i , caused by parameters p_j and p_k together: $V(E(Y_i|p_j, p_k))$

It can be used for the calculation of the *second order uncertainty index*:

$$S_{kj(i)} = \frac{V(E(Y_i|p_k, p_j)) - V(E(Y_i|p_k)) - V(E(Y_i|p_j))}{V(Y_i)}$$

This index shows the interaction of parameters p_j and p_k

The n -th order uncertainty index can be obtained in a similar way.

Example: a model has three parameters: a, b, c

The total index:

$$S_{a(i)}^{\text{tot}} = S_{a(i)} + S_{ab(i)} + S_{ac(i)} + S_{abc(i)}$$

parameter j has no correlations:

$$S_{j(i)} = S_{j(i)}^{\text{tot}}$$

interactions of parameter j :

$$S_{j(i)}^{\text{tot}} - S_{j(i)}$$

81

Sensitivity indices 3

- Global method
- Application of pseudo random numbers allow the fast calculation of the integrals
- Calculates the the first and higher order effects
- Calculates the total effect
- Takes into account the *pdf* of the parameters
- Requires much computer time
(about 25000 runs for 50 parameters)

82

Surface response methods (SRMs)

A whole family of the global sensitivity analysis methods is based on the idea that the original model (e.g. an ODE or PDE based complex model) is approximated by a simpler function and the global sensitivity analysis is carried out with the help of the simpler model.

Gaussian process emulator methods

Uses metamodels based on the assumption that for target outputs

$\mathbf{Y} = \mathbf{f}(\mathbf{x})$, the value of \mathbf{Y} at an unknown value of \mathbf{x} follows a multivariate Gaussian distribution. Suitable for systems with a small number of main effects and only weak parameter interactions.

Polynomial chaos expansion (PCE) methods

Polynomial chaos (PC; also called Wiener chaos expansion) is a non-sampling-based method to determine evolution of uncertainty in dynamical system, when there is probabilistic uncertainty in the system parameters. (Wiener, 1938)

High-dimensional model representation (HDMR) methods

To be discussed in details later.

83

Polynomial chaos expansion (PCE)

It is not related to „chaos” in the dynamical systems theory way.

It has been used several times in combustion modelling.

M. T. Reagan, H. N. Najm, B. J. Debusschere, O. P. Le Maitre, O. M. Knio, R. G., Ghanem: Spectral stochastic uncertainty quantification in chemical systems. *Combust. Theor. Model.* **8**, 607-632 (2004)

D.A. Sheen, X. You, H. Wang, T. Løvås: Spectral uncertainty quantification, propagation and optimization of a detailed kinetic model for ethylene combustion. *Proc. Combust. Inst.* **32**, 535-542 (2009)

x_i, x_j uncertain Arrhenius parameters A , scaled to interval $[-1, +1]$
description of model response $\eta_r(\mathbf{x})$ with a second order polynomial:

$$\eta_r(\mathbf{x}) = \eta_{r,0} + \sum_{i=1}^m a_{r,i} x_i + \sum_{i=1}^m \sum_{j \geq i}^m b_{r,i,j} x_i x_j$$

The uncertainty in \mathbf{x} may be expressed as a polynomial expansion of basis random variables ξ ,

$$\mathbf{x} = \mathbf{x}^{(0)} + \sum_{i=1}^m \alpha_i \xi_i + \sum_{i=1}^m \sum_{j \geq i}^m \beta_{ij} \xi_i \xi_j + \dots,$$

84

Polynomial chaos 2

Combining the previous two equations:

$$\eta_r(\xi) = \eta_r(\mathbf{x}^{(0)}) + \sum_{i=1}^m \hat{\alpha}_{r,i} \xi_i + \sum_{i=1}^m \sum_{j \geq i}^m \hat{\beta}_{r,ij} \xi_i \xi_j + \dots,$$

where $\hat{\alpha}_r = \frac{1}{2} \mathbf{I}_m \mathbf{a}_r$ $\hat{\beta}_r = \frac{1}{4} \mathbf{I}_m^T \mathbf{b}_r \mathbf{I}_m$

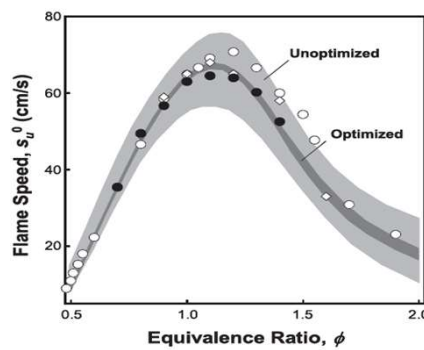
⇒ the overall model prediction is given by its nominal value plus uncertainty contributions from each rate coefficient. The overall output variance may then be represented as the sum over terms involving the coefficients of the equivalent expansion:

$$\sigma_r(\xi)^2 = \sum_{i=1}^m \hat{\alpha}_{r,i}^2 + 2 \sum_{i=1}^m \sum_{j>i}^m \hat{\beta}_{r,ij}^2 + \sum_{i=1}^m \sum_{j>i}^m \hat{\beta}_{r,ij}^2$$

D.A. Sheen, X. You, H. Wang, T. Løvås: Spectral uncertainty quantification, propagation and optimization of a detailed kinetic model for ethylene combustion. *Proc. Combust. Inst.* **32**, 535-542 (2009)

Polynomial chaos 3

A typical result from Sheen *et al.* (2009):



Light grey: prior uncertainty of ethylene–air flame velocity from the uncertainty factors f of Baulch *et al.* (2004).

Dark grey: posterior sensitivities from the optimized model.

Symbols: experimental data.

D.A. Sheen, X. You, H. Wang, T. Løvås: Spectral uncertainty quantification, propagation and optimization of a detailed kinetic model for ethylene combustion. *Proc. Combust. Inst.* **32**, 535-542 (2009)

HDMR method

High Dimensional Model Representation

The simulation results are approximated by a polynomial of the parameters:

$$Y(\mathbf{x}) = Y_0 + \sum_{i=1}^n Y_i(x_i) + \sum_{1 \leq i < j \leq n} Y_{ij}(x_i, x_j) + \dots$$

$Y(x_i)$ the only variable is parameter x_i
But the function can be even an 8th order polynomial!

$Y(x_i, x_j)$ the variables are parameters x_i and x_j
Two variables only, but it can also be a high-order polynomial!

T. Ziehn, A. S. Tomlin: GUI-HDMR - A software tool for global sensitivity analysis of complex models.
Environ. Model. Soft. **24**, 775-785 (2009)

87

HDMR-method 2

Types:

cut HDMR

The polynomial is generated from a reference point

random sampling HDMR (RS-HDMR):

Generation of random points in a parameter domain,
fitting polynomials to these points

Examples:

Approximation with base functions: $Y_i(x_i) = \sum_{r=1}^k \alpha_r^i \varphi_r(x_i)$

Partial variances: $D_i = \sum_{r=1}^{k_i} (\alpha_r^i)^2$

Sensitivity indices: $S_{i_1, \dots, i_s} = \frac{D_{i_1, \dots, i_s}}{D}, \quad 1 \leq i_1 < \dots < i_s \leq m$

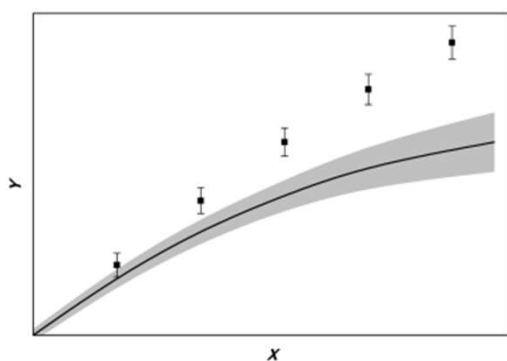
88

Comparison of the methods

| | local | Morris | MC LHS | sens. index |
|--------------------------------|------------|----------------------|--------|-------------|
| input variance | ✓ | ✓ | ✓ | ✓ |
| input <i>pdf</i> | ✗ | ✗ | ✓ | ✓ |
| output <i>pdf</i> | ✗ | ✗ | ✓ | ✗ |
| output variance | ✓ (linear) | ✗ | ✓ | ✓ (biased) |
| CPU requirement? | ✓ 1 | 2110 | 3000 | 16280 |
| Individual contributions | ✓ (linear) | ✓ (only qualitative) | ✗ | ✓ |
| global? | ✗ | ✓ | ✓ | ✓ |
| info about the non-linearities | ✗ | ✓ (only qualitative) | ✗ | ✓ |

Uncertainty analysis: What is it good for?

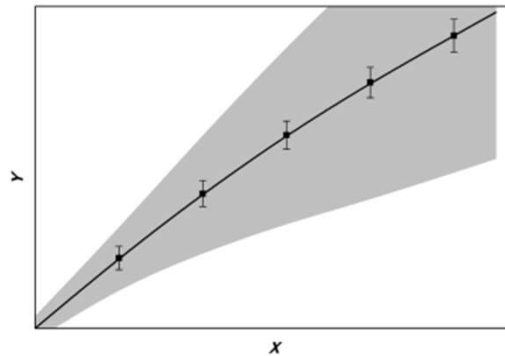
Is the structure of the model OK?



if the experimental data are correct and
 if the uncertainty regions of the parameters are well known
 BUT the uncertainty regions of measured and simulated results
 do not overlap \Rightarrow the structure of the model is bad (wrong equations!)

What is it good for? 2

Is the model well established?

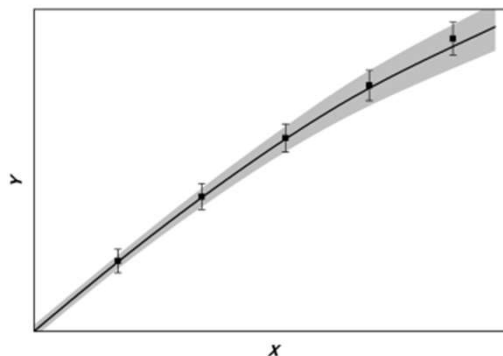


if the uncertainty of the simulated results is much wider than the uncertainty of the data
 \Rightarrow any simulation result can be obtained with the parameters
 \Rightarrow the model is not useful

91

What is it good for? 3

Are the model parameters well known?



the uncertainty ranges of the data overlap with the uncertainty of the simulation results; the two uncertainty ranges are similar
 \Rightarrow the model is OK,
 but the uncertainty of the simulation results can be decreased,
 if the critical parameters (to be identified by uncertainty analysis)
 are determined with smaller uncertainty

92

Summary of uncertainty analysis methods

Local uncertainty analysis

one parameter is changed at a time;
based on partial derivatives
can be calculated quickly

Screening methods

several parameters are changed in wide parameter ranges
intermediate computer time requirement
Morris method

Global uncertainty analysis

all parameters are changed simultaneously
according to their joint *pdf*
requires much computer time
e.g. Monte Carlo method (with Latin hypercube sampling)

93

Topic 6: Uncertainty of the thermodynamic and kinetic parameters

uncertainty of thermodynamic data,
Active Thermochemical Tables (ATcT),

direct and indirect measurements,

estimation of uncertainty for gas kinetic rate coefficients,

EXAMPLE:

applications of several uncertainty analysis methods to a
methane flame model

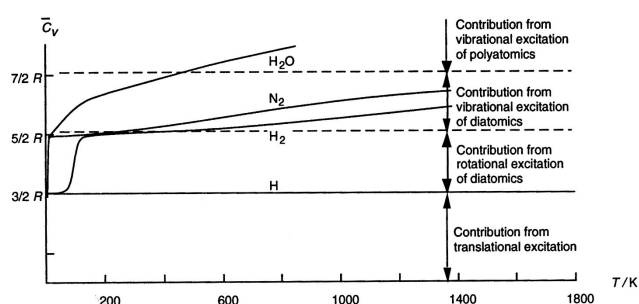
Temperature dependence of thermodynamic data

NASA polynomials

$$\frac{H^\theta}{RT} = a_1 + \frac{a_2}{2}T + \frac{a_3}{3}T^2 + \frac{a_4}{4}T^3 + \frac{a_5}{5}T^4 + \frac{a_6}{T}$$

$$\frac{c_p}{R} = a_1 + a_2T + a_3T^2 + a_4T^3 + a_5T^4$$

$$\frac{S^\theta}{R} = a_1 \ln T + a_2T + \frac{a_3}{2}T^2 + \frac{a_4}{3}T^3 + \frac{a_5}{4}T^4 + a_7$$



95

Using thermodynamic data in combustion simulations

ΔH_f \Rightarrow calculation of heat production in a reacting mixture
 \rightarrow calculation of temperature changes
 \Rightarrow calculation of $\Delta_r G^0$

c_p \Rightarrow calculation of temperature changes

ΔS \Rightarrow calculation of $\Delta G = \Delta H - T\Delta S$
 \rightarrow calculation of the equilibrium constant
 \rightarrow calculation of the rate coefficient of reverse reactions

96

Uncertainty of thermodynamic data

thermodynamic data influence the reaction kinetic calculations in two ways:

- Calculated temperature
- Calculation of the rate coefficients of backward reaction steps

Thermodynamic data used:

- heat capacity (can be calculated using statistical thermodynamics)
- entropy (can be calculated using statistical thermodynamics)
- standard enthalpy of formation (measurement or high level calculation)



- The databases contain the recommended values and variances
- Are the enthalpies of formation correlated?

97

Uncertainty of thermodynamic data

c_p and ΔS can be calculated from the IR spectrum
using methods of statistical thermodynamics

- ΔH_f
- can be computed
(for small molecules only; not easy)
 - can be determined experimentally by
 - measuring the equilibrium constant of a reaction
→ reaction enthalpy → enthalpy of formation
 - measuring ionization energy by mass spectrometry

98

Uncertainty of thermodynamic data 2

Typical uncertainty of ΔH_f (1σ):

molecules and small radicals: 0.1-0.5 kJ/mole

e.g. CO= 0.17 kJ/mole, CH₄= 0.4 kJ/mole, CH₃=0.4 kJ/mole

large radicals: 1.0 – 5.0 kJ/mole

e.g. HO₂= 3.35 kJ/mole, CH₂OH= 4.2 kJ/mole

less known radicals: 8-10 kJ/mole

e.g. HCCO= 8.8 kJ/mole, CH₂HCO= 9.2 kJ/mole

99

Determination of the enthalpies of formation

Methods for the determination of enthalpies of formation ΔH_f :

- 1) direct experimental determination:
calorimetry; synthesis from reference state elements
 $\text{H}_2 + \frac{1}{2} \text{O}_2 = \text{H}_2\text{O}$ applicable for few compounds only
- 2) direct experimental determination from MS ionization energies
applicable for few compounds only; not very accurate
- 3) direct theoretical calculation
high level *ab initio* method required: accurate for small molecules only
- 4) generally applicable method:
indirectly from experimentally measured reaction enthalpies $\Delta_r H^\ominus$
determination of ΔH_f after a chain of calculations

100

Determination of the enthalpies of formation 2

„4) determination of ΔH_f^\ominus after a chain of calculations”

- starting from directly determined ΔH_f^\ominus values

$$\Delta_r H^\ominus = \sum_j \nu_j H_f^\ominus(j)$$

a) combining it with a $\Delta_r H^\ominus$ value provides a new ΔH_f^\ominus value
 \Rightarrow indirectly determined ΔH_f^\ominus

b) GO TO a) until we get the required ΔH_f^\ominus

\Rightarrow the chain of calculation provides the required ΔH_f^\ominus

PROBLEMS:

- Going on in the chain of calculations, the errors are accumulated

ΔH_f^\ominus values at the end of a long chain are not very accurate.

- ΔH_f^\ominus values for the same species can be obtained at the ends of two different calculation chains \Rightarrow different ΔH_f^\ominus values are obtained ?????

101

Active Thermochemical Tables (ATcT)

Idea of Branko Ruscic

<http://atct.anl.gov/>

the determination of many enthalpies of formation ΔH_f^\ominus in one step:

using n direct experimental determination: $H_f^\ominus(j) = A_j \quad j = 1, \dots, n$

using m measured $\Delta_r H^\ominus$ values: $\Delta_r H_i^\ominus = \sum_j \nu_{ij} H_f^\ominus(j) \quad j = n+1, \dots, n+m$

The aim is the determination of k values of ΔH_f^\ominus :

- if $k > n+m \Rightarrow$ not enough info
- if $k < n+m \Rightarrow$ overdetermined linear algebraic system of equations
 \Rightarrow determination of the ΔH_f^\ominus values by the least squares method

If the errors of the measurements are also taken into account

\Rightarrow **weighted least squares method**

B. Ruscic, R. E. Pinzon, M. L. Morton, G. von Laszewski, S. J. Bittner, S. G. Nijsure, K. A. Amin, M. Minkoff, A. F. Wagner: Introduction to Active Thermochemical Tables: Several „key” enthalpies of formation revisited. *J. Phys. Chem. A* **108**, 9979-9997 (2004)

Active Thermochemical Tables (ATcT) 2

NOTES:

The reason of the name: the original idea was that the tables would be „active”: on a Web site adding new measurement data all enthalpies of formation would be recalculated.

It never worked this way: Dr. Ruscic is continuously adding new measurements and sometimes publishes $\Delta_f H^\theta$ values.

Please observe the similarity and difference between ATcT and the optimization of kinetic reaction mechanisms:

- using both direct and indirect measurements
- the error of measurements is used for the calculation of the uncertainty of parameters
- **ATcT**: the simulated data are a linear functions of the parameters
- kinetics**: the simulated data are obtained by solving ODEs or PDEs (strongly nonlinear functions of parameters)

B. Ruscic, R. E. Pinzon, G. von Laszewski, D. Kodeboyina, A. Burcat, D. Leahy, D. Montoya, A. F. Wagner, Active Thermochemical Tables: Thermochemistry for the 21st Century. *J. Phys. Conf. Ser.* **16**, 561-570 (2005)

Direct and indirect measurements

Direct measurements:

- determination of the rate coefficient of a single elementary reaction at a given temperature, pressure, and bath gas
- the rate coefficient values are published

Theoretical (direct) determinations:

- TST/master equation calculations
- the rate coefficients are published at given T , p
- parameterised T , p dependence of rate coefficient k

Indirect measurements:

- a property of the whole combustion system is measured
- interpretation is based on a detailed mechanism
- e.g. laminar flame velocities, ignition delays, concentration profiles

T. Turányi, T. Nagy, I. Gy. Zsély, M. Cserhádi, T. Varga, B.T. Szabó, I. Sedyó, P. T. Kiss, A. Zempléni, H. J. Curran:
Determination of rate parameters based on both direct and indirect measurements
Int.J.Chem.Kinet., **44**, 284–302 (2012)

Rate coefficient uncertainties

Uncertainty factor f_j as defined in data evaluations

(Tsang, Warnatz, Baulch, Konnov):

uncertainty factor u_j

uncertainty parameter f_j

$$u_j = \frac{k_j^0}{k_j^{\min}} = \frac{k_j^{\max}}{k_j^0}$$

$$f_j = \log_{10}(u_j)$$

k_j^0 recommended value of the rate coefficient of reaction j

k_j^{\min} possible minimal value of k_j

k_j^{\max} possible maximal value of k_j

$\Rightarrow [k_j^{\min}, k_j^{\max}]$ is the physically realistic range for the rate coefficients

assume that $\ln k^{\min}$ and $\ln k^{\max}$ deviate 3σ from $\ln k^0$

$$\Rightarrow \sigma^2(\ln k_j) = ((f_j \ln 10)/3)^2$$

1σ uncertainty limit (assuming that u corresponds to 3σ): $l = 10^{f/3} \quad 105$

Uncertainty of k at a given temperature

Uncertainty of (direct) rate coefficient measurements:

very high quality data

uncertainty factor $u = 1.26 \Leftrightarrow f = 0.1 \Leftrightarrow \pm 8\% (1\sigma)$

typical good data

uncertainty factor $u = 2.00 \Leftrightarrow f = 0.3 \Leftrightarrow \pm 26\% (1\sigma)$

typical data

uncertainty factor $u = 3.16 \Leftrightarrow f = 0.5 \Leftrightarrow \pm 47\% (1\sigma)$

(high level) theoretical determinations:

TST/master equation calculations

best systems

uncertainty factor $u = 2.00 \Leftrightarrow f = 0.3 \Leftrightarrow \pm 26\% (1\sigma)$

multi well, main channels

uncertainty factor $u = 3.16 \Leftrightarrow f = 0.5 \Leftrightarrow \pm 47\% (1\sigma)$

multi well, minor channels

uncertainty factor $u = 10 \Leftrightarrow f = 1.0$

C. F. Goldsmith, A. S. Tomlin, S. J. Klippenstein: Uncertainty propagation in the derivation of phenomenological rate coefficients from theory: A case study of *n*-propyl radical oxidation
Proc. Combust. Inst., **34**, 177-185 (2013)

J. Prager, H. N. Najm, J. Zádor: Uncertainty quantification in the *ab initio* rate-coefficient calculation for the $\text{CH}_3\text{CH}(\text{OH})\text{CH}_3 + \text{OH} \rightarrow \text{CH}_3\text{C}(\text{OH})\text{CH}_3 + \text{H}_2\text{O}$ reaction, *Proc. Combust. Inst.*, **34**, 583-590 (2013)

Local uncertainty analysis of chemical kinetic models

$f_j \rightarrow \sigma^2(\ln k_j)$ uncertainty parameter f_j is transformed to the variance of $\ln k_j$

$\partial Y_i / \partial \ln k_j$ seminormalized local sensitivity coefficients

$\sigma_{k_j}^2(Y_i) = \left(\partial Y_i / \partial \ln k_j \right)^2 \sigma^2(\ln k_j)$
contribution of the uncertainty of parameter k_j to the variance of result Y_i

$\sigma_K^2(Y_i) = \sum_j \sigma_{k_j}^2(Y_i)$ variance of result Y_i due to kinetic uncertainties

$\sigma_{T_j}^2(Y_i) = \left(\partial Y_i / \partial \Delta_f H_{298}^\circ(j) \right)^2 \sigma^2(\Delta_f H_{298}^\circ(j))$
contribution of the uncertainty of the enthalpy of formation of species j to the variance of result Y_i

$\sigma^2(Y_i) = \sigma_K^2(Y_i) + \sigma_T^2(Y_i) = \sum_j \sigma_{k_j}^2(Y_i) + \sum_j \sigma_{T_j}^2(Y_i)$
estimated total variance of result Y_i from both kinetic and thermodynamic uncertainties

T. Turányi, L. Zalotai, S. Dóbbé, T. Bérces:
Effect of the uncertainty of kinetic and thermodynamic data on
methane flame simulation results, *Phys.Chem.Chem.Phys.*, **4**, 2568-2578 (2002)

Example: the uncertainty of methane flame simulation results

The investigated methane flames:

- one dimensional, adiabatic, freely propagating, laminar, premixed stationary flame investigated at equivalence ratios $\phi = 0.70$ (lean), 1.00 (stoichiometric), and 1.20 (rich)
- cold boundary conditions $p = 1.0$ atm and $T = 298.15$ K

Monitored outputs:

- laminar flame velocity
- maximum temperature
- maximum species concentration of H, O, OH, CH, CH₂

Uncertainty analysis of a laminar methane flame

Leeds Methane Oxidation Mechanism:
37 species and 175 reversible reactions
stationary, laminar 1D simulations

37 species: the recommended values of the enthalpies of formation and their variance was calculated from thermodynamic databases

175 reactions: uncertainty parameters f were collected from Baulch *et al.*

The investigated simulation results:

maximal flame temperature, laminar flame velocity,
maximal concentrations of radicals H, O, OH, CH, CH₂

Uncertainty analysis methods:

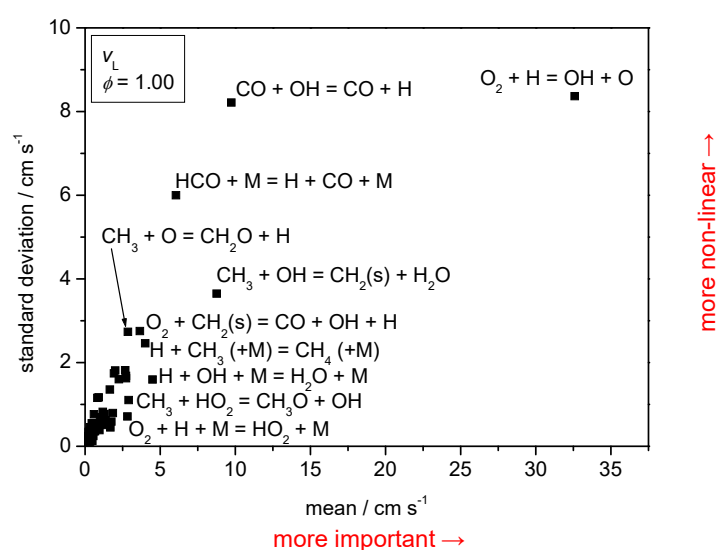
local uncertainty analysis, Morris' method,
Monte Carlo with Latin Hypercube sampling, sensitivity indices

J. Zádor, I. Gy. Zsély, T. Turányi, M. Ratto, S. Tarantola, A. Saltelli: Local and global uncertainty analyses of a methane flame model, *J. Phys. Chem. A*, **109**, 9795-9807 (2005)

109

Morris' method results ($\phi=1$)

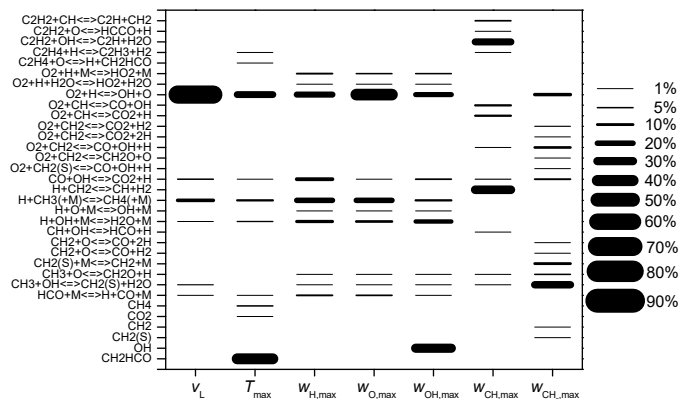
contribution of parameter uncertainties to the uncertainty of the flame velocity



110

Local uncertainty analysis results

% contribution of parameter uncertainties to the uncertainty of the simulated results

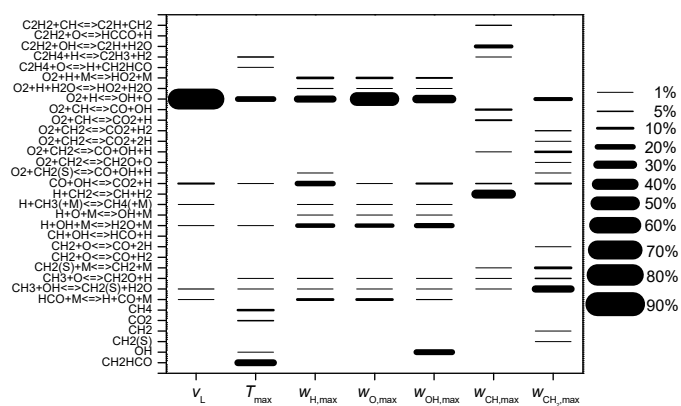


$$\phi = 1.0$$

111

Uncertainty indices

% contribution of parameter uncertainties to the uncertainty of the simulated results



$$\phi = 1.0$$

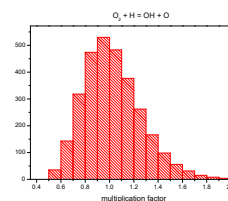
112

Assumed probability density functions of kinetic and thermodynamic parameters

The Monte Carlo and the sensitivity index methods require an assumption on the probability density functions (*pdfs*) of parameters

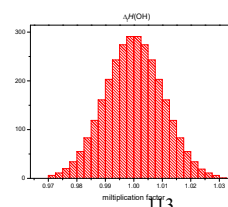
Rate coefficients:

- log-normal distribution
- σ_j was calculated from the f_j uncertainty factor
- the log-normal distribution is clipped at $\pm 3\sigma$ ($\ln k_j$)



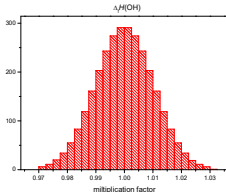
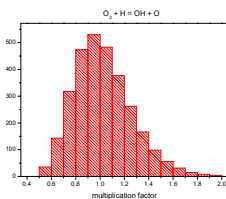
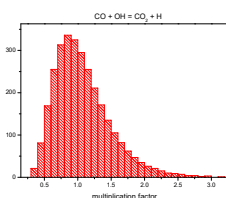
Enthalpies of formation:

- normal distribution
- σ is assessed on the basis of thermodynamic tables
- the normal distribution is clipped at $\pm 3\sigma$

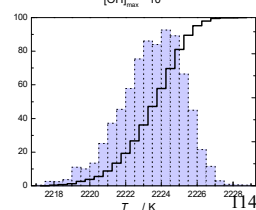
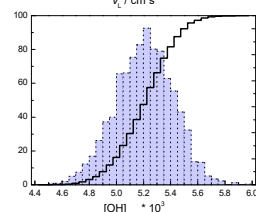
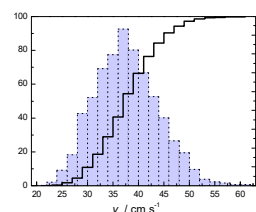


113

pdf of parameters



pdf of simulation results



3,000 Monte Carlo simulations

114

**Comparison of the results of
local and global (Monte Carlo) uncertainty analyses
for a stoichiometric, stationary, flat methane-air flame**

| | result | calculated variances from local Monte Carlo uncertainty analyses | |
|-----------------|-----------------------|---|----------|
| flame velocity | 38.1 cm/s | 4.6 cm/s | 6.2 cm/s |
| max. T | 2224.2 K | 2.8 K | 1.7 K |
| max. w_H | 2.14×10^{-4} | 14.7% | 12.6% |
| max. w_O | 1.74×10^{-3} | 13.3% | 10.4% |
| max. w_{OH} | 5.27×10^{-3} | 3.6% | 4.0% |
| max. w_{CH} | 8.07×10^{-7} | 46.3% | 49.2% |
| max. w_{CH_2} | 2.54×10^{-5} | 23.8% | 24.0% |

115

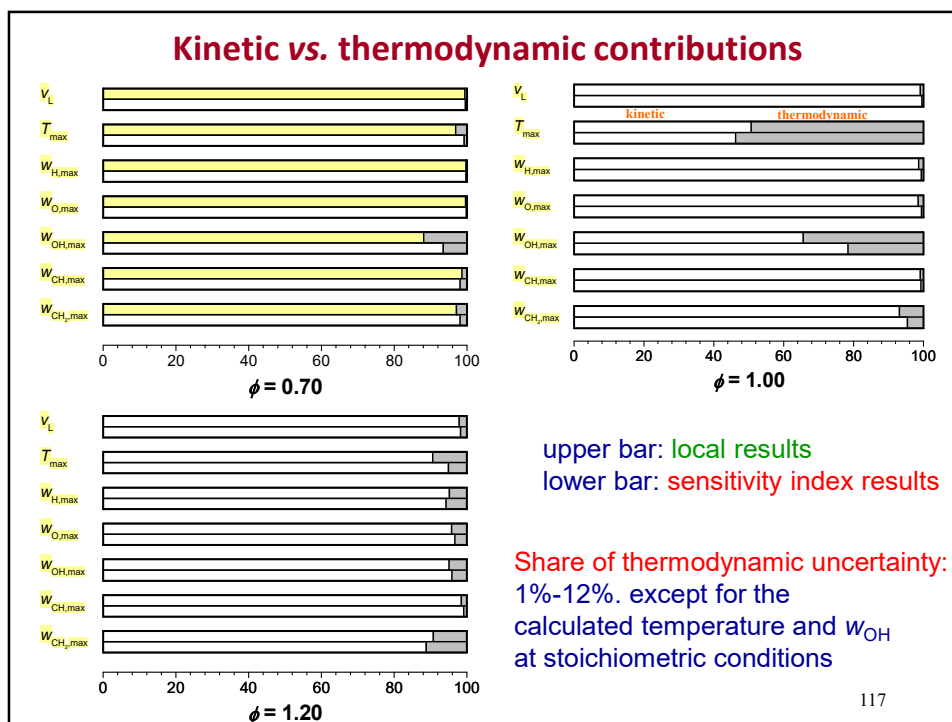
**Largest and smallest results that can be achieved with any
parameter combination, selected from the domain of
uncertainty of the parameters**

| | nominal simulation result | minimal achievable result | maximal |
|-----------------|---------------------------|------------------------------|-----------|
| flame velocity | 38.1 cm/s | 21.3 cm/s | 61.6 cm/s |
| max. T | 2224.2 K | 2217.4 K | 2228.6 K |
| max. w_H | 2.14×10^{-4} | 63.1% | 144.4% |
| max. w_O | 1.74×10^{-3} | 66.9% | 136.1% |
| max. w_{OH} | 5.27×10^{-3} | 86.4% | 114.8% |
| max. w_{CH} | 8.07×10^{-7} | 15.5% | 474.6% |
| max. w_{CH_2} | 2.54×10^{-5} | 37.9% | 219.5% |

Conclusion:

Physically unrealistic results can be obtained, even if the parameters were randomly selected from the uncertainty ranges recommended by the gas kinetics databases.
Reasons: (1) these uncertainties are based on direct measurements;
(2) correlations of uncertainties are not taken into account.

116



Global uncertainty analysis of local sensitivity coefficients

The calculated local sensitivity coefficients belong to a nominal parameter set
different parameter sets \Rightarrow different local sensitivity coefficients
(this is why these are called local ...)

local sensitivity coefficients of flame velocity
were calculated at 3000 randomly selected parameter sets

J. Zádor, I. Gy. Zsély, T. Turányi, M. Ratto, S. Tarantola, A. Saltelli: Local and global uncertainty analyses of a methane flame model, *J. Phys. Chem. A*, **109**, 9795-9807 (2005)

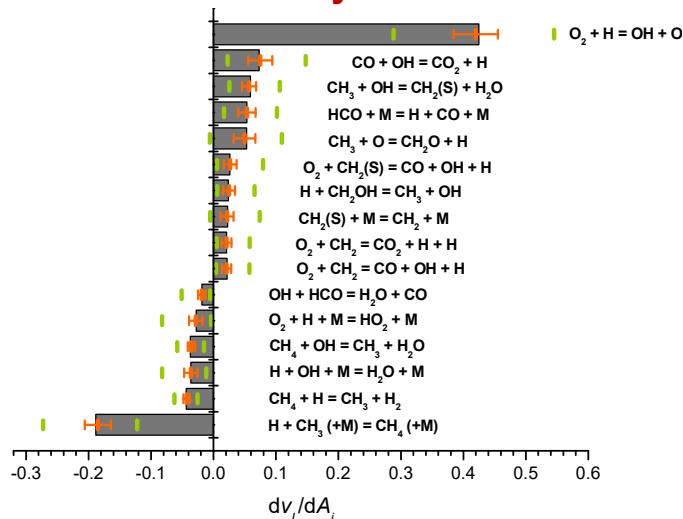
The plotted results:

- local sensitivity coefficients at the nominal set
- standard deviation of sensitivities
- the largest and the smallest calculated sensitivity coefficient



118

Global uncertainty analysis of local sensitivity coefficients 2



Conclusion:

There is a surprisingly little variation of the calculated local sensitivity coefficients with the changing parameters. The order of sensitivity coefficients is almost identical in the whole parameter space.

119

Methane flame uncertainty analysis: general conclusions

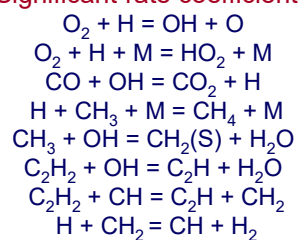
Good agreement between the calculated total variances by the local uncertainty analysis and the Monte Carlo method. (surprise)

Good agreement between the importance of parameters assessed by the local uncertainty analysis and the sensitivity indices. (surprise)

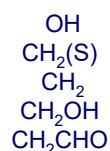
Better simulation results can be achieved, if the rate coefficients of a few reactions and the enthalpies of formation of a few species are known better (= with smaller variance)

These represent a small fraction of the total number of species/reactions.

Significant rate coefficients:



Significant enthalpies of formation:



120

Uncertainty analysis study of the laminar methane flame the points to be corrected

Which were the weak points of
the previously discussed uncertainty analysis study?

„uncertainty of the rate coefficient“ = uncertainty of Arrhenius parameter A
was considered only

What is the uncertainty of each Arrhenius parameter?

The used uncertainty parameters f were based on the direct measurements
Considering also the indirect measurements decreases the uncertainty

At the development of detailed reaction mechanisms the direct and indirect
experimental results are both considered; the nominal parameter set
contains correlations that have to be taken into account.

Considering the parameter correlations is needed

121

Topic 7: Uncertainty of the Arrhenius parameters

temperature dependence of uncertainty factor f ,

domain of uncertainty of the Arrhenius parameters,

joint uncertainty of the Arrhenius parameters,

calculation of the covariance matrix of the
Arrhenius parameters

determination of the covariance matrix of the
Arrhenius parameters from literature measurements

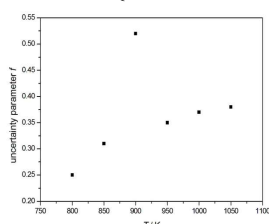
Temperature dependence of uncertainty factor f

Uncertainty parameter f is either constant (Tsang, Warnatz, Konnov)
or defined in temperature regions (Baulch *et al.* evaluations):

$$f(T) = \begin{cases} f_1 & \text{if } T \in (T_1, T_2) \\ f_2 & \text{if } T = T_3 \\ \vdots & \vdots \end{cases}$$

f_1, f_2, f_3, \dots corresponds to the actual scatter of measurements in this temperature region.

We will call them f_{original} values.

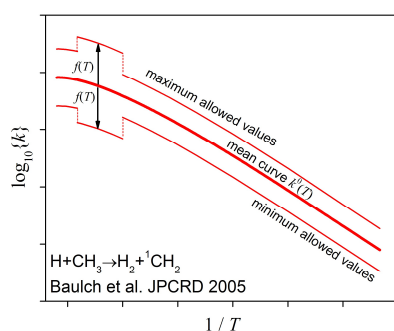


The temperature dependence of the rate coefficients imposes a relation among the uncertainty parameter f values at different temperatures.

The f_{original} values are not in accordance with the temperature dependence of the rate coefficient k

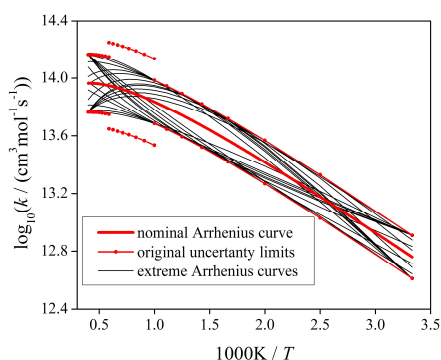
Getting consistent uncertainty factors f

Example from the Baulch *et al.* (2005) evaluation:



Solution:

Drawing the possible extreme Arrhenius curves span the realistic uncertainty limits of the rate coefficient k :



The corrected f values are called f_{extreme}

Domain of uncertainty of Arrhenius parameters

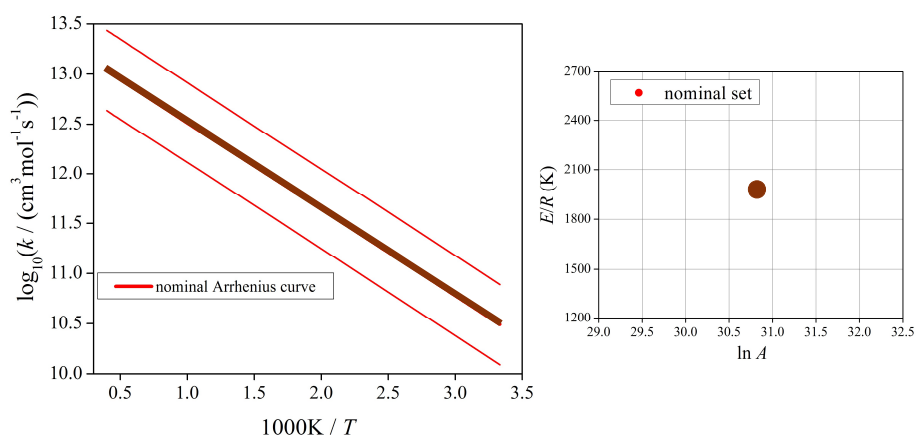
The $f_{\text{extreme}}(T)$ values define the uncertainty domain
of the rate coefficient k in interval $[T_1, T_2]$
with the temperature dependence of the rate coefficient k

The evaluations provide the uncertainty of k ,
but the real parameters of the model are Arrhenius parameters A, n, E
Better to deal with the transformed Arrhenius parameters $\ln A, n, E/R$

Statement: the extreme Arrhenius curves span
the domain of uncertainty of the Arrhenius parameters.

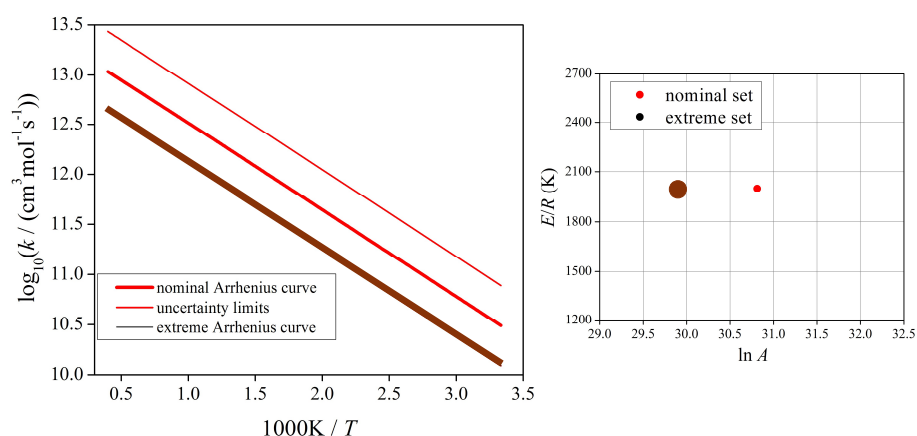
Domain of uncertainty of Arrhenius parameters

The simplest case: temperature independent uncertainty of k
two Arrhenius parameters $\ln A, E/R$



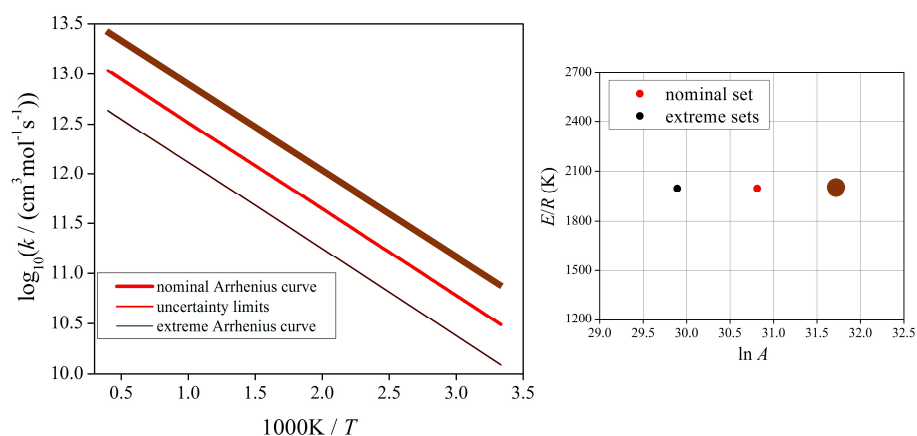
Domain of uncertainty of Arrhenius parameters

The simplest case: temperature independent uncertainty of k
two Arrhenius parameters $\ln A$, E/R



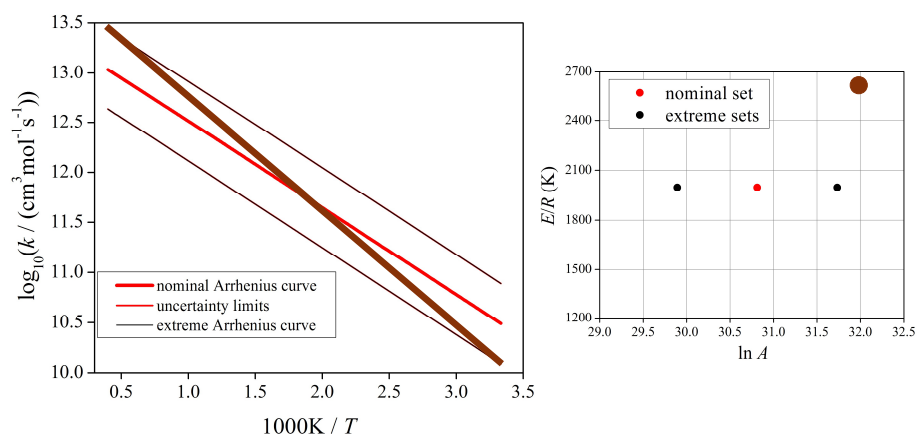
Domain of uncertainty of Arrhenius parameters

The simplest case: temperature independent uncertainty of k
two Arrhenius parameters $\ln A$, E/R



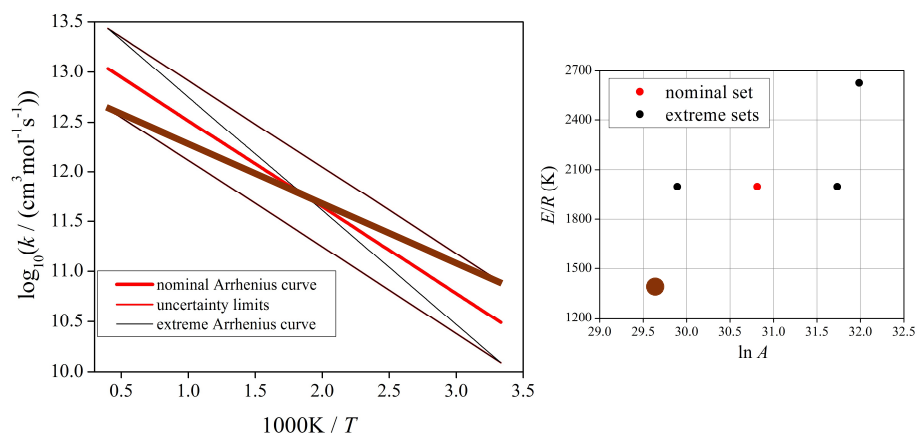
Domain of uncertainty of Arrhenius parameters

The simplest case: temperature independent uncertainty of k
two Arrhenius parameters $\ln A$, E/R



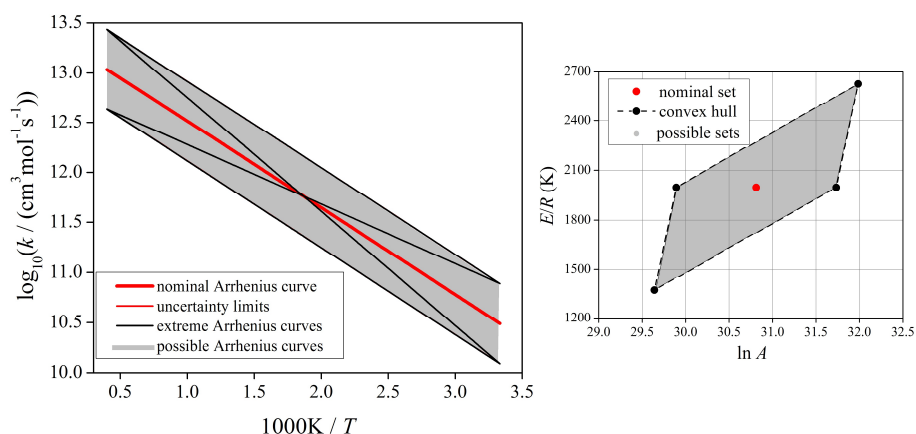
Domain of uncertainty of Arrhenius parameters

The simplest case: temperature independent uncertainty of k
two Arrhenius parameters $\ln A$, E/R



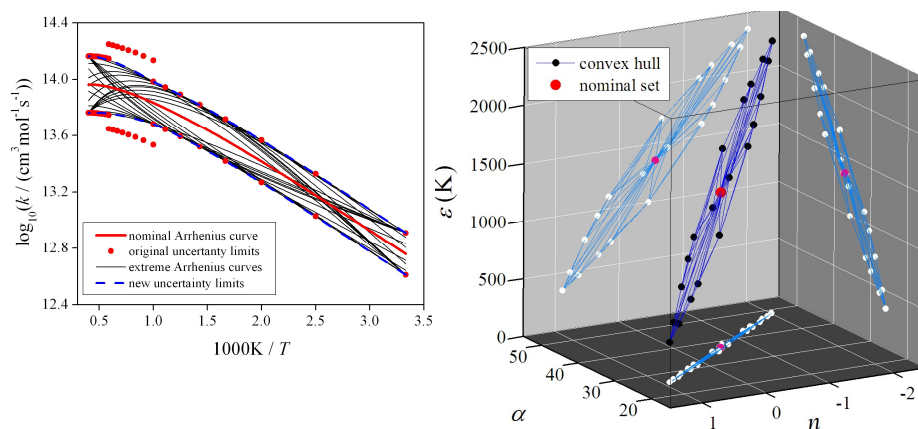
Domain of uncertainty of Arrhenius parameters

The simplest case: temperature independent uncertainty of k
two Arrhenius parameters $\ln A$, E/R



3D domain of Arrhenius parameters

The most complex case: temperature dependent uncertainty of k
three Arrhenius parameters $\alpha = \ln A$, n , $\varepsilon = E/R$
the extreme Arrhenius curves = vertices of the convex hull



Uncertainty parameter f

Definition of uncertainty factor f :

$$f(T) = \log_{10}(k^0(T)/k^{\min}(T)) = \log_{10}(k^{\max}(T)/k^0(T))$$

Calculation of the variance of $\ln k$ from uncertainty factor f :

(assuming 3σ deviation between $\log_{10} k^0$ and $\log_{10} k^{\max}$)

$$\sigma(\ln k) = \frac{\ln 10}{3} f$$

Instead of temperature dependent $\sigma(\ln k)$

the covariance matrix of the Arrhenius parameters is needed!

extended Arrhenius expression:

$$k(T) = AT^n \exp(-E/RT)$$

linearized form:

$$\frac{\ln\{k(T)\}}{\kappa(\theta)} = \underbrace{\ln\{A\}}_{\alpha} + \underbrace{n}_{n} \cdot \underbrace{\ln\{T\}}_{\theta} - \underbrace{\{E/R\}}_{\varepsilon} \cdot \underbrace{\{T\}^{-1}}_{\theta}$$

Relation between the σ of the rate coefficient and the covariance matrix of the Arrhenius parameters

Matrix-vector form of the linearized Arrhenius equation:

$$\kappa(\theta) = \mathbf{p}^T \boldsymbol{\theta}$$

$$\mathbf{p}^T := [\alpha \quad n \quad \varepsilon]$$

$$\boldsymbol{\theta}^T := [1 \quad \ln \theta \quad -\theta^{-1}]$$

The covariance matrix of the Arrhenius parameters and its relation to the uncertainty of the rate coefficient:

$$\Sigma_p = \overline{(\mathbf{p} - \bar{\mathbf{p}})(\mathbf{p} - \bar{\mathbf{p}})^T} = \begin{bmatrix} \sigma_\alpha^2 & r_{\alpha n} \sigma_\alpha \sigma_n & r_{\alpha \varepsilon} \sigma_\alpha \sigma_\varepsilon \\ r_{\alpha n} \sigma_\alpha \sigma_n & \sigma_n^2 & r_{n \varepsilon} \sigma_n \sigma_\varepsilon \\ r_{\alpha \varepsilon} \sigma_\alpha \sigma_\varepsilon & r_{n \varepsilon} \sigma_n \sigma_\varepsilon & \sigma_\varepsilon^2 \end{bmatrix}$$

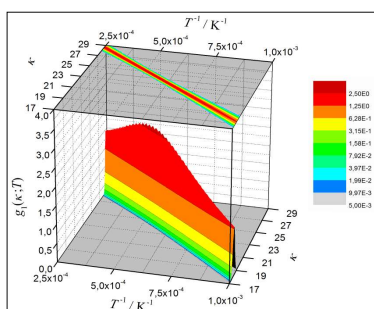
$$\sigma_\kappa(\theta) = \sqrt{\boldsymbol{\theta}^T \Sigma_p \boldsymbol{\theta}}$$

\Rightarrow the temperature dependent standard deviation of k can be calculated from a quadratic form.

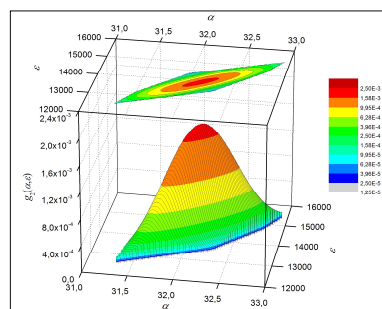
Nagy, T.; Turányi, T. Uncertainty of Arrhenius parameters
Int. J. Chem. Kinet., **43**, 359-378 (2011)

134

Example: reaction $\text{O} + \text{N}_2\text{O} \rightarrow \text{NO} + \text{NO}$



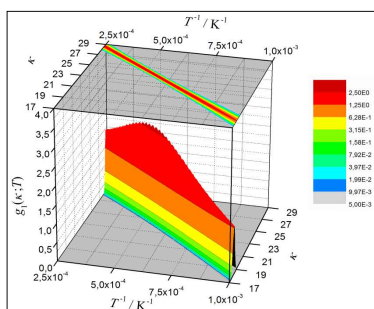
Temperature dependent
1D normal
probability density function (pdf)
of the rate coefficient
(1000 K – 4000 K)



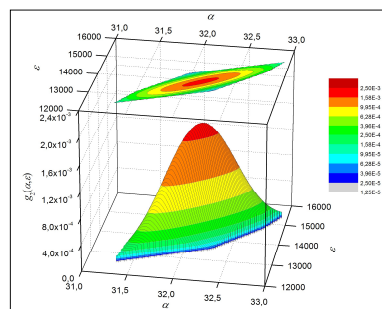
Temperature independent
multivariate joint normal
probability density function (pdf)
of the Arrhenius parameters

135

Example: reaction $\text{O} + \text{N}_2\text{O} \rightarrow \text{NO} + \text{NO}$



Temperature dependent
1D normal
probability density function (pdf)
of the rate coefficient
(1000 K – 4000 K)



Temperature independent
multivariate joint normal
probability density function (pdf)
of the Arrhenius parameters

136

Calculation of the covariance matrix of the Arrhenius parameters

$$\sigma_{\kappa}(\theta) = \sqrt{\theta^T \Sigma_p \theta}$$

For the 3-parameter Arrhenius equation:

$$\sigma_{\kappa}(\theta) = \sqrt{\sigma_{\alpha}^2 + \sigma_n^2 \ln^2 \theta + \sigma_{\varepsilon}^2 \theta^{-2} + 2r_{\alpha n} \sigma_{\alpha} \sigma_n \ln \theta - 2r_{\alpha \varepsilon} \sigma_{\alpha} \sigma_{\varepsilon} \theta^{-1} - 2r_{n \varepsilon} \sigma_n \sigma_{\varepsilon} \ln \theta \cdot \theta^{-1}}$$

variance of $\ln k$ is known
at least at 6 temperatures
(at least in 6 points)



calculation of a continuous
 $f(T)$ function



definition of the domain of
allowed A , n , E values



elements of the
covariance matrix
of Arrhenius parameters

$$\sigma_{\alpha}, \sigma_n, \sigma_{\varepsilon}, r_{\alpha n}, r_{\alpha \varepsilon}, r_{n \varepsilon}$$

Features of the uncertainty parameter f

Baulch et al. (2005):

temperature independent f (constant $f(T)$ function) about 50%

OR

a verbally defined $f(T)$ function about 50%

" $f = 0.1$ at 800 K raising to 0.2 at 2000 K "

Other sources:

NIST Chemical Kinetics Database, Tsang, Warnatz, Konnov

temperature independent f values.

Good features:

- f factors are available for several hundred reactions
- f factors are very realistic (to our experience)

Bad features:

- derivation of the f parameter is not documented
- temperature dependence is missing or not well defined
= cannot be used for the calculation of the uncertainty
of the Arrhenius parameters

⇒ Reassessment of the uncertainty parameters is needed!

https://k-evaluation.elte.hu/ website

Evaluation of high-temperature gas phase rate coefficients of elementary reactions and determination of their prior uncertainty limits

This is an interactive web site. After logging in, the users may use the database that contains Arrhenius parameters of gas phase elementary reactions determined in direct measurements, theoretical calculations or have been used in modelling studies. The users may recalculate the uncertainty limits of the rate coefficients. Please [register](#), if you want to become a user. The user status is granted by the administrator manually in two days.

You may also request to become an editor of this data base. The editors have the right to upload data sheets for new reactions and to add, delete or modify existing data sheets. The editor status may be granted to any registered user upon request to the administrator.

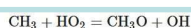
This web site was created as a part of the activity of IUPAC Task Group No. 2014-028-2-100:
"Chemical kinetics of gas-phase elementary reactions at high temperature"

The database has 169 users + 19 editors.

The database contains rate parameters for the following 208 reactions

| | | | |
|--|---|---|---|
| $\text{NCN} + \text{M} = \text{C} + \text{N}_2 + \text{M}$ | $\text{CH} + \text{C}_2\text{H}_2 = \text{products}$ | $i\text{-C}_4\text{H}_7\text{OH} = i\text{-C}_4\text{H}_7\text{OH} + \text{CH}_3$ | $n\text{-C}_4\text{H}_7\text{OH} + \text{H} = \text{C}_4\text{H}_7\text{OH} + \text{H}_2$ |
| $i\text{-C}_4\text{H}_7\text{OH} = \text{C}_2\text{H}_5 + i\text{-C}_3\text{H}_5\text{OH}$ | $i\text{-C}_4\text{H}_7\text{OH} = \text{H}_2\text{O} + i\text{-C}_4\text{H}_6$ | $i\text{-C}_4\text{H}_7\text{OH} + \text{H} = i\text{-C}_4\text{H}_7\text{OH} + \text{H}_2$ | $\text{CH} + \text{CH}_2 = \text{products}$ |
| $\text{CH} + \text{H}_2\text{O} = \text{products}$ | $\text{CH} + \text{O}_2 = \text{products}$ | $\text{NCN} + \text{NO} + \text{M} = \text{products}$ | $\text{NCN} + \text{O}_2 + \text{M} = \text{products}$ |
| $\text{NO}_2 + \text{H} = \text{NO} + \text{OH}$ | $\text{N}_2\text{O} + \text{M} = \text{N}_2 + \text{O} + \text{M}$ | $\text{N}_2\text{O} + \text{H} = \text{N}_2 + \text{OH}$ | $\text{NO} + \text{HO}_2 = \text{NO}_2 + \text{OH}$ |
| $\text{NO} + \text{H} + \text{M} = \text{HNO} + \text{M}$ | $\text{NH} + \text{NO} = \text{N}_2\text{O} + \text{H}$ | $\text{NH} + \text{OH} = \text{HNO} + \text{H}$ | $\text{HNO} + \text{H} = \text{NO} + \text{H}_2$ |
| $\text{NO} + \text{OH} + \text{M} = \text{HONO} + \text{M}$ | $\text{H} + \text{O}_2 = \text{O} + \text{OH}$ | $\text{H} + \text{O}_2 + \text{M} = \text{HO}_2 + \text{M}$ | $\text{O} + \text{H}_2 = \text{H} + \text{OH}$ |
| $\text{OH} + \text{H}_2 = \text{H}_2\text{O} + \text{H}$ | $\text{H}_2\text{O}_2 + \text{H} = \text{H}_2 + \text{HO}_2$ | $\text{H} + \text{HO}_2 = \text{OH} + \text{OH}$ | $\text{H} + \text{HO}_2 = \text{H}_2 + \text{O}_2$ |

Evaluation of a rate coefficient uncertainty



Initially uploaded on 2020-02-24 by

This datasheet is currently edited by

The content of this sheet was published in [1].

References

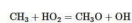
Ohm, G., Varga, T., Váró, E., Hart, S., Hase, C., Turányi, T. Development of an Ethanol Combustion Mechanism Based on a Hierarchical Optimization Approach. *Int. J. Chem. Kinet.* **2016**, *48* (8), 423–441. <https://doi.org/10.1002/kin.20998>.

Editor control panel
You are not editor of this sheet.

If you want to modify the content of this page, please request editorship.

[REQUEST EDITORSHIP](#)

The reaction in the exothermic direction:



$$\Delta_r H = -99.6 \text{ kJ mol}^{-1}$$

Reviews and modelling studies

Search

Q ...

16 of 16 items are considered. ...

| Considered | Source (s) | DOI | A | n | ERR | temp range | order | direction |
|-------------------------------------|---------------|-----|----------|------|------|------------|-------|-----------|
| <input checked="" type="checkbox"/> | Melcar, 2013 | | 1e+12 | 0.27 | -346 | 300-3000 | 2 | forward |
| <input checked="" type="checkbox"/> | Leplat, 2011 | | 8e+12 | 0 | 0 | 300-3000 | 2 | forward |
| <input checked="" type="checkbox"/> | Saxena, 2007 | | 5e+12 | 0 | 0 | 300-3000 | 2 | forward |
| <input checked="" type="checkbox"/> | Marinov, 1999 | | 7e+12 | 0 | 0 | 300-3000 | 2 | forward |
| <input checked="" type="checkbox"/> | Baulch, 2005 | | 1.81e+13 | 0 | 0 | 600-1200 | 2 | forward |

Determination of the $f(T)$ functions

We have created an interactive website
for the semiautomatic calculation of the $f(T)$ functions
(uncertainty of the rate coefficient as a function of temperature).

Major steps for a given elementary reaction in the interactive website:

- 1 collection of all direct measurements and theoretical calculations
source: NIST Chemical Kintics Database + recent reviews
- 2 forward direction: selected (direction with more data)
backward direction: converted to forward direction Arrhenius parameters
- 3 preparation of a datafile: each line one measurement/calculation
squib + temperature range + Arrhenius parameters
- 4 selection of a mean line ($\ln k - 1/T$)
in the middle of uncertainty band: almost always Baulch *et al.*, 2005
- 5 interactive elimination of outliers
- 6 calculation of „empirical“ f points at several temperatures
fitting the elements of the covariance matrix to these points
plotting the experimental/theoretical results + the recalculated $f(T)$

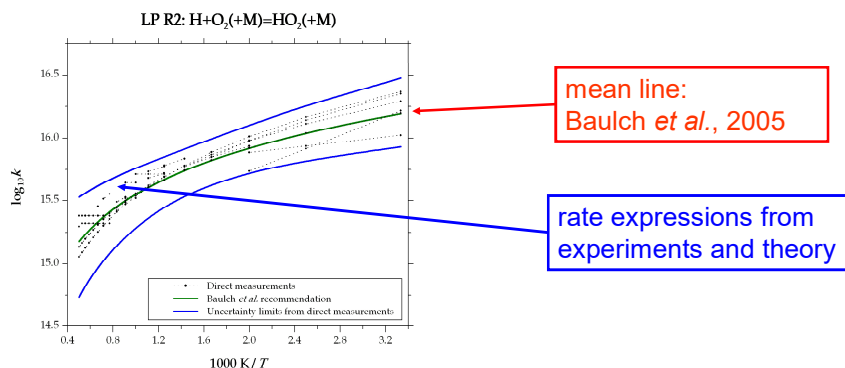
Example: reaction $\text{H} + \text{O}_2 + \text{M} = \text{HO}_2 + \text{M}$

We found about 60 experimental/theoretical rate expressions.

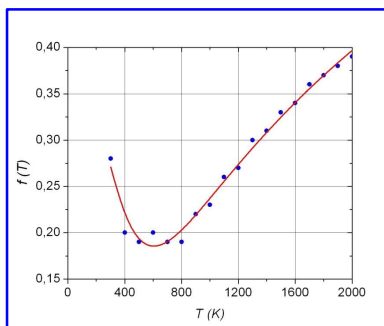
After the selection remained:

- Ar bath gas: 9 experimentally determined and
1 theoretically calculated rate coefficient expressions
- N₂ bath gas: 10 experimentally determined and
2 theoretically calculated rate coefficient expressions

used together assuming $m=0.5$ (relative collision efficiency Ar to N₂)

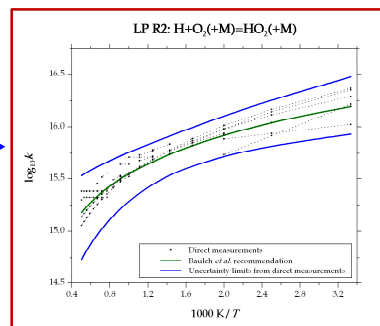


Example: reaction $\text{H} + \text{O}_2 + \text{M} = \text{HO}_2 + \text{M}$



blue dots:
distance from the extreme
experimental/theoretical values
(„empirical f points”)

red line:
calculated from the fitted
elements of the covariance matrix
 \Rightarrow *a priori* $f(T)$ function



blue line:
a priori
temperature dependent
 k^{\min} and k^{\max} bounds
calculated from the
covariance matrix
of Arrhenius parameters

Topic 8: Mechanism optimisation and determination of the posterior parameter uncertainties

steps of mechanism optimisation,

relations between the following uncertainty domains:

prior uncertainty of the input parameters,
uncertainty of the model results calculated from
the prior uncertainty of the input parameters,
uncertainty of model results measured by indirect experiments,
prior uncertainty of the input parameters,
uncertainty of the model results calculated from
the posterior uncertainty of the input parameters;

results of mechanism optimization

Uncertainty of reaction rate parameters

Reaction rate parameters:

Arrhenius parameters A , n , E ,
 3rd body collision efficiencies,
 (parameters of pressure dependence: Lindemann and Troe parameters)
 (enthalpies of formation)

a priori uncertainty of reaction rate parameters:

uncertainty of reaction rate parameters, deduced from
 available direct measurement data and theoretical calculations

a posteriori uncertainty of reaction rate parameters:

uncertainty of reaction rate parameters, deduced from fitting to
 direct measurement data + theoretical calculations results +
 indirect measurement data

145

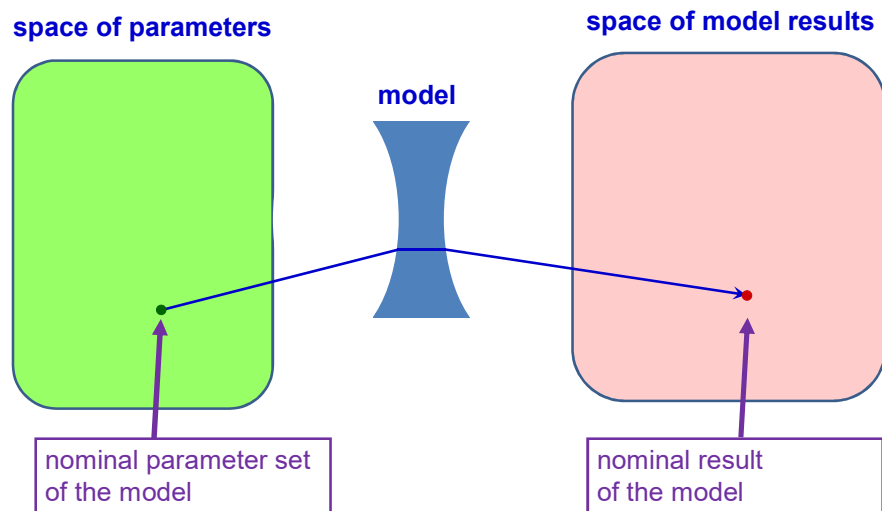
Mechanism optimisation

- 1 all indirect measurement data should be collected
that are applicable for testing a mechanism.
- 2 sensitivity analysis for finding the important reaction steps
(simulated data points with respect to the rate parameters)
the rate parameters of these reactions will be optimised
- 3 determination of the *a priori* uncertainty of the rate parameters
(= determination of the domain of allowed parameter values)
- 4 all reliable direct measurement data related to the important reactions
are collected
- 5 global parameter optimisation
considering both the indirect and direct measurement data
 ⇒ new rate parameters with physical meaning
 ⇒ *a posteriori* uncertainty domain of rate parameters

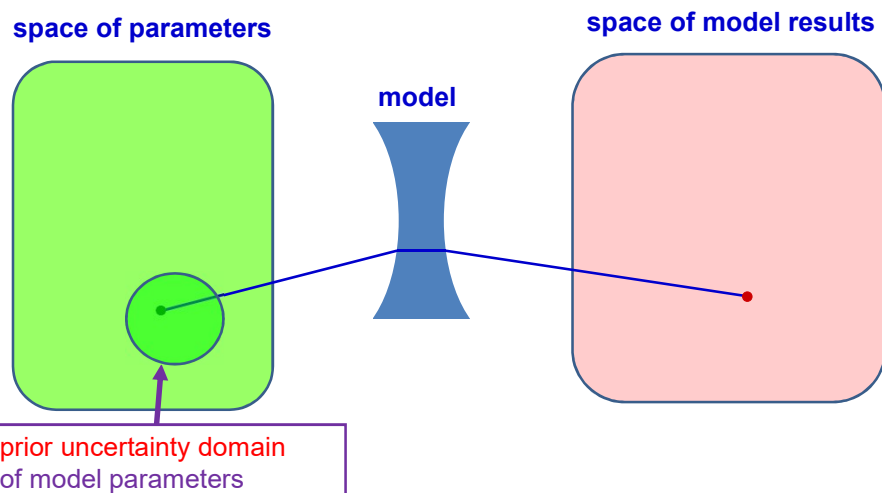
Turányi T, Nagy T, Zsély IGy, Cserhádi M, Varga T, Szabó B,
 Sedyó I, Kiss P, Zempléni A, Curran H J
 Determination of rate parameters based on both direct and indirect measurements.
Int. J. Chem. Kinet. **44**, 284–302 (2012)

146

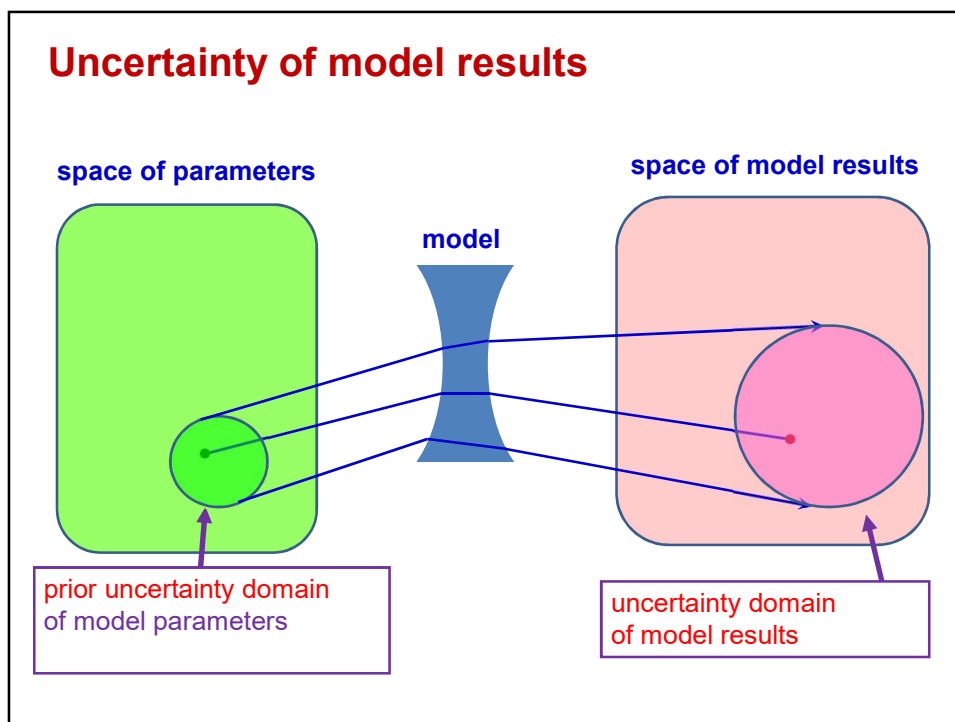
Parameters and model results



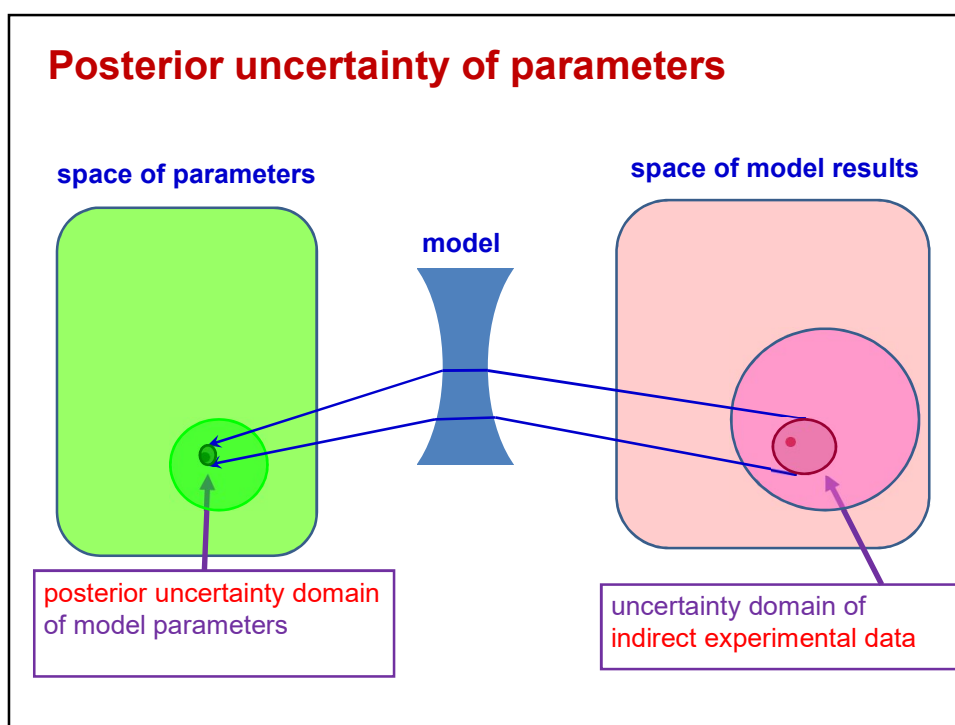
Uncertainty of model parameters



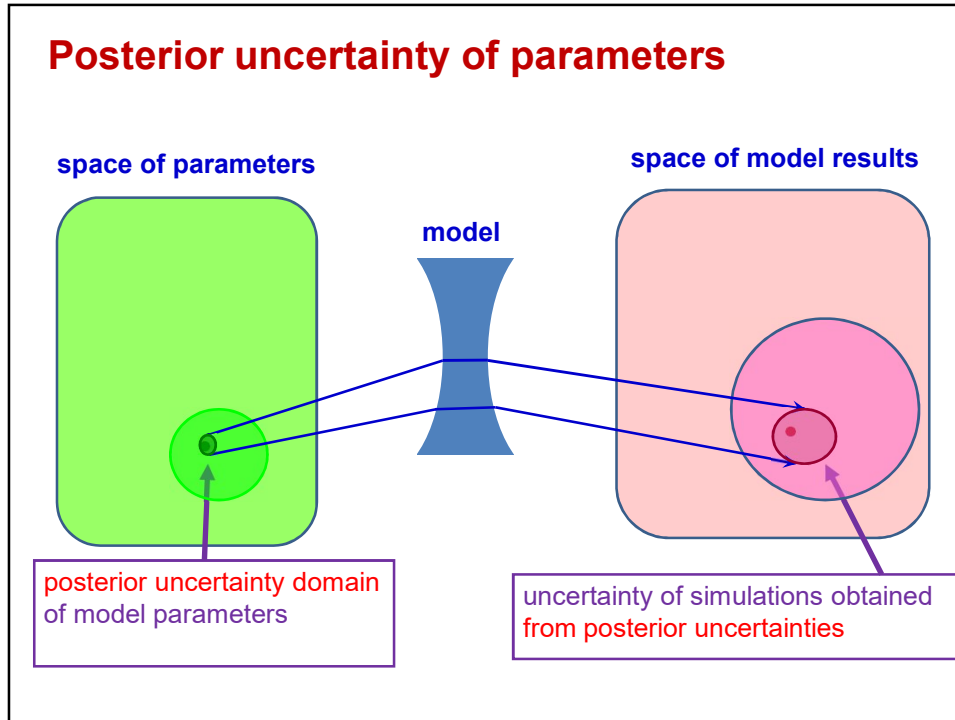
Uncertainty of model results



Posterior uncertainty of parameters



Posterior uncertainty of parameters



Optimisation and uncertainty calculation

Optimisation - minimisation of this error function by fitting the parameters **within their prior uncertainty domain**

$$E(\mathbf{p}) = \frac{1}{N} \sum_{i=1}^N \frac{1}{N_i} \sum_{j=1}^{N_i} \left(\frac{Y_{ij}^{mod}(\mathbf{p}) - Y_{ij}^{exp}}{\sigma(Y_{ij}^{exp})} \right)^2$$

Y_{ij} measured/calculated rate coefficient OR measured/calculated ignition time/flame velocity in data point j of data series i

σ standard deviation of the measured data

N_i number of data points in data series i

N number of data series (different experiments)

$$Y_{ij} = \begin{cases} y_{ij} & \text{if } \sigma(y_{ij}^{exp}) \approx \text{constant} \\ \ln y_{ij} & \text{if } \sigma(\ln y_{ij}^{exp}) \approx \text{constant} \end{cases}$$

Calculation of the covariance matrix of the estimated parameters:

Covariance matrix of experiments

Discrepancy between experiments and model

$$\Sigma_p = \left[\left(\mathbf{J}_o^T \mathbf{W} \Sigma_Y^{-1} \mathbf{J}_o \right)^{-1} \mathbf{J}_o^T \mathbf{W} \Sigma_Y^{-1} \right] (\Sigma_Y + \Sigma_\Delta) \left[\left(\mathbf{J}_o^T \mathbf{W} \Sigma_Y^{-1} \mathbf{J}_o \right)^{-1} \mathbf{J}_o^T \mathbf{W} \Sigma_Y^{-1} \right]^T$$

Results of optimisation

- **Optimised combustion model**
 - Better overall performance than any previously published model
- **Set of optimised rate parameters**
 - Optimized Arrhenius parameters
 - Optimized third body collision efficiency parameters
 - Optimized enthalpies of formation
- **Posterior covariance matrix of the optimised parameters**
 - Temperature independent
 - Uncertainty (i.e. estimated scatter) of each optimised parameter
 - Correlation coefficients between the parameter pairs

Example: optimization of a methanol and formaldehyde combustion mechanism

- **Methanol** is an alternative automotive fuel, fuel additive and feedstock in various industrial processes
- **Model system** for studies of **C₁ combustion**: important radicals include CH₂OH and CH₃O
- **Relevance** for the oxidation of higher hydrocarbons/oxygenates
- **Not all** experimentally observed **combustion characteristics** (e.g. ignition, flame propagation, speciation profiles) are **well-described** by available kinetic mechanisms

Data collection of methanol combustion

- Indirect measurements
- Direct measurements of rate coefficients
(926 data points/ 66 data sets)
- Theoretical rate determinations
(33 data sets)

| Type of measurement experimental facility | Data sets | Data points | p / atm | T / K |
|--|-----------|---------------|-----------|-----------|
| Ignition delay times | 81 | 574 | | |
| Shock tube | 67 | 421 | 0.3–51.7 | 963–2180 |
| Shock tube (CH ₂ O) | 7 | 99 | 1.6 | 1363–2304 |
| Rapid compression machine | 7 | 54 | 9.3–40.6 | 817–980 |
| Burning velocity measurements | 87 | 632 | | |
| Outwardly/ spherically propagating flame | 35 | 170 | 0.5–9.9 | 298–500 |
| Counterflow twin-flame | 5 | 90 | 1 | 298–368 |
| Heat flux method / laminar flat flame | 41 | 280 | 0.2–1 | 298–358 |
| Flame-cone method | 6 | 92 | 1 | 298–413 |
| Concentration measurements | 97 | 23,694 | | |
| Flow reactor concentration–time profiles | 18 | 1,452 | 1–20 | 752–1043 |
| Flow reactor conc.–time profiles (CH ₂ O) | 13 | 462 | 1–6 | 852–1095 |
| Flow reactor outlet concentrations | 13 | 444 | 1–98.7 | 600–1443 |
| Flow reactor outlet concentrations (CH ₂ O) | 3 | 156 | 1.05 | 712–1279 |
| Jet-stirred reactor outlet concentrations | 9 | 711 | 1–20 | 697–1200 |
| Shock tube concentration–time profiles | 14 | 12,756 | 0.3–2.5 | 1266–2100 |
| Shock tube conc.–time profiles (CH ₂ O) | 27 | 7,713 | 1.5–2.0 | 1244–1907 |

Initial mechanism for optimization

Starting point: CH₃OH/CH₂O/CO mechanism of Li *et al.* (2007)

J. Li; Z. W. Zhao; A. Kazakov; M. Chaos; F. L. Dryer; J. J. Scire Jr.,
Int. J. Chem. Kinet. 39 (2007) 109–136

Update of rate coefficients in the H₂/CO sub-mechanism

using values from our recently optimized joint hydrogen and syngas mechanism

T. Varga; C. Olm; T. Nagy; I. Gy. Zsély; É. Valkó; R. Pálvölgyi;
H.J. Curran; T. Turányi, *Int. J. Chem. Kinet.* 48 (2016) 407–422

Further modifications:

- Thermochemistry updated
S. M. Burke; J. M. Simmie; H. J. Curran,
J. Phys. Chem. Ref. Data 44 (2015) 013101
Burcat database (March 13, 2015)
- CH₃OH+HÖ₂ = CH₃Ö+H₂O₂
abstraction channel added
S. J. Klippenstein; L. B. Harding; M. J. Davis; A. S. Tomlin;
R. T. Skodje, *Proc. Combust. Inst.* 33 (2011) 351–357

Local sensitivity analysis

Important reactions in formaldehyde and methanol combustion

Brute force method (parameters varied by +5%) using the initial mechanism, shown: ($|S|_{\text{avg}} \geq 0.1$)

CH₃OH shock tube IDTs

| | |
|---|------|
| CH ₃ OH+H ₂ O ₂ = CH ₃ OH+H ₂ O ₂ | 0.80 |
| OH+OH(+M) = H ₂ O ₂ (+M) | 0.54 |
| H+O ₂ = O+OH | 0.41 |
| OH+CH ₃ (+M) = CH ₃ OH(+M) | 0.26 |
| CH ₃ OH+OH = CH ₃ O+H ₂ O | 0.24 |
| CH ₃ OH+H = CH ₃ OH+H ₂ | 0.20 |
| H ₂ O ₂ +H ₂ O = H ₂ O ₂ +O ₂ | 0.18 |
| HCO ₂ +OH = H ₂ O+O ₂ | 0.17 |
| H+H ₂ O = H ₂ +O ₂ | 0.14 |
| HCO(+M) = H+CO(+M) | 0.12 |
| OH+CH ₃ (+M) = CH ₃ OH(+M) | 0.11 |
| CH ₃ OH+O ₂ = CH ₃ OH+H ₂ O ₂ | 0.10 |
| CH ₃ OH+OH = CH ₃ OH+H ₂ O | 0.10 |

CH₂O shock tube IDTs

| | |
|---|------|
| HCO(+M) = H+CO(+M) | 0.86 |
| HCO+H ₂ O ₂ = HCO+H ₂ O ₂ | 0.53 |
| CH ₂ O+O ₂ = HCO+HO ₂ | 0.43 |
| CH ₂ O+H = HCO+H ₂ | 0.42 |
| H+O ₂ = O+OH | 0.41 |
| HCO+O ₂ = CO+HO ₂ | 0.40 |
| CH ₂ O+H = HCO+H ₂ | 0.32 |
| OH+OH(+M) = H ₂ O ₂ (+M) | 0.23 |
| HCO+H = CO+H ₂ | 0.18 |
| CH ₂ O+OH = HCO+H ₂ O | 0.16 |
| CH ₂ OH+HCO = CH ₂ O+CH ₂ O | 0.15 |
| CH ₂ O+M = CO+H ₂ +M | 0.13 |
| CH ₂ O+O = HCO+OH | 0.12 |
| CH ₂ O+CH ₃ = HCO+CH ₄ | 0.10 |
| H+HO ₂ = H ₂ +O ₂ | 0.10 |
| CH ₂ OH+M = CH ₂ O+H+M | 0.10 |

CH₃OH RCM IDTs

| | |
|---|------|
| CH ₃ OH+H ₂ O ₂ = CH ₃ OH+H ₂ O ₂ | 1.00 |
| OH+OH(+M) = H ₂ O ₂ (+M) | 0.55 |
| OH+OH(+M) = H ₂ O ₂ (+M) | 0.31 |
| H ₂ O ₂ +H ₂ O = H ₂ O ₂ +O ₂ | 0.28 |
| H ₂ O ₂ +H ₂ O = H ₂ O ₂ +O ₂ | 0.19 |
| CH ₃ O+HO ₂ = HCO+H ₂ O ₂ | 0.13 |
| CH ₃ OH+O ₂ = CH ₃ OH+H ₂ O ₂ | 0.10 |

CH₃OH burning velocities

| | |
|--|------|
| H+O ₂ = O+OH | 0.99 |
| HCO(+M) = H+CO(+M) | 0.60 |
| CO+OH = CO ₂ +H | 0.52 |
| H ₂ O+H = OH+OH | 0.38 |
| CH ₃ OH+OH = CH ₃ O+H ₂ O | 0.35 |
| H ₂ O+OH = H ₂ O+O ₂ | 0.32 |
| H+H ₂ O = H ₂ +O ₂ | 0.30 |
| HCO+O ₂ = CO+HO ₂ | 0.29 |
| H+OH+M = H ₂ O+M | 0.23 |
| H+O ₂ (+M) = HO ₂ (+M) | 0.23 |
| HCO+OH = CO+H ₂ O | 0.18 |
| CH ₃ O+M = CH ₂ O+H+M | 0.18 |
| OH+OH(+M) = H ₂ O ₂ (+M) | 0.17 |
| CH ₃ OH+H = CH ₃ OH+H ₂ | 0.16 |
| OH+H ₂ = H+H ₂ O | 0.15 |
| HCO+H = CO+H ₂ | 0.14 |

CH₃OH speciation data

| | |
|---|------|
| CH ₃ OH+H ₂ O ₂ = CH ₃ OH+H ₂ O ₂ | 0.36 |
| CH ₃ OH+OH = CH ₃ O+H ₂ O | 0.29 |
| CH ₃ OH+O ₂ = CH ₃ OH+H ₂ O ₂ | 0.25 |
| CH ₃ OH+OH = CH ₃ OH+H ₂ O | 0.25 |
| OH+OH(+M) = H ₂ O ₂ (+M) | 0.23 |
| H ₂ O ₂ +OH = H ₂ O+O ₂ | 0.23 |
| CH ₂ O+OH = HCO+H ₂ O | 0.21 |
| H ₂ O+H ₂ O = H ₂ O ₂ +O ₂ | 0.20 |
| H+O ₂ = O+OH | 0.20 |
| CO+OH = CO ₂ +H | 0.20 |
| CH ₃ O+M = CH ₂ O+H+M | 0.20 |
| CH ₃ OH+H = CH ₃ OH+H ₂ | 0.19 |
| CH ₃ O+HO ₂ = HCO+H ₂ O ₂ | 0.19 |
| CH ₃ +HO ₂ = CH ₂ +O ₂ | 0.18 |
| H+O ₂ (+M) = HO ₂ (+M) | 0.18 |
| CH ₂ OH+M = CH ₂ O+H+M | 0.17 |
| HCO(+M) = H+CO(+M) | 0.16 |
| CH ₂ +H = HCO+H ₂ | 0.16 |
| CH ₂ +HO ₂ = CH ₂ O+OH | 0.15 |
| HO ₂ +HO ₂ = H ₂ O ₂ +O ₂ | 0.15 |
| OH+CH ₃ (+M) = CH ₃ OH(+M) | 0.15 |

CH₂O speciation data

| | |
|--|------|
| HCO(+M) = H+CO(+M) | 0.46 |
| CH ₂ O+H = HCO+H ₂ | 0.38 |
| CH ₂ O+O ₂ = HCO+HO ₂ | 0.34 |
| HCO+O ₂ = CO+HO ₂ | 0.30 |
| CH ₂ O+HO ₂ = HCO+H ₂ O ₂ | 0.30 |
| CH ₂ O+M = CO+H ₂ +M | 0.27 |
| CH ₂ OH+HCO = CH ₂ O+CH ₂ O | 0.27 |
| CH ₂ OH+M = CH ₂ O+H+M | 0.19 |
| CH ₂ OH+HCO = CH ₂ OH+CH ₂ O | 0.19 |
| OH+OH(+M) = H ₂ O ₂ (+M) | 0.17 |
| H+O ₂ = O+OH | 0.17 |
| CH ₂ O+M = HCO+H+M | 0.17 |
| CH ₂ O+OH = HCO+H ₂ O | 0.13 |
| CO+OH = CO ₂ +H | 0.13 |
| CH ₂ O+O = HCO+OH | 0.12 |
| OH+OH(+M) = H ₂ O ₂ (+M) | 0.12 |
| HCO+HO ₂ = CO ₂ +H+OH | 0.12 |
| HO ₂ +H = OH+OH | 0.12 |
| HO ₂ +OH = H ₂ O+O ₂ | 0.12 |
| HO ₂ +HO ₂ = H ₂ O ₂ +O ₂ | 0.11 |
| HCO(+M) = H+CO(+M) | 0.11 |
| CH ₂ OH+O ₂ = CH ₂ O+HO ₂ | 0.11 |
| HCO+H = CO+H ₂ | 0.11 |
| HO ₂ +HO ₂ = H ₂ O ₂ +O ₂ | 0.10 |

Optimized reactions (this work)

Already optimized H₂/CO reactions

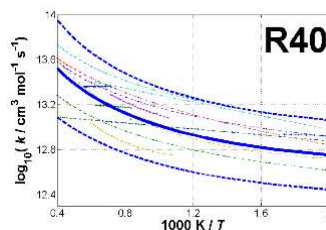
Not optimized reactions

Mechanism optimization

57 Arrhenius parameters of 17 reactions optimized

| No. | Reaction | f_{prior} |
|---------|--|--------------------|
| R14/R15 | H ₂ O ₂ +H ₂ O ₂ = H ₂ O ₂ +O ₂ | 0.30–0.70 |
| R37 LPL | CH ₂ O+M = CO+H ₂ +M | 0.50 |
| R38 | CH ₂ O+H = HCO+H ₂ | 0.60 |
| R40 | CH ₂ O+OH = HCO+H ₂ O | 0.34–0.43 |
| R41 | CH ₂ O+O ₂ = HCO+HO ₂ | 1.20 |
| R47 | CH ₃ +H ₂ O ₂ = CH ₃ O+OH | 0.46–0.76 |
| R53 | CH ₃ +H ₂ O ₂ = CH ₄ +O ₂ | 1.00 |
| R60 | CH ₂ OH+O ₂ = CH ₂ O+HO ₂ | 0.50 |
| R67 LPL | CH ₃ O+M = CH ₂ O+H+M | 0.84–1.24 |
| R77 HPL | OH+CH ₃ = CH ₃ OH | 0.34–0.84 |
| R77 LPL | OH+CH ₃ +M = CH ₃ OH+M | 1.20 |
| R80 | CH ₃ OH+H = CH ₂ OH+H ₂ | 0.44–1.07 |
| R81 | CH ₃ OH+H = CH ₃ O+H ₂ | 1.70 |
| R83 | CH ₃ OH+OH = CH ₃ O+H ₂ O | 0.70 |
| R84 | CH ₃ OH+OH = CH ₂ OH+H ₂ O | 0.46–0.87 |
| R85 | CH ₃ OH+O ₂ = CH ₂ OH+HO ₂ | 0.80 |
| R87 | CH ₃ OH+HO ₂ = CH ₂ OH+H ₂ O ₂ | 1.10 |
| R88 | CH ₃ OH+HO ₂ = CH ₃ O+H ₂ O ₂ | 0.70 |

T. Nagy; É. Valkó; I. Sedyó; I. Gy. Zsély; M. J. Pilling;
T. Turányi, *Combust. Flame* 162 (2015) 2059–2076



Mechanism optimization 2

Optimization targets:

- 517 Shock tube, 59 RCM ignition delay points
- 153 Laminar burning velocity points
- 2,508 Flow reactor species concentration points
- 706 Jet-stirred reactor species concentration points
- 20,460 Shock tube species concentration points
- 926 Direct measurements of reaction rate coefficients
- 33 Theoretical determinations of reaction rate coefficients

Polynomial surrogate model ("response surfaces")

used for computationally expensive **flame simulations**

Hierarchical optimization strategy:

Step-by-step inclusion of reactions and optimization targets

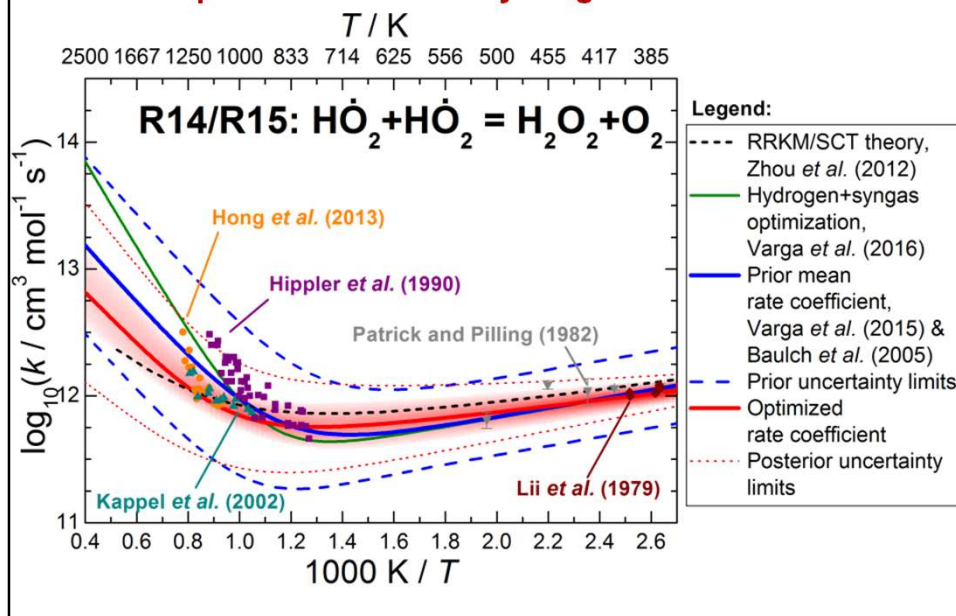
Mechanism optimization results

| No. | Reaction | f_{prior} | $f_{\text{posterior}}$ | $f_{\text{posterior+H}_2/\text{CO}}$ | | When also considering all sensitive H ₂ /CO reactions: |
|---------|---|--------------------|------------------------|--------------------------------------|---|--|
| R14/R15 | $\text{HO}_2 + \text{HO}_2 = \text{H}_2\text{O}_2 + \text{O}_2$ | 0.30–0.70 | 0.08–0.71 | 0.09–0.57 | ↘ | |
| R37 LPL | $\text{CH}_2\text{O} + \text{M} = \text{CO} + \text{H}_2 + \text{M}$ | 0.50 | 0.09–0.12 | 0.09–0.12 | → | |
| R38 | $\text{CH}_2\text{O} + \text{H} = \text{HCO} + \text{H}_2$ | 0.60 | 0.08–0.10 | 0.09–0.11 | → | |
| R40 | $\text{CH}_2\text{O} + \text{OH} = \text{HCO} + \text{H}_2\text{O}$ | 0.34–0.43 | 0.22–0.30 | 0.19–0.27 | ↘ | |
| R41 | $\text{CH}_2\text{O} + \text{O}_2 = \text{HCO} + \text{HO}_2$ | 1.20 | 0.19–0.20 | 0.18–0.20 | → | |
| R47 | $\dot{\text{C}}\text{H}_3 + \text{HO}_2 = \text{CH}_3\dot{\text{O}} + \text{OH}$ | 0.46–0.76 | 0.26–0.49 | 0.26–0.38 | ↘ | |
| R53 | $\dot{\text{C}}\text{H}_3 + \text{HO}_2 = \text{CH}_4 + \text{O}_2$ | 1.00 | 0.25–0.45 | 0.25–0.32 | ↘ | |
| R60 | $\dot{\text{C}}\text{H}_2\text{OH} + \text{O}_2 = \text{CH}_2\text{O} + \text{HO}_2$ | 0.50 | 0.27–0.38 | 0.27–0.33 | ↘ | |
| R67 LPL | $\text{CH}_3\dot{\text{O}} + \text{M} = \text{CH}_2\text{O} + \text{H} + \text{M}$ | 0.84–1.24 | 0.16–0.26 | 0.16–0.21 | → | |
| R77 HPL | $\text{OH} + \dot{\text{C}}\text{H}_3 = \text{CH}_3\text{OH}$ | 0.34–0.84 | 0.20–0.31 | 0.19–0.28 | ↘ | |
| R77 LPL | $\text{OH} + \dot{\text{C}}\text{H}_3 + \text{M} = \text{CH}_3\text{OH} + \text{M}$ | 1.20 | 0.07–0.39 | 0.07–0.27 | ↘ | |
| R80 | $\text{CH}_3\text{OH} + \text{H} = \dot{\text{C}}\text{H}_2\text{OH} + \text{H}_2$ | 0.44–1.07 | 0.18–0.27 | 0.17–0.24 | → | |
| R81 | $\text{CH}_3\text{OH} + \text{H} = \text{CH}_3\dot{\text{O}} + \text{H}_2$ | 1.70 | 0.24–0.38 | 0.24–0.31 | → | |
| R83 | $\text{CH}_3\text{OH} + \text{OH} = \text{CH}_3\dot{\text{O}} + \text{H}_2\text{O}$ | 0.70 | 0.13–0.44 | 0.12–0.25 | ↘ | |
| R84 | $\text{CH}_3\text{OH} + \text{OH} = \dot{\text{C}}\text{H}_2\text{OH} + \text{H}_2\text{O}$ | 0.46–0.87 | 0.19–0.41 | 0.18–0.40 | → | |
| R85 | $\text{CH}_3\text{OH} + \text{O}_2 = \dot{\text{C}}\text{H}_2\text{OH} + \text{HO}_2$ | 0.80 | 0.78–1.01 | 0.72–0.91 | ↘ | |
| R87 | $\text{CH}_3\text{OH} + \text{HO}_2 = \dot{\text{C}}\text{H}_2\text{OH} + \text{H}_2\text{O}_2$ | 1.10 | 0.20–0.25 | 0.16–0.21 | ↘ | |
| R88 | $\text{CH}_3\text{OH} + \text{HO}_2 = \text{CH}_3\dot{\text{O}} + \text{H}_2\text{O}_2$ | 0.70 | 0.15–0.42 | 0.15–0.26 | ↘ | |

and the corresponding
H₂/CO data

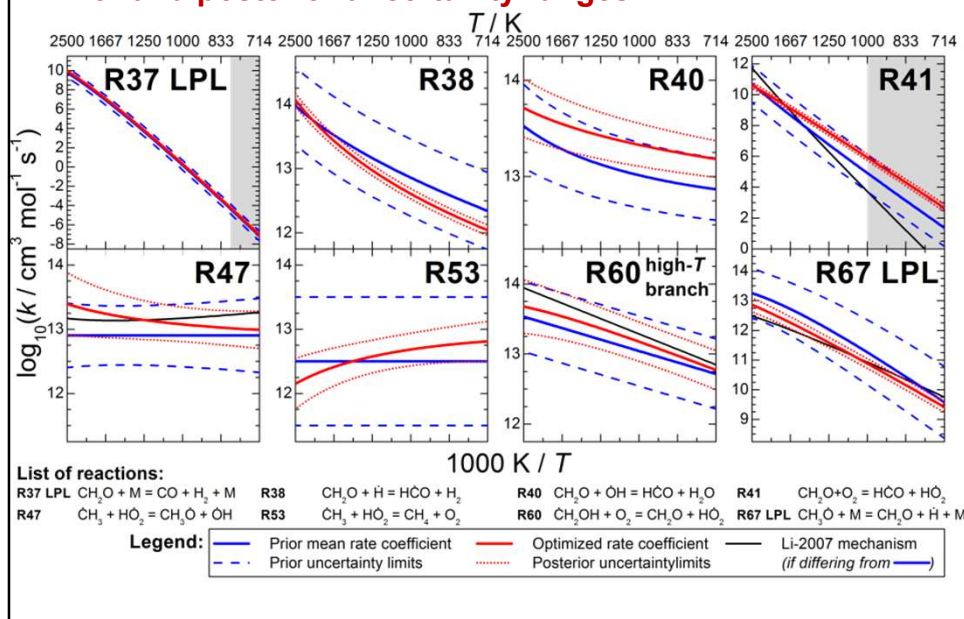
Arrhenius plots (I)

Prior and posterior uncertainty ranges



Arrhenius plots (II)

Prior and posterior uncertainty ranges



Mechanism comparison results

Error function values for each type of data and overall

| Mechanism | Ignition delay times | | Average error function value | | Concentration profiles | | Overall |
|---------------------|----------------------|-------------------|------------------------------|--------------------|------------------------|----------------------|----------------------|
| | CH ₃ OH | CH ₂ O | Burning velocities | CH ₃ OH | CH ₃ OH | CH ₂ O | |
| AAU-2008 | 28.4 | 2.6 | no transport | 21.3 | 18.9 | — | — |
| Alzueta-2001 | 103.9 ^a | 11.3 | no transport | 32.1 | 15.9 | — | — |
| Christensen-2016 | 35.4 | 3.3 | 5.2 | 15.7 | 8.4 | 16.3 | 16.3 |
| Hamdane-2012 | 41.2 | 6.4 | (72.2) | 109.6 | 12.9 | (59.8) | (59.8) |
| Klippenstein-2011 | 131.8 | 3.4 | 1.7 | 14.9 | 6.4 | 41.5 | 41.5 |
| Li-2007 | 7.6 | 3.4 | 1.9 | 14.8 | 6.4 | 6.9 | 6.9 |
| Rasmussen-2008 | 32.2 | 5.2 | 17.9 | 40.9 | 12.3 | 25.3 | 25.3 |
| CaltechMech2.3-2015 | 51.4 | 2.5 | 3.0 | 15.9 | 6.4 | 19.7 | 19.7 |
| Johnson-2009 | 11.8 | 10.9 | no transport | 19.9 | 13.1 | — | — |
| Kathrotia-2011 | 10.7 | 8.2 | [3.0] | 60.9 | 43.0 | [23.6] | [23.6] |
| Konnov-2009 | 54.6 | 7.5 | [76.0] | 25.6 ^b | 37.2 | [51.7] ^b | [51.7] ^b |
| Leplat-2011 | 410.5 ^a | 6.1 | 22.2 | 52.6 | 38.1 | 131.6 ^a | 131.6 ^a |
| Marinov-1999 | 260.7 | 20.7 | (14.1) | 36.7 | 30.4 | (90.4) | (90.4) |
| SanDiego-2014 | 24.7 | 1.6 | 3.8 | 31.4 | 10.0 | 16.2 | 16.2 |
| SaxenaWilliams-2007 | 86.2 | 1.7 | 2.3 | 17.3 | 9.6 | 30.0 | 30.0 |
| USC-II-2007 | 602.8 ^a | 2.3 | (8.5) | 27.8 | 19.1 | (178.4) ^a | (178.4) ^a |
| Aramco1.3-2013 | (41.3) | (11.1) | (4.3) | (16.0) | (12.7) | (18.6) | (18.6) |
| NUIG-16.09-2016 | (51.6) | (11.0) | (4.2) | (20.0) | (12.4) | (22.2) | (22.2) |
| Initial mechanism | 8.1 | 2.3 | 2.1 | 15.1 | 12.4 | 8.1 | 8.1 |
| Optimized mechanism | 6.8 | 2.0 | 1.6 | 12.0 | 6.3 | 5.9 | 5.9 |
| No. of data sets | 74 | 7 | 87 | 54 | 43 | 265 | 265 |
| No. of data points | 475 | 99 | 632 | 15,363 | 8,331 | 24,900 | 24,900 |

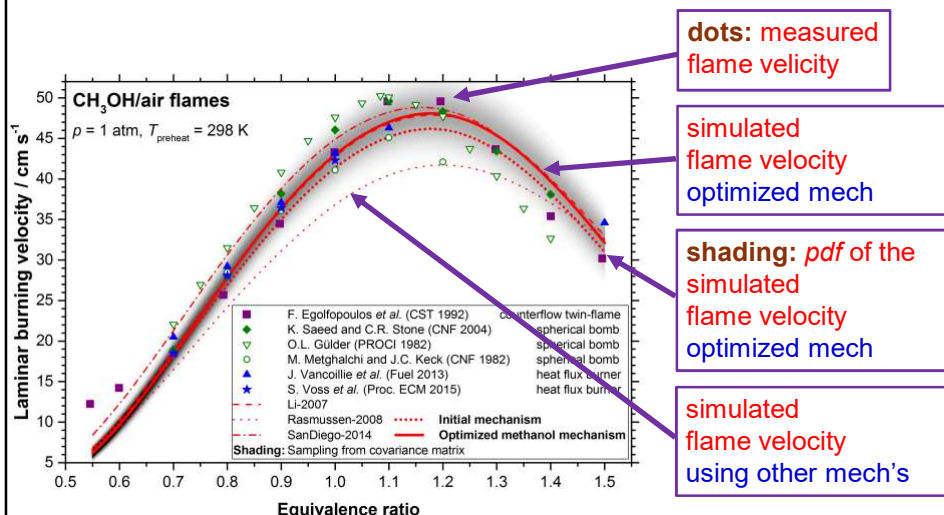
$$E = \frac{1}{N} \sum_{i=1}^N \frac{1}{N_i} \sum_{j=1}^{N_i} \left(\frac{Y_{ij}^{\text{mod}} - Y_{ij}^{\text{exp}}}{\sigma(Y_{ij}^{\text{exp}})} \right)^2$$

$E = 9$: data can be described within a 3σ uncertainty

Improvement
for all types
of data!

Comparison of simulation results

Propagation of rate coefficient posterior uncertainties



Summary

- **New optimized mechanism** for **methanol** and **formaldehyde combustion** simulations
- **Best reproduction** of indirect experimental data, while optimized rate coefficients are **consistent with direct measurements** and **theoretical calculations** within their uncertainty limits
- Determination of the **posterior uncertainty domain** of the rate parameters

C. Olm, T. Varga, É. Valkó, H. J. Curran, T. Turányi:
Uncertainty quantification of a newly optimized methanol and formaldehyde combustion mechanism
Combust. Flame, **186**, 45-64 (2017)

Topic 9: Time-scale analysis

Lifetime and its interpretation for various systems,
stiff systems, slow and fast variables,
slow manifolds in dynamical systems,
modes, calculation of the dynamical dimension,
stability analysis of stationary and dynamic systems

Lifetimes and time scales

Half life:

Time period needed for the concentration of a species to decrease to $\frac{1}{2}$, if during this time it is not produced and the concentrations of all other species remains identical.

Lifetime:

Time period needed for the concentration of a species to decrease to $1/e$, if during this time it is not produced and the concentrations of all other species remains identical.

Single first order reaction : $Y = Y_0 e^{-kt}$

$A \rightarrow P$

$$\text{lifetime: } \tau = \frac{1}{k} \qquad \text{half life: } \tau_{1/2} = \frac{\ln 2}{k}$$

Several first order reactions

(e.g. in photochemistry the reactions of an excited species):

$A \rightarrow P_1$

$\rightarrow P_2$

$\rightarrow P_3$

$$Y = Y_0 e^{-(k_1+k_2+k_3)t}$$

$$\text{lifetime: } \tau = \frac{1}{(k_1 + k_2 + k_3)}$$

Lifetime

Atmospheric chemistry:

small radical concentrations \Rightarrow radical-radical reactions are missing
(e.g. $2 \text{CH}_3 \rightarrow \text{C}_2\text{H}_6$) \Rightarrow no Y_i^2 type terms in the kinetic system of ODEs

P_i effect of producing steps

L_i effect of consuming steps

Production rate of Y_i :

$$dY_i/dt = P_i - L_i Y_i$$

Y_i lifetime:

$$\tau = \frac{1}{L_i}$$

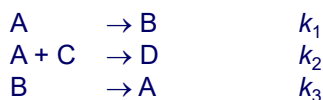
General reaction mechanism:

$$Y_i \text{ lifetime: } \tau = -\frac{1}{j_{ii}} \quad \text{where } j_{ii} = \frac{\partial f_i}{\partial Y_i}$$

j_{ii} is the i^{th} diagonal element of the Jacobian

168

Example



Production rate of species A :

$$da/dt = -k_1 a - k_2 ac + k_3 b$$

$$da/dt = k_3 b - (k_1 + k_2 c) a$$

„Atmospheric chemical" lifetime:

$$dY_i/dt = P_i - L_i Y_i \quad \tau_A = 1/L_A = 1/(k_1 + k_2 c)$$

General lifetime:

$$j_{AA} = \frac{\partial (da/dt)}{\partial a} = -(k_1 + k_2 c) \quad \tau_A = -1/j_{AA} = 1/(k_1 + k_2 c)$$

169

Slow variables and fast variables

The concentration of a single species is changed by $\Delta y'_i$
and the concentration change of the other species is negligible:

$$\Delta y'_i(t) = \Delta y'_i{}^0 e^{j_{ii} t}$$

short lifetime species = the effect of perturbation decreases rapidly =
the perturbed trajectory converges very fast to the the original trajectory

⇒ **fast variable**

long lifetime species = the effect of perturbation does not decrease rapidly
= the original and the perturbed trajectory are „parallel"

⇒ **slow variable**

Consequences:

- fast variables „forget" their initial value
- the values of fast variables are determined by the values of the other variables
- the „slow/fast variable" classification is independent of the actual change of the variables in time (dY_i/dt)

170

Eigenvector-eigenvalue decomposition of the Jacobian

$$\Lambda = \mathbf{W} \mathbf{J} \mathbf{V} \quad \mathbf{J} = \left\{ \frac{\partial f_i}{\partial Y_j} \right\}$$

Λ diagonal matrix that contains the eigenvalues (complex eigenvalues!)

\mathbf{W} matrix of left eigenvectors (row vectors)

\mathbf{V} matrix of right eigenvectors (column vectors)

denote \mathbf{W}_f the matrix of left eigenvectors, related to small negative $\text{Re}(\lambda)$
(„eigenvectors related to fast directions”)

Features: the left and right eigenvectors are orthonormed:

$$\mathbf{I} = \mathbf{W} \mathbf{V} \quad \mathbf{I} = \mathbf{V} \mathbf{W} \quad \text{therefore:} \quad \mathbf{J} = \mathbf{V} \Lambda \mathbf{W}$$

171

Stiff systems 1

The eigenvalues define the time scales of a model: $t_i = 1/|\text{Re}(\lambda_i)|$

Very different time scales \Rightarrow stiff mathematical models

Mathematicians' definition of stiffness:

the ratio of the longest and shortest time scale

stiffness ratio S_1

$$S_1 = \frac{1}{\min_i |\text{Re}(\lambda_i)|} \quad / \quad \frac{1}{\max_i |\text{Re}(\lambda_i)|}$$

longest time scale shortest time scale

$$S_1 = \max_i |\text{Re}(\lambda_i)| / \min_i |\text{Re}(\lambda_i)|$$

Gear, C. W., Numerical Initial-Value Problems in Ordinary Differential Equations,
Englewood Cliffs: Prentice Hall, 1971

172

Stiff systems 2

Physicists' and chemists' definition of stiffness:
the ratio of the characteristic („typical”) time scale and the shortest time scale

stiffness ratio S_2

$$S_2 = \frac{\tau}{\frac{1}{\max_i |\operatorname{Re}(\lambda_i)|}}$$

characteristic time scale shortest time scale

$$\text{stiffness ratio } S_2 = \tau \max_i |\operatorname{Re}(\lambda_i)|$$

τ is the characteristic time scale of the system

A model is considered stiff, if the stiffness ratio is large (e.g. 10^8 - 10^{12})

The stiff systems of differential equations:

- ⇒ can be solved with special algorithms only
(„backward differentiation formulas”, „implicit solvers”)
- ⇒ stiffness changes with changing concentrations

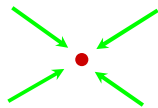
173

Stability analysis of a stationary system

differential equation of the system $d\mathbf{Y}/dt = \mathbf{f}(\mathbf{Y}, \mathbf{p})$

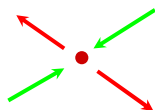
in the stationary point $d\mathbf{Y}/dt = \mathbf{0}$

Stable stationary point: we move it out, goes back



Jacobian $\mathbf{J} = \begin{Bmatrix} \frac{\partial f_i}{\partial y_j} \end{Bmatrix}$ the real parts of
all eigenvalues are negative

Unstable stationary point: we move it out, goes away



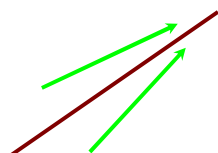
There exist at least one eigenvalue of the Jacobian
having positive real part

174

Stability analysis of a moving system

differential equation of the system $dY/dt = f(Y, p)$

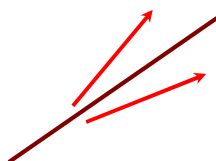
Stable trajectory: we move it out, goes back to the original trajectory



Jacobian $J = \begin{Bmatrix} \frac{\partial f_i}{\partial y_j} \end{Bmatrix}$ the real parts of all eigenvalues are negative

Unstable trajectory:

we move it out, goes away



There exist at least one eigenvalue of the Jacobian that the real part of it is positive

Chemical example: autocatalytic runaway, explosions

175

Slow manifolds in dynamical systems

Assume that the manifolds are attracting

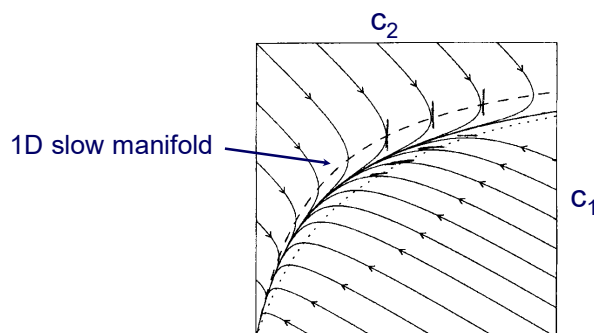
(no strong autocatalysis, no explosion)

In the space of variables (in chemical kinetics: concentrations) the fast moving points approach a given object (called slow manifolds) and move slowly along it.

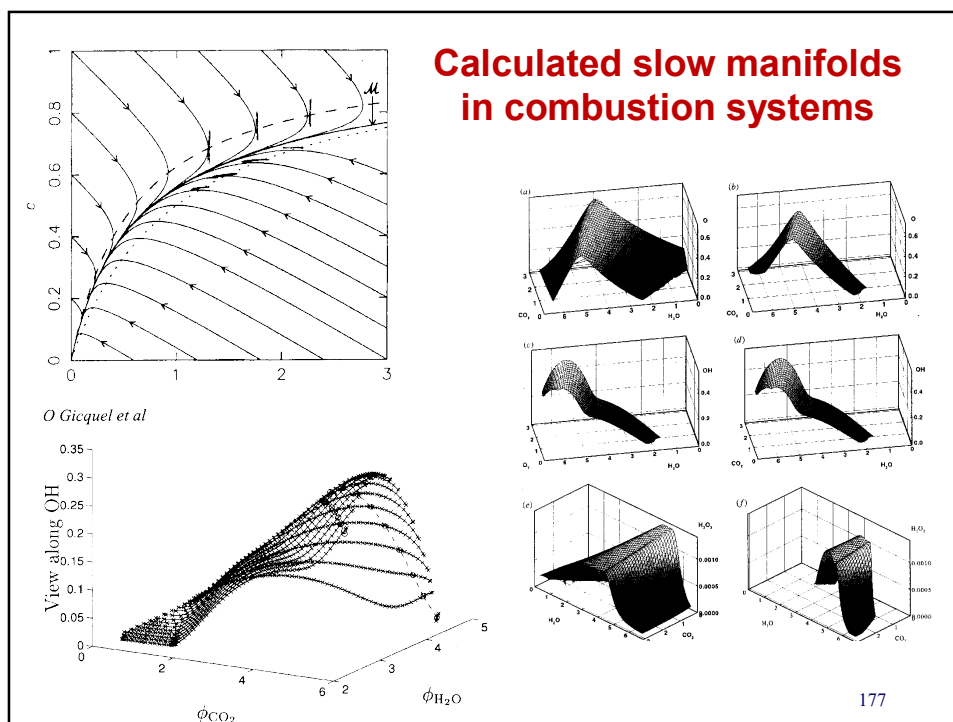
2D manifold : the trajectories approach a plane

1D manifold: the trajectories approach a (curved) line

0D manifold: the trajectories approach the equilibrium point



176



Modes

Previous assumption: „The concentration of a single species is changed by Δy_i and the concentrations of the other species are not changed”

This is approximately true if the concentration of the changed species is low and its lifetime is short.

Usually changing the concentration of a single species induces the change of the concentrations of several other species.

⇒ A more general approach:

the concentrations of several species are changed simultaneously by $\Delta \mathbf{Y}$

linear approach

to the change of the perturbation:

$$\frac{d(\Delta \mathbf{Y})}{dt} \approx \frac{\partial \mathbf{f}}{\partial \mathbf{Y}} \Delta \mathbf{Y} = \mathbf{J} \Delta \mathbf{Y}$$

The solution of this ODE: (assuming that the Jacobian does not change during the short time of relaxation)

$$\Delta \mathbf{Y}(t) = e^{\mathbf{J}\tau} \Delta \mathbf{Y}(t_1) \quad \Rightarrow \quad \Delta Y_i = C_1 e^{\lambda_1 \tau} + C_2 e^{\lambda_2 \tau} + C_3 e^{\lambda_3 \tau} + \dots + C_n e^{\lambda_n \tau}$$

where $\tau = t - t_1$ is the elapsed time from the start of perturbation

178

Modes 2

introducing new variables: \mathbf{z} vector of modes

c.f. normal coordinates in spectroscopy

$$\text{calculation of mode } z_i: \quad z_i = \mathbf{w}_i \mathbf{Y} \quad \mathbf{z} = \mathbf{W} \mathbf{Y}$$

where \mathbf{w}_i is the i -th row of matrix \mathbf{W}

$$\text{calculation of concentration } y_i: \quad Y_i = \mathbf{v}_i \mathbf{z} \quad \mathbf{Y} = \mathbf{V} \mathbf{z}$$

where \mathbf{v}_i is the i -th column of matrix \mathbf{V}

$$\text{the transformed kinetic system of ODEs: } \frac{d\mathbf{z}}{dt} = \mathbf{W} \mathbf{f}(\mathbf{V}\mathbf{z}), \quad \mathbf{z}_0 = \mathbf{W} \mathbf{Y}_0$$

If perturbation $\Delta\mathbf{Y}$ is towards direction \mathbf{w}_1 , then $z_1 \neq 0$,
but for all the other j directions $z_j = 0$.

$$\text{The change of } z_i \text{ after perturbation} \quad \Delta z_i(t) = \Delta z_i^0 e^{\lambda_i t}$$

IMPORTANT: the Jacobian changes in the space of concentrations,
therefore transformation $\mathbf{Y} \rightarrow \mathbf{z}$ also changes with \mathbf{Y} !

179

Modes 3

Denote \mathbf{z}_f the fast modes:

$$\tilde{\mathbf{Y}}(t) = \mathbf{Y}(t) + \Delta\mathbf{Y}(t)$$

$$\frac{d\tilde{\mathbf{Y}}}{dt} = \frac{d(\mathbf{Y} + \Delta\mathbf{Y})}{dt} = \mathbf{f}(\mathbf{Y}, \mathbf{p}) + \frac{d\Delta\mathbf{Y}}{dt}$$

$$\frac{d\mathbf{z}}{dt} = \mathbf{W} \mathbf{f}(\mathbf{V}\mathbf{z}), \quad \mathbf{z}_0 = \mathbf{W} \mathbf{Y}_0$$

$$\frac{dz_i}{dt} = \mathbf{w}_i \mathbf{f} = \mathbf{w}_i \mathbf{f}(\mathbf{Y}^m) + \mathbf{w}_i \frac{d\Delta\mathbf{Y}}{dt} = \frac{d\Delta z_i}{dt}$$

Let i belong to a fast mode and let
 \mathbf{Y}^m be a point on the manifold.

$$\mathbf{W}_i \mathbf{f}(\mathbf{Y}^m) = 0$$

Therefore, for mode i :

$$\frac{d\Delta z_i}{dt} = \mathbf{w}_i \mathbf{f}$$

180

Modes 4

From the previous page: $\frac{d \Delta z_i}{d t} = \mathbf{w}_i \mathbf{f}$

The modes can be perturbed independently from each other:

$$\frac{d \Delta z_i}{d t} = \lambda_i \Delta z_i$$

Comparing the two equations above:

$$\mathbf{w}_i \mathbf{f} = \lambda_i \Delta z_i$$

$$\Delta z_i = \mathbf{w}_i \mathbf{f} / \lambda_i$$

where Δz_i is the distance from manifold i

181

Calculation of the dynamical dimension

$$\Delta z_i = \mathbf{w}_i \mathbf{f} / \lambda_i$$

Δz_i distance from the slow manifold towards direction \mathbf{w}_j

If $|\Delta z_i| < z_{\text{threshold}} \Rightarrow$ this mode is (almost) on the manifold

Assume that there are n_r modes relaxed onto the corresponding slow manifold.

n number of variables in the model
 n_c number of conserved properties
 = number of zero eigenvalues of the Jacobian
 n_r number of relaxed modes

actual dynamical dimension: $n_D = n - n_c - n_r$

182

Change of the dynamical dimension during the course of a chemical reaction

n number of species in the mechanism
 n_c number of conserved properties
 (e.g. number of elements in a closed system)

If the initial composition is randomly selected, initially the trajectory is moving in a $(n - n_c)$ dimensional space
 (change of elementary composition by chemical reactions is forbidden)

If all eigenvalues of the Jacobian are negative:

- all manifolds are attractive
- the actual dynamical dimension is continuously decreasing
- finally it $n_D = 1$ (moving along a line) and the $n_D = 0$ (equilibrium point)

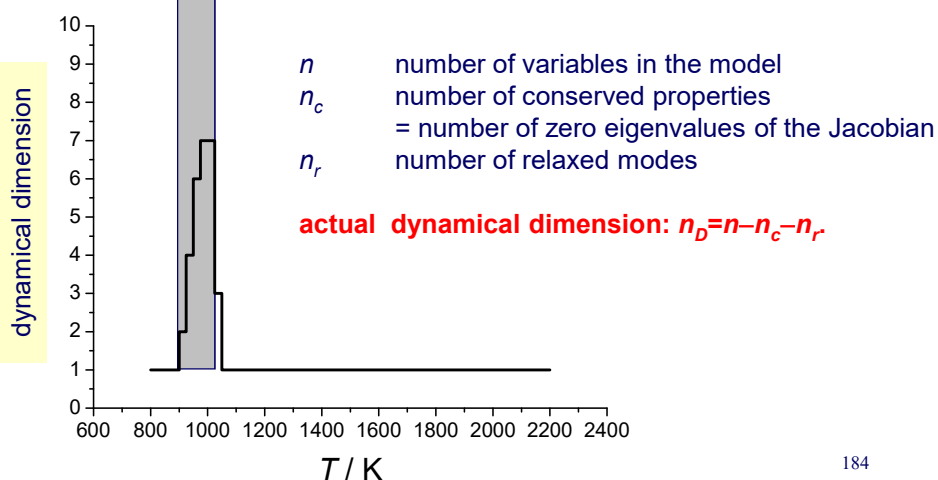
If some eigenvalue(s) of the Jacobian are positive:

- some manifolds are repellent
- the actual dynamical dimension is increasing
- the case of autocatalytic runaways (including explosions)

183

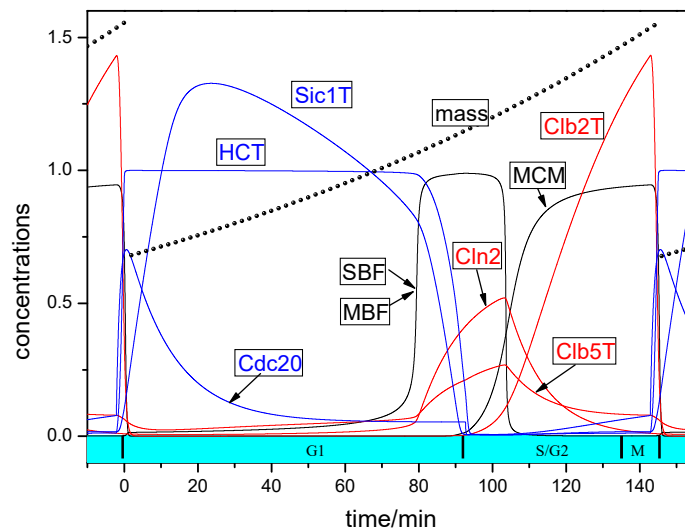
Change of dimension during adiabatic hydrogen/air explosion

grey region: here the largest eigenvalue is positive

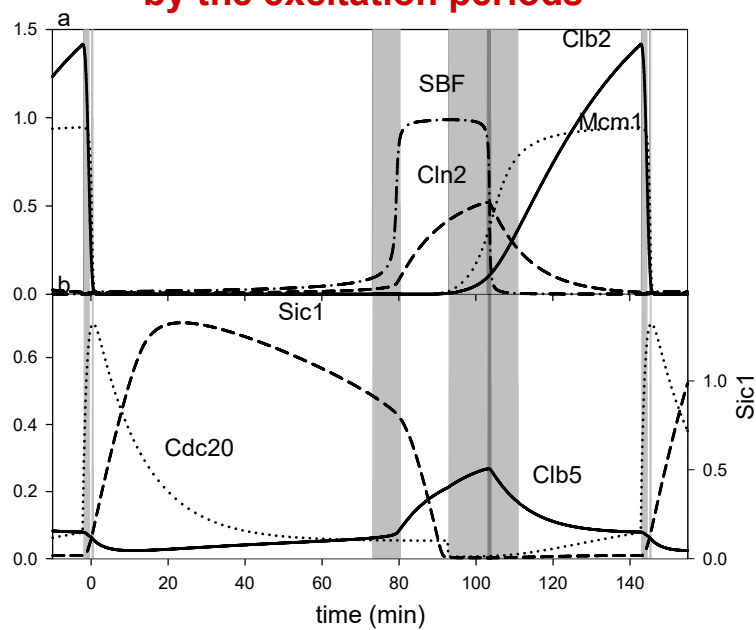


184

Change of protein concentrations during a cell cycle



Concentration changes are affected by the excitation periods



Need for the reduction of large reaction mechanisms

Increasing knowledge in chemical kinetics
 \Rightarrow increasing size of reaction mechanisms

Typical sizes of detailed reaction mechanisms:

high temperature combustion: 30-100 species, 200-500 reaction steps
 low temperature combustion: 500 species, 10000 reaction steps
 tropospheric chemistry: 500 species, 10000 reaction steps

Large mechanisms are not for humans:

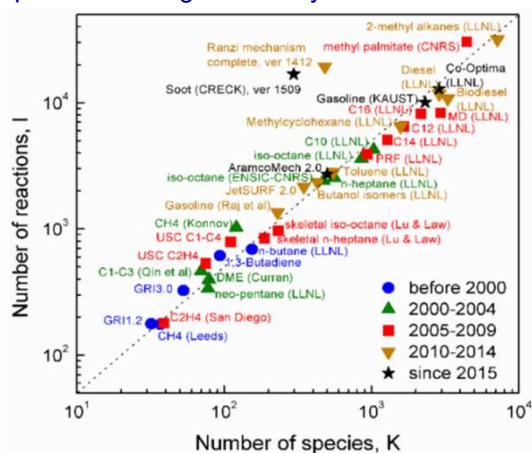
Small reduced mechanisms are needed for the

- understanding of the chemical processes
- fast calculation of chemistry

Reaction mechanisms are getting larger

The reaction mechanisms are getting larger, because

- increasing chemical knowledge
- faster computers with larger memory are available



F.N. Egolfopoulos, N. Hansen, Y. Ju, K. Kohse-Höinghaus, C.K. Law, F. Qi,
Prog. Energy Combust. Sci. **43** (2014) 36–67.

190

Need for the reduction of large reaction mechanisms 2.

Practical requirement:

simulation of spatially distributed systems with complex geometry.
The simulations must be fast and accurate.

The usual strategy: mechanism reduction at a series of simplified conditions, like plug-flow reactors, PSRs, 1D laminar flames.

These simple models together cover all the conditions in the model having complex geometry.

Is this a good approximation or an oversimplification?

I. Gy. Zsély, T. Turányi: Thermal and diffusion couplings do not affect mechanism reduction
Phys.Chem.Chem.Phys., **5**, 3622-3631 (2003)

Advantages of mechanism reduction

1 Spatially homogeneous system

- described by an ordinary system of differential equations
fast numerical simulation
a few minutes simulation time of a model having several thousand species and several ten thousands of reactions
- nobody understands such a big mechanism.
a skeleton model is needed to understand the chemistry

2 Spatially inhomogeneous system

- described by a partial system of differential equations
very slow numerical simulation
method of operator splitting is frequently used
the chemistry and the advection/diffusion is simulated separately:

$$\frac{d\mathbf{c}(\mathbf{r},t)}{dt} = \mathbf{f}(\mathbf{r},t,\mathbf{c}) + \Theta(\mathbf{r},t,\mathbf{c},\nabla\mathbf{c},\nabla^2\mathbf{c})$$

Most of the computer time (e.g. 99%) is used for solving the chemical kinetic equations

Mechanism reduction offers a
good possibility for speeding up the calculations!

192

Advantages of mechanism reduction 2

The original mechanism is not the „real one“, because ...

- the reaction mechanisms contain thermal average rate coefficients and the concentrations represent the thermal average quantum state of species
- selection of the list of species depend on the sensitivity of the applied chemical analytical methods
- some species are known to be present, but most models do not contain them.
Example: species CHO^+ in hydrocarbon flames
- almost all mechanisms contain redundant species and reactions, because presence of such species/reactions do not cause error
- none of the original mechanisms are general, but these have been created for a given domain of (y, p, T)

it is not „unfair“ to reduce reaction mechanisms, since...

- the domain of applicability of a reaction mechanism may be smaller than the original domain of validity
- it is OK if the simulation results change less due to reduction than the accuracy of the validation experiments (say 5% or 10%)
- we interest in the concentrations of some species only, not all calculated species concentrations.

193

Overview of mechanizmus reduction methods

I. without considering time scale separation

1. selection of a submechanism

elimination of redundant species and redundant reactions
⇒ skeleton mechanism; smaller ODE

2. lumping of reactions and species

⇒ smaller mechanism, smaller ODE

II. based on time scale separation

1. Simplification of the ODE: QSSA, partial equilibrium (PE)

⇒ coupled ODE and algebraic equations

2. Numerical representation of kinetic information:

ILDLM, ISAT, repromodelling
⇒ numerically stored kinetic equations:
look-up tables, polynomials, ANNs

194

Removal or redundant reactions the classic rate-of-production analysis

The traditional method: **rate-of-production analysis (ROPA)**:

The percentage contribution of **each reaction step** to the formation and removal of **each species** is investigated in several time points.

A reaction step can be **eliminated**, if its contribution is less then (say) 5% to the formation/removal of any species.

Example:

$$\frac{dx}{dt} = -k_1xy + k_2ya - 2k_3x^2 + k_4xa - 0,5k_5xy$$

$$\frac{dx}{dt} = \begin{matrix} \text{all producing terms} \\ + k_2ya + k_4xa \end{matrix} \quad \begin{matrix} \text{all consumption terms} \\ - k_1xy - 2k_3x^2 - 0,5k_5xy \end{matrix}$$

contribution of reaction step 4 to the producing terms

Easy to understand and easy to calculate.

BUT: large amount of data have to be considered
if there are many time point, reaction steps and species.

195

Table of contributions calculated by KINALC for a methane pyrolysis simulation

| | | | | | |
|-------------|--------------|---------|------------|---------------------------------|--|
| CH4 | | | | | |
| | | Rate : | -1.082E-08 | | |
| No | Contribution | | # | reaction | |
| 1 | -1.17547E-08 | 34.8 %C | 152 | C2H3+CH4 => C2H4+CH3 | |
| 2 | 9.13403E-09 | 39.8 %P | 151 | C2H4+CH3 => C2H3+CH4 | |
| 3 | -7.16821E-09 | 21.2 %C | 140 | CH=CCH2.+CH4 => CH=CCH3+CH3 | |
| 4 | -5.71162E-09 | 16.9 %C | 136 | CH2=CHCH2.+CH4 => CH2=CHCH3+CH3 | |
| 5 | 3.72978E-09 | 16.2 %P | 139 | CH=CCH3+CH3 => CH=CCH2.+CH4 | |
| 6 | 3.60756E-09 | 15.7 %P | 135 | CH2=CHCH3+CH3 => CH2=CHCH2.+CH4 | |
| 7 | 3.45436E-09 | 15.0 %P | 143 | C2H6+CH3 => C2H5+CH4 | |
| CH3 | | | | | |
| | | Rate : | 4.636E-10 | | |
| No | Contribution | | # | reaction | |
| 1 | -1.69871E-08 | 22.7 %C | 7 | 2CH3 => C2H6 | |
| 2 | 1.17547E-08 | 15.6 %P | 152 | C2H3+CH4 => C2H4+CH3 | |
| 3 | -9.13403E-09 | 12.2 %C | 151 | C2H4+CH3 => C2H3+CH4 | |
| 4 | 7.84580E-09 | 10.4 %P | 8 | C2H6 => 2CH3 | |
| C2H2 | | | | | |
| | | Rate : | 1.996E-09 | | |
| No | Contribution | | # | reaction | |
| 1 | 6.06561E-09 | 44.1 %P | 81 | CH2=CHCH2. => C2H2+CH3 | |
| 2 | -5.12527E-09 | 43.6 %C | 82 | C2H2+CH3 => CH2=CHCH2. | |
| 3 | 3.86101E-09 | 28.1 %P | 190 | C2H3 (+M) => H+C2H2 (+M) | |
| 4 | -3.15073E-09 | 26.8 %C | 189 | H+C2H2 (+M) => C2H3 (+M) | |
| 5 | -1.15098E-09 | 9.8 %C | 67 | C2H2+CH3 => CH=CCH3+H | |

196

Principal component analysis of the sensitivity matrix: PCAS

Another approach for the identification of redundant reaction steps (= identification of redundant parameters)

It has been discussed in the local sensitivity analysis section.

In several time points the normalized local sensitivity matrix \mathbf{S}_r is calculated, component matrix $\tilde{\mathbf{S}}$ is formed and the eigenvector-eigenvalue analysis of matrix $\tilde{\mathbf{S}}^T \tilde{\mathbf{S}}$ is carried out.

$$\tilde{\mathbf{S}} = \begin{bmatrix} \tilde{\mathbf{S}}_1 \\ \tilde{\mathbf{S}}_2 \\ \vdots \\ \tilde{\mathbf{S}}_n \end{bmatrix}$$

$$\tilde{\mathbf{S}}_r = \{(p_k / Y_i)(\partial Y_i(t_r) / \partial p_k)\}$$

eigenvector j : \mathbf{u}_j defines the parameters acting together for influencing the concentrations at time t_r

eigenvalue i : λ_i indicates the importance of the parameter group.

A reaction step is **important**, if all species concentrations are considered in the objective function and if the corresponding rate parameter belongs to an **important parameter group** (large λ_i) and it is **important within the parameter group** (large eigenvector element).

197

Principal component analysis of the rate sensitivity matrix: PCAF

the normed \mathbf{F} matrix is calculated in several time points r

$$\tilde{\mathbf{F}}_r = \{(p_k / f_i)(\partial f_i(t_r) / \partial p_k)\}$$

eigenvector-eigenvalue analysis of matrix $\tilde{\mathbf{F}}_r^T \tilde{\mathbf{F}}_r$

eigenvector j : \mathbf{u}_j defines the parameters acting together for influencing the production rates at time t_r

eigenvalue i : λ_i indicates the importance of the parameter group.

A reaction step is **important at time r** , if all species production rate are considered in the objective function and if the corresponding rate parameter belongs to an **important parameter group** (large λ_i) and it is **important within the parameter group** (large eigenvector element).

A reaction step is **important in a time interval**, if it is important at least in a single time point

T. Turányi, T. Bérces, S. Vajda: Reaction rate analysis of complex kinetics systems
Int.J.Chem.Kinet., **21**, 83-99 (1989)

198

PCAS and PCAF are basically different

PCAF

- investigation of **reaction rates**, which depend on the **actual concentrations** only
- analysis in **time points**
- change of importance in time can be investigated
- **F** calculated analytically

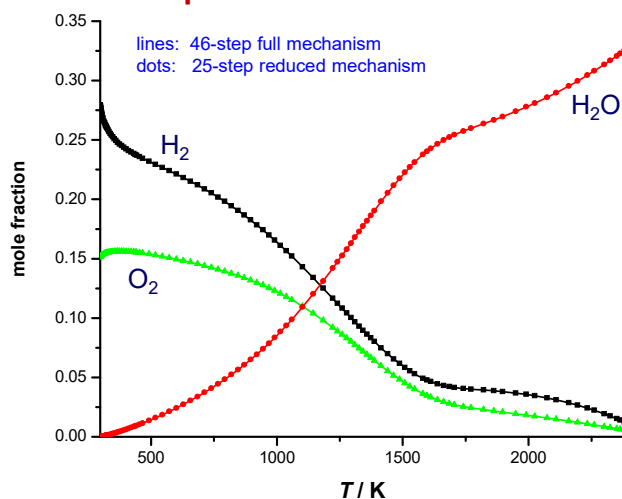
PCAS

- investigation of **sensitivity functions**, which depend on the prehistory of the simulation
- analysis belongs to a **time interval**
- direct inspection of the change of simulation results; close connection to parameter estimation
- **S** calculated numerically

In all investigated cases PCAF and PCAS provided exactly the same reduced mechanisms.

199

Example: H₂-air flame mechanism reduction PCAS and PCAF provided identical reduced mechanisms



I. Gy. Zsély, T. Turányi: The influence of thermal coupling and diffusion on the importance of reactions: The case study of hydrogen-air combustion, *Phys.Chem.Chem.Phys.*, **5**, 3622-3631(2003)

Integer programming methods

$$\dot{\mathbf{y}} = \mathbf{v}\mathbf{R}(\mathbf{y})$$

$d \mathbf{y}/d t$ production rates belonging to the full mechanism

\mathbf{v} stoichiometric matrix

\mathbf{R} rates of the reaction steps

$$\dot{\mathbf{z}} = \mathbf{v}\mathbf{D}\mathbf{R}(\mathbf{z})$$

$d \mathbf{z}/d t$ production rates belonging to the reduced mechanism

\mathbf{D} diagonal matrix:

$d_{ii} = 0$ the reaction step is missing from the reduced mech

$d_{ii} = 1$ the reaction step is present in the reduced mech

The aim is finding the reduced mechanism having k reaction steps with minimal deviation between the production rates of the full and reduced mechanisms by varying vector \mathbf{d} .

$$\begin{aligned} & \min \|\mathbf{y} - \mathbf{z}\| \\ & \text{subject to} \\ & \dot{\mathbf{y}} = \mathbf{v}\mathbf{R}(\mathbf{y}), \quad \mathbf{y}(0) = \mathbf{y}_0 \\ & \dot{\mathbf{z}} = \mathbf{v}\mathbf{D}\mathbf{R}(\mathbf{z}), \quad \mathbf{z}(0) = \mathbf{z}_0, \quad 0 \leq t \leq b \\ & \sum_{i=1}^N d_{ii} = k, \quad d_{ii} = 0 \text{ or } 1 \end{aligned}$$

L. Petzold, W. Zhu: Model reduction for chemical kinetics: An optimization approach. *AIChE Journal* **45**, 869-886 (1999)

201

Integer programming methods 2.

5-step full mechanism $\Rightarrow 2^5 - 1$ possible reduced mechanisms

\Rightarrow trial of all combinations does not work

\Rightarrow a classic integer programming problem

several approaches were suggested by Petzold and Zhu:

- greedy algorithm: elimination of the least important reactions first
- elimination of reactions first via the elimination of redundant species
- all variants require much computer time

Further improvements:

Androulakis: branch and bound algorithm, which splits the feasible region of input values into smaller subregions (branching) with the subregions forming a search tree.

Another approach: the simulation error
(deviation between the solutions of the reduced and full models)
is investigated instead of the deviations of the production rates.

I. P. Androulakis: Kinetic mechanism reduction based on an integer programming approach. *AIChE J.* **46**, 361-371 (2000)

202

Genetic algorithm-based methods

Again, the reduced mechanism is represented by a **d** vector with elements of either 1 or 0.

The conceptual background and the terminology is based on **evolution**

candidate reduced mechanisms (called **individuals**):

| | |
|--------------|------------|
| Individual 1 | 1100101010 |
| Individual 2 | 1100111000 |
| Individual 3 | 1100100011 |
| Individual 4 | 1110001010 |

fitness criterion agreement of the reduced mechanism with the full mech

genetic operators: cross over and mutation

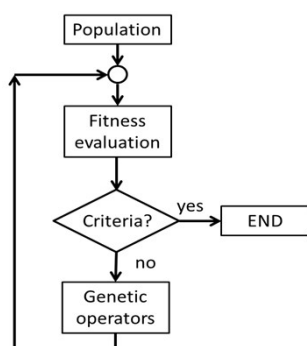
cross over exchange of sections of two individuals

mutation changing 0 to 1 OR 1 to 0 in an individual

203

Genetic algorithm-based methods 2

- 1 random population of reduced mechanisms is produced.
- 2 the fitness is evaluated (comparison of the full and reduced mechs)
- 3 if a good enough reduced mech is found ⇒ **END**
- 4 variants of the reduced mechanisms are produced by genetic operators
- 5 the newly produced mechs are added to the population;
the poor individuals are replaced by the new ones ⇒ **GOTO 2**



EVOLUTION: some of the the new individuals are at least not worse than the previous ones
⇒ **improvement is expected**

K. Edwards, T. F. Edgar, V. I. Manousiouthakis:
Kinetic model reduction using genetic algorithms.
Comput. Chem. Eng. **22**, 239-246 (1998)

N. Sikalo, O. Hasemann, C. Schulz, A. Kempf, I. Wloka:
A genetic algorithm-based method for the
automatic reduction of reaction mechanisms.
Int. J. Chem. Kinet. **46**, 41–59 (2014)

204

Topic 11: Reduction of reaction mechanisms 2: Elimination of redundant species

reaction rate and Jacobian-based methods for species removal,

species elimination via trial and error,
connectivity method (CM)

simulation error minimization connectivity method (SEM-CM)
directed relation graph (DRG) method
DRG-aided sensitivity analysis (DRG-SA),
DRG with error propagation (DRGEP)
path flux analysis method (PFA)

comparison of methods for species elimination

Identification of redundant species

important species and important features

- examples for important features: ignition delay time, period time
- alternative name: target species (DRG terminology)

The aim of the simulations is the accurate calculation of the
important features and the concentrations of the important species

In different simulations the important species/features can be different
even if the applied mechanism is identical.

necessary species

These are needed for the accurate calculation of the important features and
the concentrations of the important species

redundant species

- not important and not necessary species
- can be eliminated from the mechanisms

T. Turányi: Reduction of large reaction mechanisms, *New J.Chem.*, **14**, 795-803 (1990)

206

Removal of redundant species 2

Approach 1: elimination of species one-by-one via trial calculations

The consuming reactions of each species is deleted one-by-one; the effect on the important species/reactions is investigated.

Problem: not effective enough; some species can be eliminated only together (e.g. participating in fast preequilibrium reactions)
elimination of species groups \Rightarrow too many possibilities

Approach 2: Which species are directly linked to the important species?

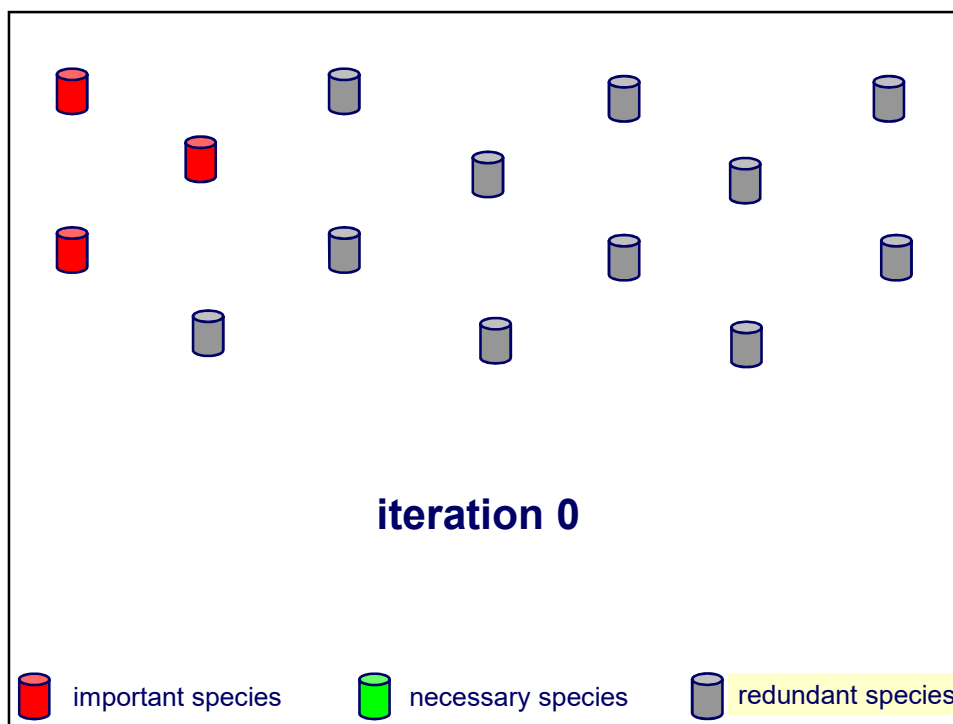
(this approach cannot handle the reproduction of important features)

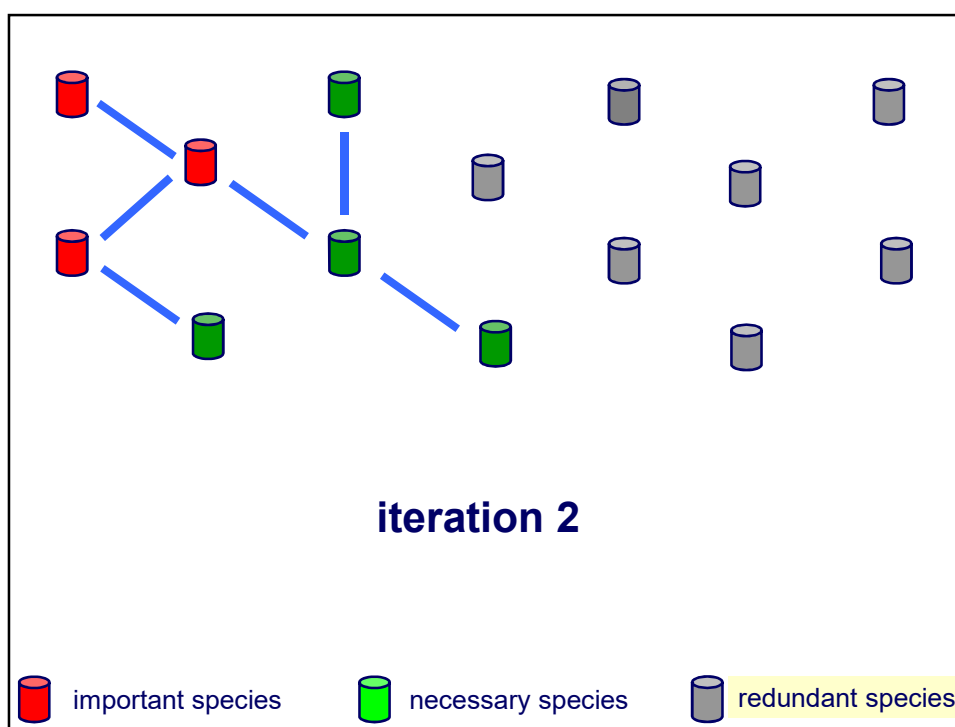
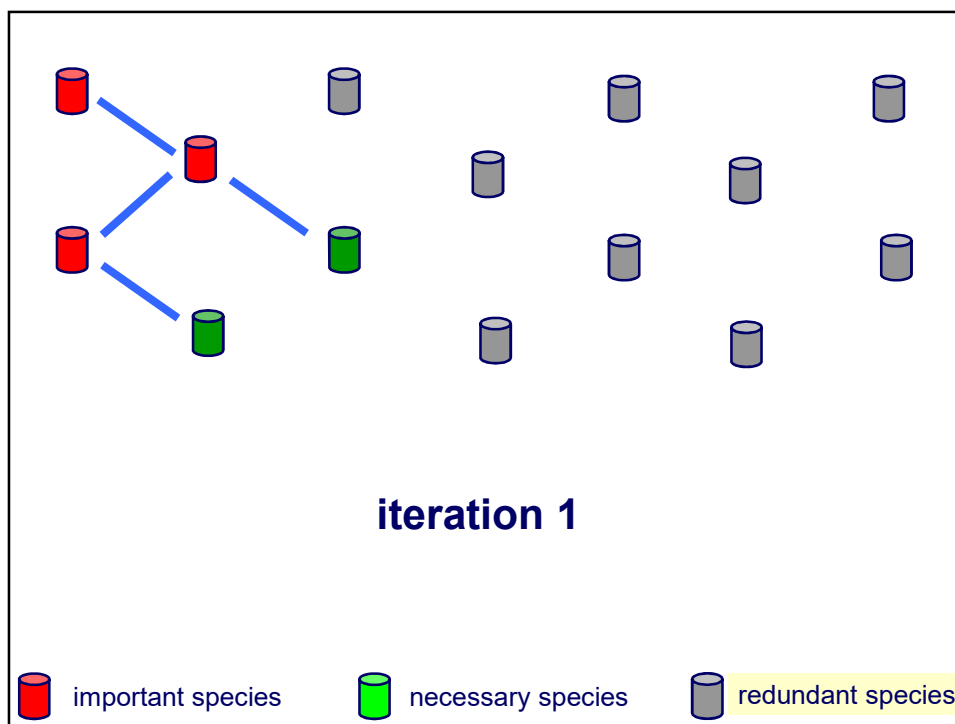
Step 1: using an appropriate method, the direct link of each species to the important species is investigated (detection of „species group 1“).

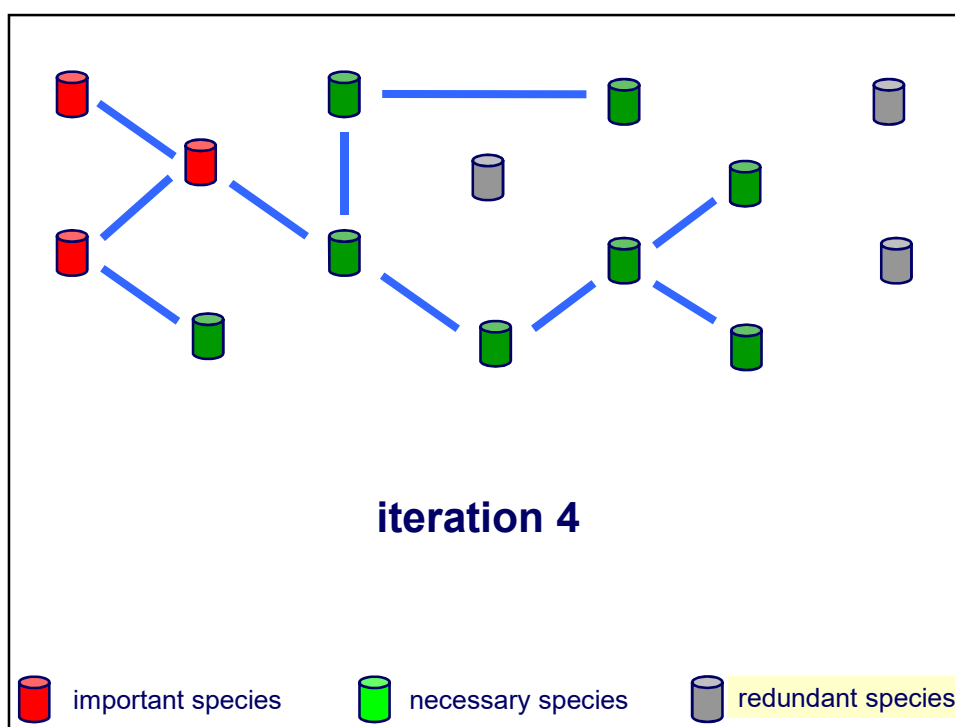
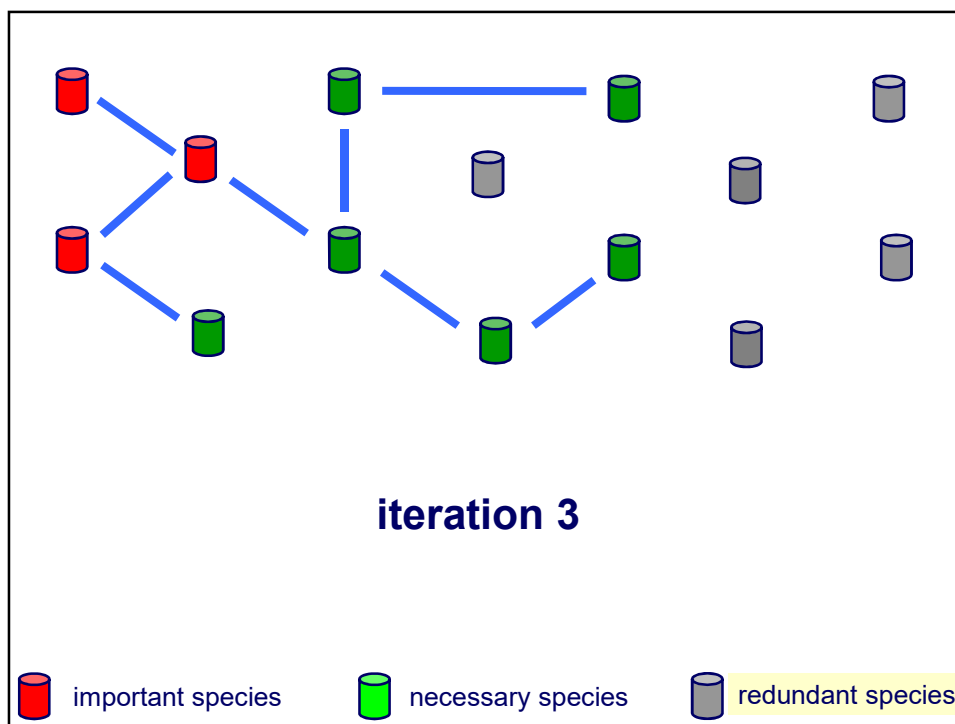
Step 2: assessment of the link of each species to the „species group 1“. The newly identified closely linked species are added to the group, forming „species group 2“.

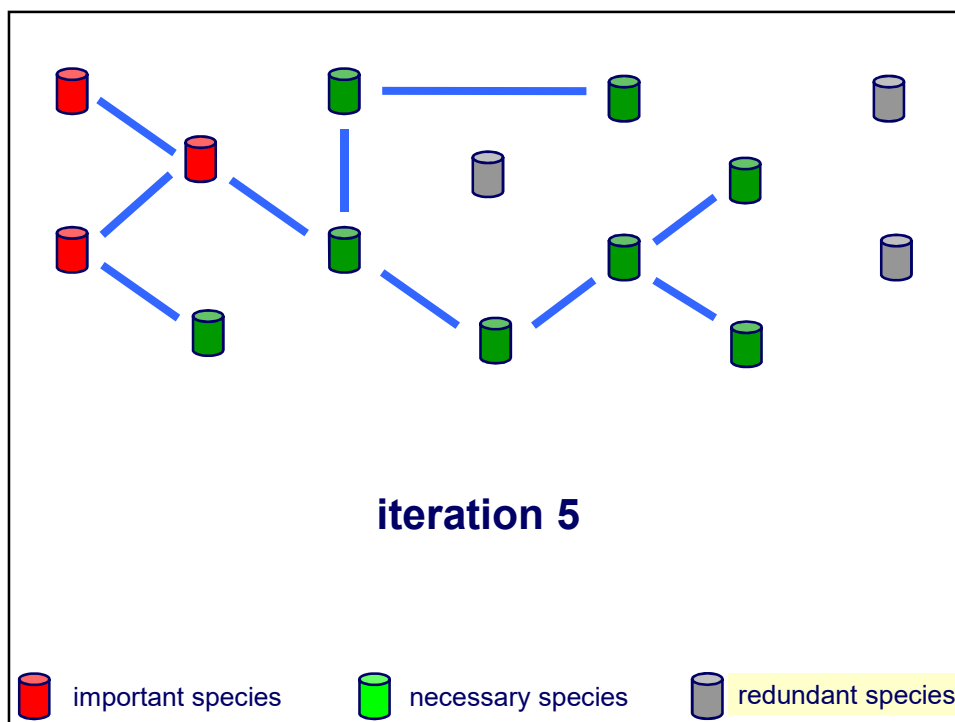
Step n : The iteration is repeated, until no species is closely linked to „species group $(n-1)$ “

207









Connectivity Method

An element of the **normalized Jacobian** shows the effect of changing the concentration of species i on the production rate of species j :

$$\bar{J}_{ij} = (c_i / f_j) (\partial f_j / \partial c_i)$$

B_i characterizes the strength of the direct link of species i to the group of important species:

$$B_i = \sum_{j \in \text{group}} \bar{J}_{ij}^2$$

In an iterative process all species are identified that are strongly connected directly or through other species to the group of important species.

The procedure is repeated at each selected time.

T. Turányi: Reduction of large reaction mechanisms, *New J.Chem.*, **14**, 795-803 (1990)

Connectivity Method 2.

advantages and disadvantages

Advantages:

- Simple, fast
- Available in KINALC
- Works well for small mechanisms

Disadvantages:

The iteration is stopped, when a gap appears in the range of B_i values.

BUT

The best threshold is different from case to case.

The user has to select the threshold manually.

If there is a large number of species (500), there is **no obvious gap!**

The **special role of important species diminishes** after many iterations; this may lead to the selection of redundant species.

Directed Relation Graph (DRG) Method

The mechanism is represented by **nodes** and **vertices**.

Each species is a **node**.

The procedure starts from the important species (called here „target species“)

A **vertex** is drawn if the corresponding reaction has a significant contribution to the production rate of the species represented by the node.

This effect is characterized by the following measure:

$$R_{i \rightarrow j}^{(Lu)} = \frac{\sum_{\alpha \in C(i,j)} |v_{i\alpha} r_{\alpha}|}{\sum_{\alpha \in R(i)} |v_{i\alpha} r_{\alpha}|}$$

- $R(i)$ set of reactions that are related to species i
 $C(i,j)$ set of reactions in which both species i and j participate
 $v_{i\alpha}$ stoichiometric coefficient of species i in reaction α
 r_{α} net reaction rate (the difference of the forward and backward rates)

T. Lu, C. K. Law: A directed relation graph method for mechanism reduction.
Proc. Comb. Inst., **30** (2005) 1333–1341.

DRG Method 2

Importance of species i :
$$I_i^{(\text{DRG})} = \begin{cases} 1 & \text{if species } i \text{ is a target species} \\ \max_{j \in S} (\min(R_{j \rightarrow i}, I_j^{(\text{DRG})})) & \text{otherwise} \end{cases}$$

S full set of chemical species

$R_{i \rightarrow j}$ connection weight

$R_{i \rightarrow j} = 0$ the two species are not connected

$I_i^{(\text{DRG})}$ is calculated iteratively using a minimum-cost graph search algorithm

if $I_i^{(\text{DRG})} < \epsilon$ species i is considered to be redundant for the simulation of the target species.

DRG+restart Method

tactic 1: getting a reduced mechanism in one step
by applying a large ϵ

tactic 2: getting a larger reduced mechanism by applying a smaller ϵ

- new simulation with the reduced mechanism
- new calculation of the r values
(different r values since the mechanism is different!)
- new reduction with (the same or larger) smaller ϵ

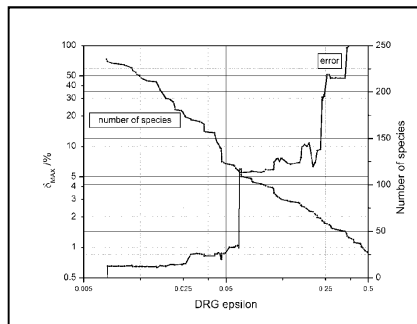
Lu and Law found that this two-stage approach
(called DRG+restart) is more effective and
allows the removal of further species at the second stage.

T. Lu, C. K. Law: Linear time reduction of large kinetic mechanisms with directed relation graph:
n-heptane and *iso*-octane. *Combust. Flame*, **144** (2006) 24–36..

Directed Relation Graph (DRG) Methods

advantages

- simple, very fast



disadvantages

- ε is not directly related to the error of the reduced mechanism
- decreasing ε does not always decrease the error of reduction
- very small fluxes of important species is also reproduced
⇒ selection of redundant species
- every selected species becomes equally important
⇒ selection of redundant species

DRGASA method

DRGASA: DRG-aided sensitivity analysis

misleading name:

- calculation of sensitivities is not included
- the DRG-estimation is checked using simulations

- 1 redundant species are selected by DRG using large ε
- 2 a second group of species is also identified using DRG with smaller ε
- 3 A series of simulations are carried out where the consequences of eliminating these species (one-by-one) are investigated using a series of simulations.

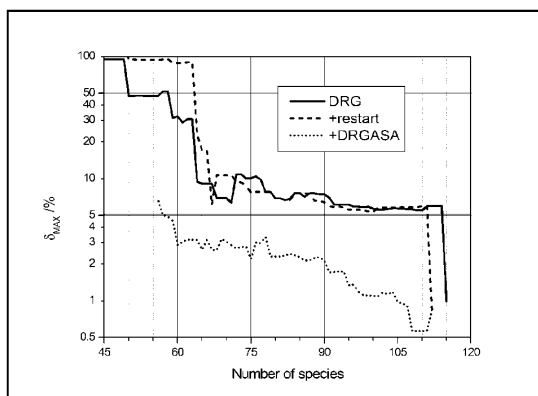
DRGASA method is more effective than the basic DRG approach, because it investigates the simulation error directly. This simulation error belongs to the group of important species, and therefore the DRGASA indicates less species to be necessary than the original method for a prescribed error limit.

DRG vs. DRG-restart vs. DRGASA methods

Case study: reduction of a methane partial oxidation mechanism

full mechanism: 6874 reaction steps of 345 species

maximal simulation errors of the mechanisms as function of species number, for the original DRG DRG-restart and DRGASA methods



DRG+restart is slightly better (sometimes) than DRG

DRGASA is much better than DRG

T. Nagy, T. Turányi: Reduction of very large reaction mechanisms using methods based on simulation error minimization, *Combust. Flame*, **156**, 417–428 (2009)

Directed Relation Graph with Error Propagation: DRGEP method

Alternative definition of the weight of the vertices; distinguishing reactions that create or destroy species i

$$R_{i \rightarrow j}^{(Pep)} = \frac{\left| \sum_{\alpha \in C(i,j)} \nu_{i\alpha} r_{\alpha} \right|}{\max \left(\sum_{\alpha \in R(i)} (\nu_{i\alpha} r_{\alpha})^+, \sum_{\alpha \in R(i)} (\nu_{i\alpha} r_{\alpha})^- \right)} \quad \begin{array}{l} (.)^+ \text{ selects the positive terms} \\ (.)^- \text{ selects the negative terms} \end{array}$$

This equation calculates the sum of the rates belonging to the pair of species (i, j) to the total rate of formation or destruction of species i .

Importance index:
$$I_i^{(DRGEP)} = \begin{cases} 1 & \text{if species } i \text{ is a target species} \\ \max_{j \in S} (R_{j \rightarrow i} \cdot I_j^{(DRGEP)}) & \text{otherwise} \end{cases}$$

if $I_i^{(DRGEP)} < \epsilon$ species i is considered to be redundant for the simulation of the target species.

P. Pepiot-Desjardins, H. Pitsch: An efficient error-propagation-based reduction method for large chemical kinetic mechanisms, *Combust. Flame*, **154**, 67-81 (2008)

DRGEP method 2

advantages

- simple, very fast

disadvantages

- ε is not directly related to the error of the reduced mechanism
- decreasing ε does not always decrease the error of reduction
- very small fluxes of important species is also reproduced
⇒ selection of redundant species
- ~~every selected species becomes equally important~~
~~⇒ selection of redundant species~~

Path Flux Analysis (PFA) method

The first generation production (P_A) and consumption (C_A) fluxes of species A:

$$P_A = \sum_i \max(\nu_{A,i} \omega_i, 0)$$

$$C_A = \sum_i \max(-\nu_{A,i} \omega_i, 0)$$

$\nu_{A,i}$ stoichiometric coefficient of species A in reaction i
 ω_i net reaction rate (the difference of the forward and backward rates)

The production (P_{AB}) and consumption (C_{AB}) fluxes of species A via species B

$$P_{AB} = \sum_i \max(\nu_{A,i} \omega_i \delta_B^i, 0)$$

$$C_{AB} = \sum_i \max(-\nu_{A,i} \omega_i \delta_B^i, 0)$$

δ_B^i is unity if species B is involved in the i -th reaction and 0 otherwise

W. T. Sun, Z. Chen, X. L. Gou, Y. G. Ju: A path flux analysis method for the reduction of detailed chemical kinetic mechanisms *Combust. Flame* **157**, 1298-1307 (2010)

PFA method 2

Flux ratio: share of a particular production and consumption path via species B to the total production and consumption flux of species A.

The first generation flux ratios for the production and consumption of species A via species B are defined as:

$$r_{AB}^{pro-1st} = \frac{P_{AB}}{\max(P_A, C_A)}$$

$$r_{AB}^{con-1st} = \frac{C_{AB}}{\max(P_A, C_A)}$$

$$r_{AB} = \max(r_{AB}^{pro-1st}, r_{AB}^{con-1st})$$

Starting from the set of important species, using the relation $r_{AB} > \varepsilon$, the set of other necessary species are identified.

Common features of the CM/DRG/DRGEP/PFA methods

The method is based on the investigation of the kinetic system of ODEs.

The size of the reduced mechanism is controlled by a threshold (B_i or ε); this threshold is not directly related to the error of simulation.

The analysis is carried out at several reaction times (concentration sets)
The final reduced mechanism is the union of the reduced mechanisms obtained at the different concentration sets

Only one or few reduced mechanisms are produced and therefore the error of reduction is checked only once or few times.

New strategy for mechanism reduction:

Simulation error minimization (SEM)

Definition of error calculation

relative error \Rightarrow overemphasizes large relative deviations
of small concentrations

absolute error \Rightarrow deviations of small concentrations
are neglected

mixed error:

$$\delta_i(t_j) = 2 \frac{c_i^{\text{red}}(t_j) - c_i^{\text{full}}(t_j)}{c_i^{\text{full}}(t_j) - c_{i,\text{MAX}}^{\text{full}}} \approx \begin{cases} \frac{c_i^{\text{red}}(t_j) - c_i^{\text{full}}(t_j)}{c_i^{\text{full}}(t_j)} & \text{if } c_i^{\text{full}}(t_j) \sim c_{i,\text{MAX}}^{\text{full}} \quad \approx \text{relative error} \\ \frac{c_i^{\text{red}}(t_j) - c_i^{\text{full}}(t_j)}{c_{i,\text{MAX}}^{\text{full}}/2} & \text{if } c_i^{\text{full}}(t_j) \ll c_{i,\text{MAX}}^{\text{full}} \quad \approx \text{scaled absolute error} \end{cases}$$

where

$c_i^{\text{full}}(t_j)$ concentration from the full mechanism

$c_i^{\text{red}}(t_j)$ concentration from the reduced mechanism

$c_{i,\text{MAX}}^{\text{full}} = \max_j c_i^{\text{full}}(t_j)$ maximal value of c_i^{full}

definition of worst case error: $\delta_{i,\text{MAX}} = \max_j |\delta_i(t_j)|$
 $\delta_{\text{MAX}} = \max_i \delta_{i,\text{MAX}}$

Consistency of a reduced mechanism

The aim is to produce a consistent reduced mechanism.

A mechanism is called **consistent**, if all species are **living**.

living species:

has nonzero concentration

or

produced from another species

or

has inflow term (e.g. in PSR)

complementary set of species:

species that are not yet selected, but

selection of these species

yields at least one additional selected reaction

Note: unions of complementary sets are also complementary sets

Looking for strongly connected species - the problem of selecting important reactions



A is the only important species

non-zero initial concentrations: A, D

zero initial concentrations: B, C

Proper reduced mechanism: $A + B \rightarrow C \quad D \rightarrow B$

Connectivity method selects B and D as necessary
(or B only at the initial time).

Rule 1: a reaction is selected, if all of its species are necessary
⇒ some important reactions are not selected,
including $A + B \rightarrow C$

or

Rule 2: a reaction is selected, if any of its species is necessary
⇒ redundant reactions are also selected

SEM-CM steps

1 initiation

- simulations using the full mechanism
- selection of the representative time points
- saving concentration sets and Jacobian matrices in these points
- identification of the important species by the modeller
⇒ initially these species are the selected species

2 identification of complementary sets of species

Complementary sets of species are looked for
to the group of currently selected species
by going through all reaction steps one-by-one.

These sets may contain each other or overlap.

SEM-CM**3 ranking the complementary sets**

The strength of the direct link of the complementary set k , to the group of selected species is characterized by

$$C_k = \frac{1}{n_k} \sum_{j \in \text{set}} B_j = \frac{1}{n_k} \sum_{j \in \text{set}} \sum_{i \in \text{group}} \bar{J}_{ij}^2$$

Each complementary set is ranked according to their C_k values.

4 generation of extended sets of species

Several complementary sets exist with similarly strong links to the group of selected species.

Building procedure to **depth level m** generates m extended sets of species by adding each complementary set up to rank m to the current group of selected species. This procedure is repeated at each reaction time t_k .

SEM-CM**5 generation of consistent reduced mechanisms**

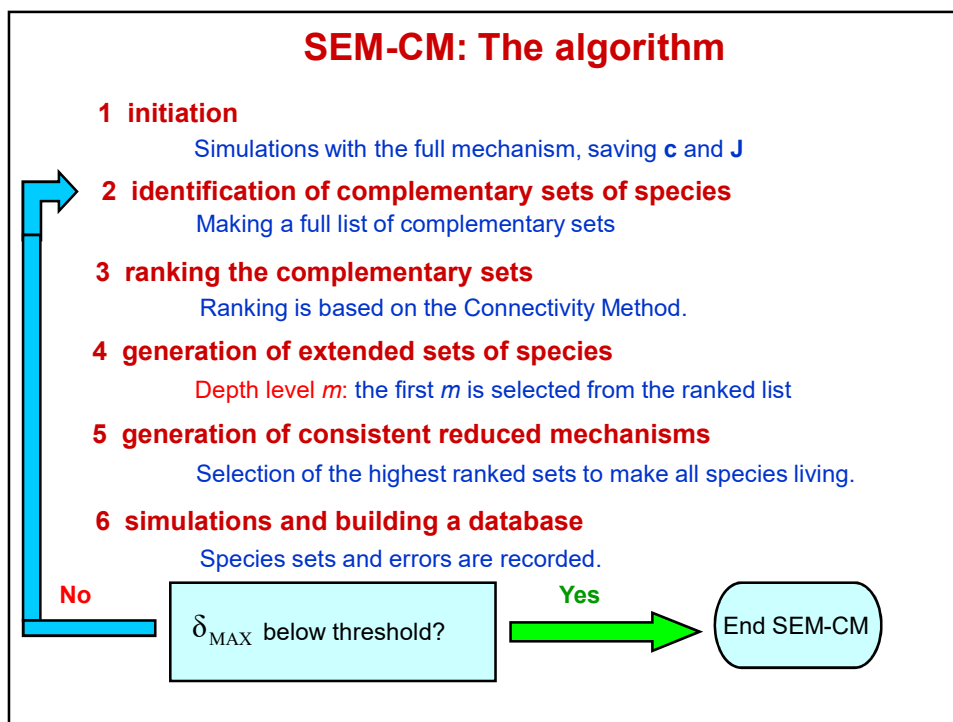
Non-living species are identified and the corresponding complementary sets are determined. A living species at time t_k is formed previously from living species. Maximum values of the previous Jacobians are used for ranking the complementary sets:

$$\bar{C}_k = \frac{1}{n_k} \sum_{j \in \text{set}} \bar{B}_j = \frac{1}{n_k} \sum_{j \in \text{set}} \sum_{i: \text{non-living and selected}} \bar{M}_{ij}^2 \quad \bar{M}_{ij}(t_k)^2 = \max_{1 \leq k} \bar{J}_{ij}(t_1)^2$$

Species belonging to the highest ranked complementary set are added to the group of selected species. This procedure is repeated, until all species become living.

6 simulations and building a database

Each generated reduced mechanism is investigated via a simulation. Reduction errors are recorded.



SEM-PCAF: PCAF with simulation error minimization

Step 1: Identification of redundant reactions

Based on the PCAF method, many reduced mechanisms are generated by trying various thresholds for eigenvalues and eigenvector elements.

Step 2: Making the reduced mechanisms to be consistent

Some of the obtained reduced mechanisms contain not-living species. Producing reactions of these species are restored. The most important producing reactions (based on F-matrix analysis) are added.

Step 3: Finding the fastest reduced mechanism with small simulation error

Simulations are carried out; errors and required CPU time are recorded. Many different reduced mechanisms may have similarly small error.

The reduced mechanism associated with the fastest simulation within a 2% margin of reduction error is selected as the best one.

Example:**gas-phase chemistry in solid-oxide fuel cells
the partial oxidation of methane**

Solid-oxide fuel cells (SOFCs): power source for electric-driven vehicles.

Can be operated with hydrocarbon fuels.

Air is added to the hydrocarbon fuel to prevent deposit formation.

⇒ slow partial oxidation of the hydrocarbon before reaching the anode

Dean mechanism: homogeneous gas-phase chemistry
in the anode channel of natural gas fuelled SOFCs.
Partial oxidation of methane up to high conversion.

Reduction is needed for **computer optimization**
of fuel cell geometry and operating conditions.

235

**Gas-phase chemistry in solid-oxide fuel cells:
partial oxidation of methane 2**

Full Dean mechanism: 345 species and 6874 irreversible reactions.

It was investigated at a typical set of SOFC conditions:

$T = 900\text{ }^{\circ}\text{C}$ (1173.15 K)

$p = 1\text{ atm}$ (101325 Pa)

isothermal and isobaric conditions

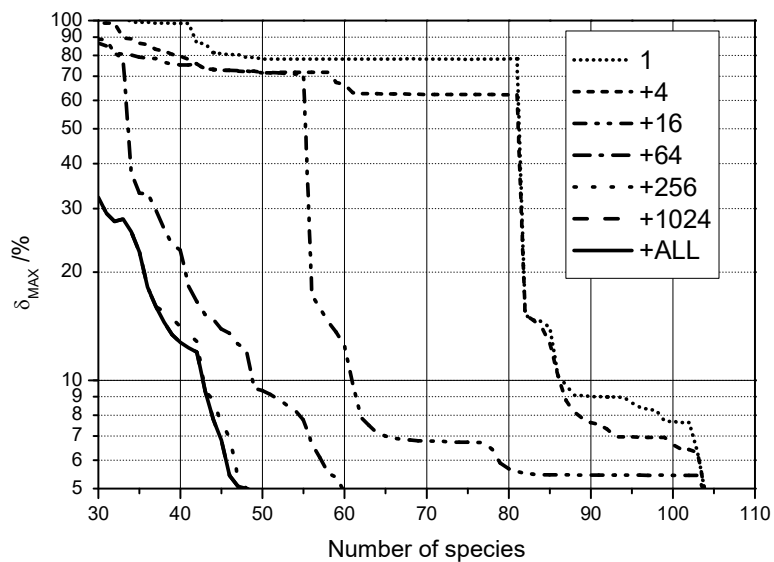
30.0 % v/v methane and 70.0 % v/v air

12 important species:

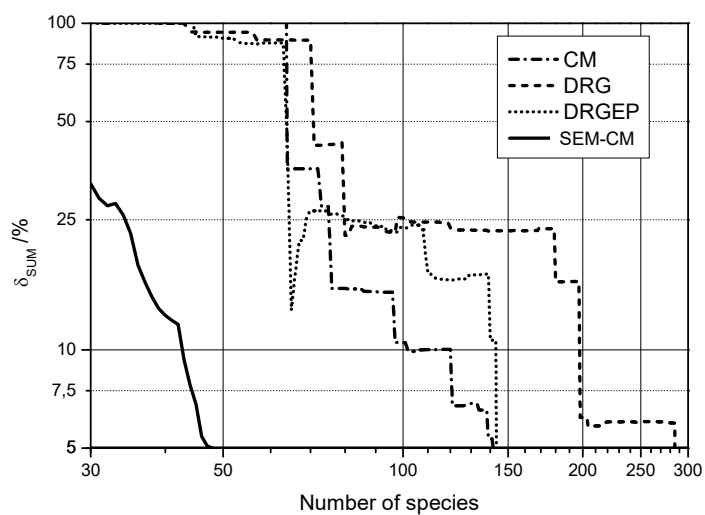
CH_4 , N_2 , O_2 , H_2 , H_2O , CH_2O , CO , CO_2 , C_2H_2 , C_2H_4 , C_2H_6 , C_6H_6 .
(the mole fraction of these species exceed 0.001)

236

Testing the “depth level” of SEM-CM



Comparison of methods CM, DRG, DRGEP, SEM-CM simulation error vs. number of species

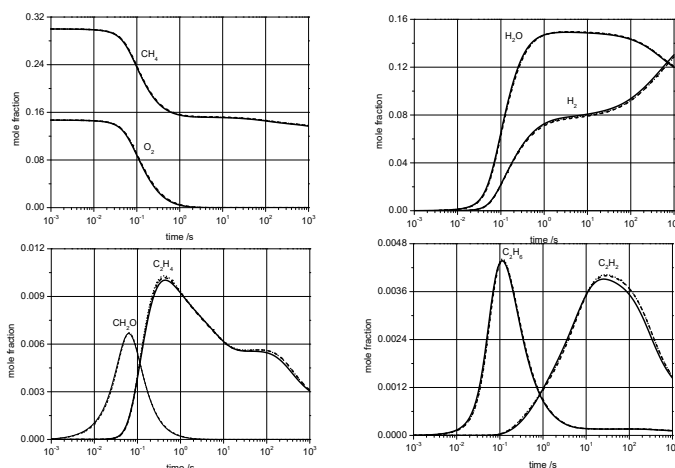


SOFC chemistry example: comparison of the obtained reduced mechanisms at 5% maximal error

| | | | |
|---------------------|-------------|----------------|--------------------|
| original mechanism: | 345 species | 6874 reactions | |
| DRG reduction | 286 species | 5637 reactions | 1.34 times faster |
| DRGEP reduction | 144 species | 2482 reactions | 6.18 times faster |
| CM reduction | 139 species | 2494 reactions | 5.57 times faster |
| SEM-CM reduction | 47 species | 613 reactions | 58.4 times faster |
| SEM-CM + SEM-PCAF | 47 species | 297 reactions | 103.0 times faster |

CPU for the generation of the reduced mechanism (Athlon XP 2500+ PC):
 (hh:mm:ss) DRG: 00:15:00 DRGEP: 00:04:40 CM: 00:01:30
 SEM-CM(256): 9:29:00 SEM-CM(all): 18:10:00

Testing the obtained reduced mechanisms



| | |
|----------------------------------|---------------------------------------|
| _____ full mechanism | 6,874 reactions of 345 species |
| ----- result of SEM-CM | 613 reactions of 47 species |
| result of SEM-CM+ SEM-PCAF | 297 reactions of 47 species |

Almost identical concentrations can be obtained with a much smaller mechanism!

Summary

1. In all current methods for the elimination of redundant species and redundant reactions from a large reaction mechanism one or few reduced mechanisms are generated. The controlling parameter of the method is not directly related to the error of reduction.
2. New reduction philosophy: **SIMULATION ERROR MINIMIZATION**
Thousands of candidate reduced mechanisms are generated in a guided way. The best mechanism (smallest reduction error and/or fastest simulation) is accepted.
3. **SEM-CM**: guided building up of a series of consistent reduced mechanisms, starting from the important species.
4. **SEM-PCAF**: optimized PCAF method for the elimination of redundant reactions
5. **SEM-CM** and **SEM-PCAF** together are very effective for the reduction of large reaction mechanisms

T. Nagy, T. Turányi: Reduction of very large reaction mechanisms using methods based on simulation error minimization, *Combust. Flame*, **156**, 417–428 (2009)

Topic 12: Reduction of reaction mechanisms 4: Lumping

reaction lumping;

species lumping:

linear lumping,
general nonlinear methods,
chemical lumping,
continuous lumping

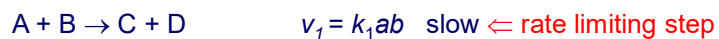
Reaction lumping

Lumping paralel reaction pathways



It generates exactly the same kinetic system of ODEs
Computer time is not saved

Reaction lumping based on the rate limiting step



Less stiff ODEs, computer time is saved

243

Species lumping

The mathematical definitions:

$$\frac{d\mathbf{Y}}{dt} = \mathbf{f}(\mathbf{Y}) \quad \text{Original kinetic system of ODEs, dimension of } \mathbf{Y} \text{ is } n$$

$$\frac{d\hat{\mathbf{Y}}}{dt} = \hat{\mathbf{f}}(\hat{\mathbf{Y}}) \quad \text{ODE for the lumped variables dimension } n' \leq n$$

$$\hat{\mathbf{Y}} = \mathbf{h}(\mathbf{Y}) \quad \text{Definition of lumped variables}$$

\mathbf{h} linear function \Rightarrow linear lumping
 \mathbf{h} nonlinear function \Rightarrow nonlinear lumping

identical solutions \Rightarrow exact lumping
almost identical solutions \Rightarrow approximate lumping

$\mathbf{Y}, \hat{\mathbf{Y}}$ some elements of these two vectors are identical
 \Rightarrow constrained lumping

244

Linear species lumping

$$\hat{\mathbf{Y}} = \mathbf{M}\mathbf{Y}$$

New variables are obtained by multiplying the original variable vector with a matrix

$$\mathbf{Y} = \mathbf{M}^{-1}\hat{\mathbf{Y}}$$

Regaining the original concentrations

\mathbf{M}

Lumping matrix ($n \times n'$)

Jacobian is constant

(= first order reactions only)

⇒ exact lumping is possible

Jacobian is not constant

⇒ no exact lumping

methods for approximate lumping
do not work well

245

Species lumping – a chemical approach

Lumping is frequently used in an intuitive way
„chemical approach”

If species with similar reactions and reactivity are present:

⇒ these species are lumped

⇒ concentration of the lumped species

= sum of the concentrations of the member species

called as the „*family method*” in atmospheric chemistry

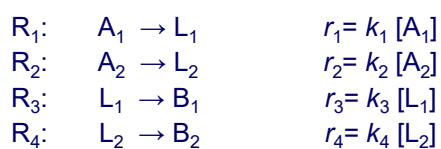
A more involved approach:

the reactivity of the member species are different

concentration of the lumped species

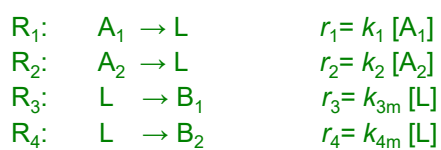
= **weighted** sum of the concentrations of the member species ²⁴⁶

Species lumping – a chemical approach



Species lumping: $[L] = [L_1] + [L_2]$

The mechanism after species lumping:



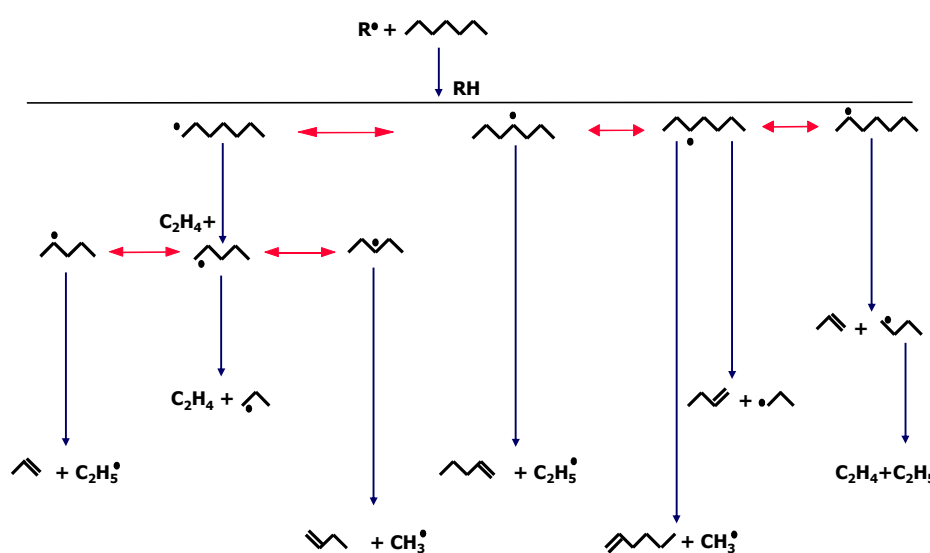
New rate coefficients:

$$k_{3m} = k_3 * [L_1]/[L]$$

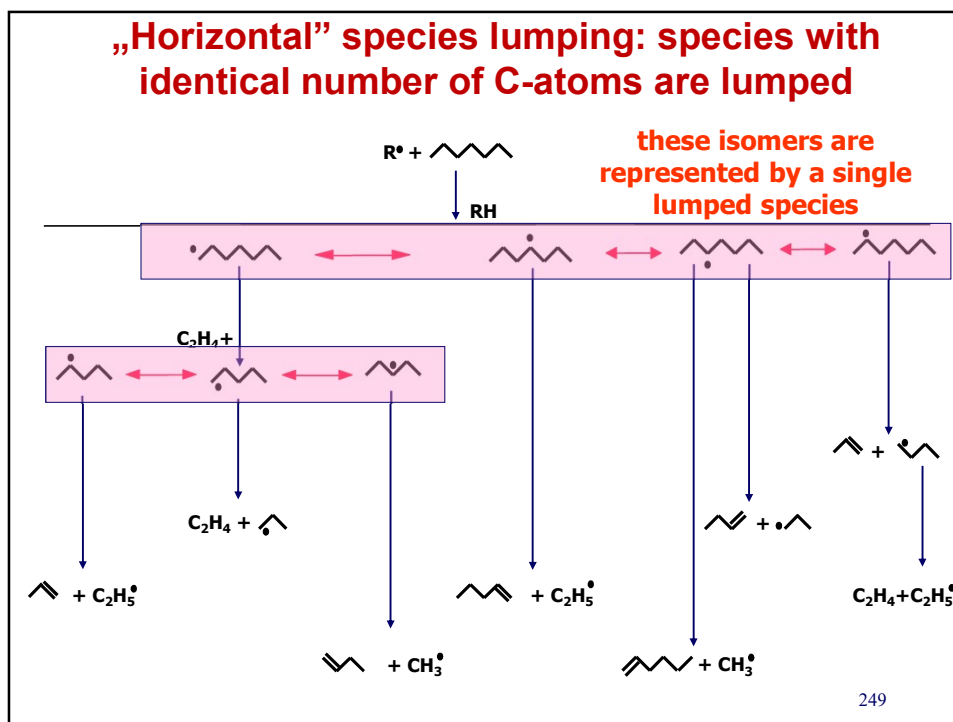
$$k_{4m} = k_4 * [L_2]/[L]$$

247

H abstraction reactions of *n*-heptane



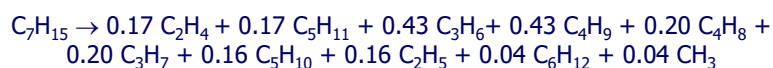
248



The lumped reaction obtained

reaction rates of the parallel reactions can be calculated at a given temperature \Rightarrow stoichiometric coefficients of the lumped reaction

The obtained lumped reaction at 1000 K:



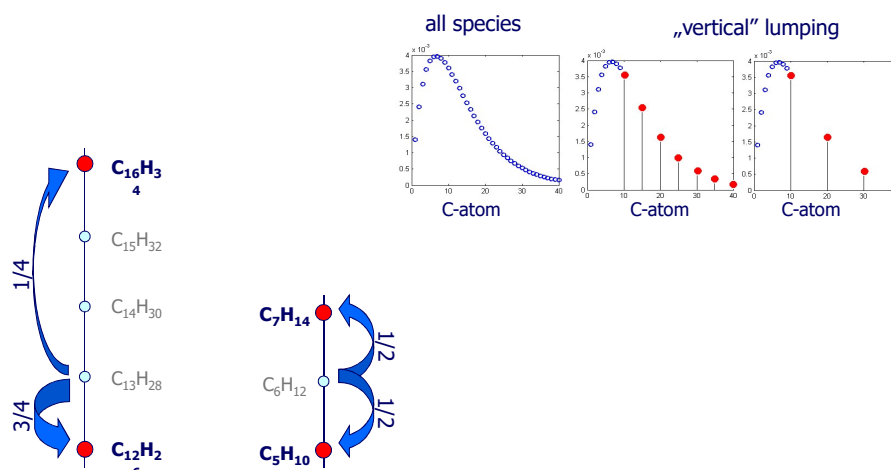
The stoichiometric coefficients of the lumped reaction change very little with changing temperature

| | 800 | 1000 | 1200 | 1500 |
|------------------------------------|------|------|-------|-------|
| CH₃ | 0.03 | 0.04 | 0.044 | 0.045 |
| C₂H₅ | 0.21 | 0.16 | 0.13 | 0.11 |
| C₃H₇ | 0.18 | 0.20 | 0.21 | 0.23 |
| C₄H₉ | 0.43 | 0.43 | 0.42 | 0.41 |
| C₅H₁₁ | 0.15 | 0.17 | 0.196 | 0.205 |

E. Ranzi, M. Dente, A. Goldaniga, G. Bozzano, T. Faravelli: Lumping procedures in detailed kinetic modeling of gasification, pyrolysis, partial oxidation and combustion of hydrocarbon mixtures. *Prog. Energy Combust. Sci.* **27**, 99-139 (2001)

„Vertical” species lumping

Similar types of species are identified (e.g. *n*-alkane, iso-alkane, alkene, ...), and these are represented by surrogate species having similar ranges of carbon atoms.



251

n-heptane primary oxidation reactions

Detailed Scheme

135 Primary reactions

38 Intermediate radicals

30 Primary products
(retaining nC_7 structure)

3 *n*-heptenes
8 cyclic-ethers
4 hydroperoxides
15 keto-hydroperoxides

Lumped Scheme

15 Primary lumped reactions

4 Intermediate lumped radicals

4 Primary lumped products

1 lumped *n*-heptene
1 lumped cyclic-ether
1 lumped hydroperoxide
1 lumped keto-hydroperoxide

252

Continuous lumping

Continuous species

species in a petroleum feedstocks, polymerisation systems

- very large numbers of species (several hundred thousands)
- can be ordered according to a chemical or physical feature (e.g. molecular weight)
- a feature is a continuous function of the ordering variable (e.g. the melting point and the reactivity of the oligomers is a smooth function of the number of monomer units in the oligomer species.)

Using probability density function (*pdf*) of the feature instead of the concentrations of the individual species

= the many discrete species are represented by a continuum

The chemical reactions modify this *pdf*.

R. Aris, G. R. Gavalas: On the theory of reactions in continuous mixtures
Philos. Trans. R. Soc. A **260**, 351-393 (1966)

M.S. Okino, M.L. Mavrouniotis: Simplification of mathematical models of chemical reaction systems. *Chem. Rev.* **98**, 391-408 (1998)

253

Topic 13: Reduction of reaction mechanisms 4: Time scales

history of the quasi steady-state approximation,

calculation of the local QSSA error,

interpretation of QSSA,

Computational Singular Perturbation (CSP)

reduction of models in reaction kinetics with direct calculation of slow manifolds (ILDIM),
reaction diffusion manifolds (REDIM)

repro-modelling

History of the quasi-steady state approximation

1913 – 1960: analytical solution of the kinetic ODEs

Bodenstein (1913): analytical solution to the equations of the H_2/Br_2 reaction system

Szemenjov (1939): applied the QSSA for a part of the intermediates only

1960 – 1971: conversion of the stiff ODEs to non-stiff ODEs

Edelson (1973) claimed that the stiff ODEs can already be solved directly (no need for the QSSA); nobody can assess the error introduced by the application of the QSSA \Rightarrow **QSSA should be banned**

1971 – : production of skeleton models from detailed mechanisms for solving PDEs

theoretical study of the QSSA method: (about 60 articles)

main lines:

- justification of the application of QSSA for small mechanisms
- singular perturbation: analytical investigation of small systems

An early general article and its commented English translation.

We developed this line further, see the following coming pages.

D. A. Frank-Kamenetskii: Условия применимости метода Боденштейна в химической кинетике (Conditions for the applicability of the Bodenstein method in chemical kinetics) *Ж. Физ. Хим.* (Zh. Fiz. Him.) **14**, 695-700 (1940)

T. Turányi, J. Tóth: Comments to an article of Frank-Kamenetskii on the quasi-steady-state approximation. *ACH Models In Chemistry* **129**, 903-907 (1992)

255

Quasi-steady-state approximation (QSSA)

The original kinetic system of differential equations:

$$d\mathbf{c}/dt = \mathbf{f}(\mathbf{c}, \mathbf{k}), \quad \mathbf{c}(0) = \mathbf{c}_0$$

The concentration vector is divided to two parts:

$\mathbf{c}^{(1)}$ concentration vector of non-QSSA species

$\mathbf{c}^{(2)}$ concentration vector of QSSA species

The Jacobian:
$$\mathbf{J} = \begin{pmatrix} \mathbf{J}^{(11)} & \mathbf{J}^{(12)} \\ \mathbf{J}^{(21)} & \mathbf{J}^{(22)} \end{pmatrix} = \begin{pmatrix} \partial \mathbf{f}^{(1)} / \partial \mathbf{c}^{(1)} & \partial \mathbf{f}^{(1)} / \partial \mathbf{c}^{(2)} \\ \partial \mathbf{f}^{(2)} / \partial \mathbf{c}^{(1)} & \partial \mathbf{f}^{(2)} / \partial \mathbf{c}^{(2)} \end{pmatrix}$$

Quasi-steady-state approximation:

$$d\mathbf{c}^{(1)}/dt = \mathbf{f}^{(1)}(\mathbf{c}, \mathbf{k})$$

$$\mathbf{0} = \mathbf{f}^{(2)}(\mathbf{c}, \mathbf{k})$$

$$\mathbf{c}(0) = \mathbf{c}_0$$

\Leftarrow denote $\mathbf{C}^{(2)}$ the concentration vector calculated from the algebraic equation

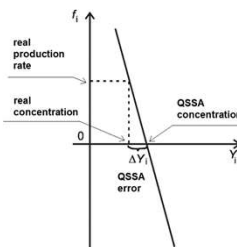
256

The local error of the QSSA

$$\Delta \mathbf{c} = \mathbf{c}^{(2)} - \mathbf{C}^{(2)} \quad \text{Local error of the QSSA}$$

Taylor expansion of the production rate of the QSSA species at the QSSA concentrations:

$$\frac{d\mathbf{c}^{(2)}}{dt} = \underbrace{\mathbf{f}^{(2)}(\mathbf{c}, \mathbf{k})}_{\mathbf{0}} \Big|_{\mathbf{c}=\mathbf{C}} + \mathbf{J}^{(22)} \Delta \mathbf{c}^{(2)}$$



Calculation of the local error for several QSSA species:

$$d\mathbf{c}^{(2)}/dt = \mathbf{J}^{(22)} \Delta \mathbf{c}^{(2)}$$

Calculation of the local error for a single QSSA species:

$$\frac{dc_i}{dt} = J_{ii} \Delta c_i \quad \Rightarrow \quad -\Delta c_i = \left(\frac{-1}{J_{ii}} \right) \frac{dc_i}{dt}$$

error of QSSA approximation = lifetime × production rate of the species

T. Turányi, A. S. Tomlin, M. J. Pilling: On the error of the quasi-steady-state approximation. J. Phys. Chem. **97**, 163-172 (1993)

257

Example: QSSA error at methane pyrolysis

The QSSA local error of **each** species at 50 s

| | relative error | absolute error |
|------------------|----------------|-----------------------|
| 19. CH3 | -6.200E-01 % | -2.631E-13 mole/cm**3 |
| 20. CH3CH2CH3 | -5.284E-01 % | -4.568E-14 mole/cm**3 |
| 21. CH.=CHCH2CH3 | 5.050E-01 % | 3.022E-21 mole/cm**3 |
| 22. (CH3)2C=CH. | 4.889E-01 % | 1.708E-19 mole/cm**3 |
| 23. C2H5 | 4.013E-01 % | 2.989E-16 mole/cm**3 |
| 24. CH≡CCH2. | -3.385E-01 % | -4.109E-14 mole/cm**3 |
| 25. CH2=CHCH=CH2 | 3.062E-01 % | 8.733E-13 mole/cm**3 |
| 26. CH.=CHCH3 | 3.030E-01 % | 4.148E-18 mole/cm**3 |
| 27. C2H3 | 2.612E-01 % | 1.241E-16 mole/cm**3 |
| 28. CH2=CHCH2. | 2.134E-01 % | 1.153E-14 mole/cm**3 |
| 29. CH≡CCH3 | -2.040E-01 % | -1.283E-11 mole/cm**3 |
| 30. CH2 | 1.591E-01 % | 1.041E-20 mole/cm**3 |
| 31. C | -1.366E-01 % | -8.633E-30 mole/cm**3 |
| 32. CH2=C.CH3 | 1.364E-01 % | 5.094E-18 mole/cm**3 |
| 33. CH2S | 1.025E-01 % | 5.811E-23 mole/cm**3 |
| 34. H | 7.083E-02 % | 1.699E-16 mole/cm**3 |
| 35. CH2=C=CH2 | -6.929E-02 % | -1.209E-12 mole/cm**3 |

258

Direct calculation of slow manifolds

\mathbf{y}^M a point „on the surface” of the manifold

$\mathbf{f}(\mathbf{y}^M)$ velocity of the point
„on the surface” of the manifold

\mathbf{W}_s tangent plane of the manifold
in this point (includes vector \mathbf{f})

\mathbf{W}_f vector of fast directions
linearly independent of \mathbf{W}_s

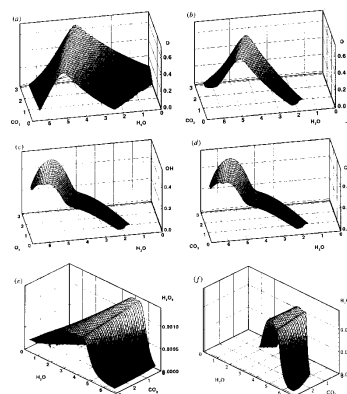
$\mathbf{f}(\mathbf{y}^M)$ this vector is orthogonal
to the \mathbf{w}_f vectors:

$$\mathbf{W}_f \mathbf{f}(\mathbf{y}^M) = 0$$

1. Selection of the dimension (denote n_D)
2. Selection of n_D variables used for parameterization (vector \mathbf{x}).
The equation above defines all other concentrations that belong to the manifold as a function of vector \mathbf{x} .

PROBLEM: numerically ill-conditioned task, because vectors \mathbf{W}_f have frequently almost identical direction.

259



Numerical determination of slow manifolds

Numerically more stable is the
Schur decomposition of the Jacobian:

$$\mathbf{Q}^T \mathbf{J} \mathbf{Q} = \begin{pmatrix} \mathbf{J}'^{(11)} & \mathbf{J}'^{(12)} \\ 0 & \mathbf{J}'^{(22)} \end{pmatrix}$$

eigenvalues of matrix \mathbf{N}_s $\lambda_1, \lambda_2, \dots, \lambda_m$

eigenvalues of matrix \mathbf{N}_f $\lambda_{m+1}, \dots, \lambda_n$ and $\text{Re}(\lambda_i) \geq \text{Re}(\lambda_j)$ if $i < j$,
thus \mathbf{Q}_f belongs to the fast modes.

The following equation is solved: $\mathbf{Q}_f(\mathbf{Y}) \mathbf{f}(\mathbf{Y}) = 0$

ILDM: Intrinsic Low-Dimensional Manifolds

Using the ILDM in simulations: a look-up table contains

- the change of parameterizing variables in time ($d\mathbf{Y}_p/dt$)
- the related values of all other concentrations

simulations =

solution of the small ODE + search in the table

260

REDIM: reaction diffusion manifolds

In most of these slides the reduction of spatially homogeneous chemical kinetic systems is discussed.

However, in some systems the chemical reactions and the effect of chemical flows have to be simulated together:

$$\frac{\partial \Psi}{\partial t} = \mathbf{F}(\Psi) - \vec{v} \cdot \text{grad} \Psi + \frac{1}{\rho} \text{div} \mathbf{D} \text{grad} \Psi$$

- Ψ is the vector of thermokinetic state
with elements specific enthalpy h , the pressure P , mass fractions w_i
- \mathbf{F} chemical source term
- \vec{v} flow velocity
- ρ density
- \mathbf{D} matrix of transport coefficients

V. Bykov, U. Maas: The extension of the ILDM concept to reaction-diffusion manifolds.
Combust. Theory Model. **11**, 839-862 (2007)

261

REDIM: reaction diffusion manifolds 2

Possible cases:

- 1 fast chemistry – slow transport:
the concentration changes are dictated by the chemistry only

- 2 fast chemistry – moderately fast transport:
the manifolds are dictated by the chemistry
with perturbation by the diffusion

U. Maas, S. B. Pope: Laminar flame calculations using simplified chemical kinetics based on intrinsic low-dimensional manifolds. *Proc. Combust. Inst.* **25**, 1349-1356 (1994)

- 3 fast chemistry – fast transport:
a joint manifold has to be determined,
dictated by both the chemistry and the diffusion
⇒ REDIM: reaction-diffusion manifolds

U. Maas, V. Bykov: The extension of the reaction/diffusion manifold concept to systems with detailed transport models. *Proc. Combust. Inst.* **33**, 1253-1259 (2011)

262

Computational Singular Perturbation (CSP)

Assume that there are M fast modes in an n -variate dynamical system
Denote Ω an $(n-m)$ -dimensional manifold

vectors $\mathbf{a}_i, i = 1, \dots, M$ span the fast subspace

vectors $\mathbf{a}_i, i = M+1, \dots, n$ span the manifold

$$\mathbf{A}_r = [\mathbf{a}_1, \mathbf{a}_2, \dots, \mathbf{a}_m]$$

$$\mathbf{A}_s = [\mathbf{a}_{m+1}, \mathbf{a}_{m+2}, \dots, \mathbf{a}_n]$$

production rates: $\mathbf{f} = \mathbf{f}_{\text{fast}} + \mathbf{f}_{\text{slow}}$

fast directions of production rates:

$$\mathbf{f}_{\text{fast}} = \mathbf{A}_r \mathbf{z}$$

production rates along the surface:

$$\mathbf{f}_{\text{slow}} = \mathbf{A}_s \mathbf{z}$$

fast amplitudes

$$\mathbf{z}_{\text{fast}} = \mathbf{B}_r \mathbf{f}$$

slow amplitudes

$$\mathbf{z}_{\text{slow}} = \mathbf{B}_s \mathbf{f}$$

Matrices \mathbf{A} and \mathbf{B} are orthogonal

S. H. Lam, D. A. Goussis: Understanding complex chemical kinetics with computational singular perturbation. *Proc. Combust. Inst.* **22**, 931-941 (1988)

263

CSP 2

Matrices \mathbf{A} and \mathbf{B} are obtained by an iterative „refinement procedure”
from the Jacobian

The value of the amplitude allows sorting the modes:

z always zero

conserved property

in classic kinetics: e.g. element conservation

z was large \Rightarrow now z almost zero

exhausted mode

in classic kinetics: QSSA, partial equilibrium

z almost zero \Rightarrow may become large

dormant mode

in classic kinetics: pool component on the actual time scale

z large now

active mode

movement of the trajectory along the manifold

264

CSP 3

The CSP analysis is based on the application of a series of pointers:

1 CSP Participation Index

z_k^m denotes the contribution of the k -th reaction step to the m -th fast amplitude:

$$z^m = z_1^m + z_2^m + \dots + z_{N_r}^m \approx 0$$

$$z^m = \mathbf{b}^m \mathbf{f}, \quad m=1, \dots, M \quad \text{amplitude of the } m\text{-th fast mode}$$

$$z_k^m = (\mathbf{b}^m \mathbf{v}_k) r_k \quad \begin{array}{l} \mathbf{v}_k \text{ stoichiometric vector of reaction } k \\ r_k \text{ rate of reaction } k \end{array}$$

$$P_k^m = \frac{z_k^m}{\sum_j |z_j^m|} \quad \text{CSP Participation Index}$$

The sum of the absolute values of P_k^m is equal to unity. A relatively large P_k^m value indicates that the k -th reaction step is a significant participant in the m -th equilibrium.

D. A. Goussis, P. D. Kourdis: Glycolysis in *saccharomyces cerevisiae*:
Algorithmic exploration of robustness and origin of oscillations. *Math. Biosci.* **243**, 190–214 (2013)

CSP 4

2 CSP Importance Index

contribution of the k -th reaction step to the evolution of the n -th variable on the manifold

$$f_{slow}^n = f_{slow}^{n,1} + f_{slow}^{n,2} + \dots + f_{slow}^{n,N_r}$$

$$f_{slow}^{n,k} = \sum_{j=M+1}^{N_s} a_j^n (\mathbf{b}^j \mathbf{v}_k) r_k, \quad k=1, \dots, N_r \quad \begin{array}{l} a_j^n \text{ denotes the } n\text{-th element of} \\ \text{column vector } \mathbf{a}_j \text{ in matrix } \mathbf{A}_s \end{array}$$

$$I_k^n = \frac{f_{slow}^{n,k}}{\sum_j |f_{slow}^{n,k}|} \quad \text{CSP Importance Index}$$

The sum of the absolute values of I_k^n is equal to unity. A relatively large I_k^n value indicates that the k -th reaction step has a significant contribution to the change of the n -th variable on the manifold.

CSP 5

3 CSP Pointer (earlier name: „radical pointer”)

Identification of variables (*i.e.* species concentrations) that have a large contribution to the exhausted modes.

$$\mathbf{D}_m = \text{diag}[\mathbf{a}_m \mathbf{b}^m] \quad \text{CSP Pointer}$$

A value of D_m^i close to unity indicates that the i -th variable is strongly connected to the m -th mode and its corresponding time-scale.

D_m^i identifies the QSS-species and the non-QSS-species participating in fast equilibria

Application of CSP for mechanism reduction: a non-stiff reduced model can be obtained that well describes the change of modes belonging to the characteristic time-scale of the system.

M. Valorani, F. Creta, D. A. Goussis, J. Lee, H. Najm: An automatic procedure for the simplification of chemical kinetic mechanisms based on CSP. *Combust. Flame* **146**, 29–51 (2006)

Repromodelling

Stages of reduction of a detailed reaction mechanism

original stiff ODE, many variables **SLOW SIMULATION**

→ making a **skeleton mechanism**
(by elimination of redundant species and reactions, lumping)
FASTER

skeleton mechanism → manifold based mathematical model (ODE)

skeleton mechanism → difference equations obtained by the repromodelling method **FASTEST**

Principle of repromodelling:

The chemical kinetic model is simulated several thousand times at different conditions. A polynomial is fitted to the simulation results. In the further simulations the fitted polynomial is used, instead of solving again the differential equations.

268

Repromodel from skeleton models

We have a skeleton mechanism having few species.

The kinetic simulation has a natural timescale and natural time step Δt .

The solutions of the ODE (calculated concentrations) are printed at every Δt times:

$\mathbf{c}(t)$, $\mathbf{c}(t+\Delta t)$, $\mathbf{c}(t+2\Delta t)$, $\mathbf{c}(t+3\Delta t)$, etc.

Building a database from the simulation results:

$\mathbf{c}(t) \rightarrow \mathbf{c}(t+\Delta t)$

$\mathbf{c}(t+\Delta t) \rightarrow \mathbf{c}(t+2\Delta t)$

$\mathbf{c}(t+2\Delta t) \rightarrow \mathbf{c}(t+3\Delta t)$

Fitting function \mathbf{G} to the data: $\mathbf{c}(t+\Delta t) = \mathbf{G}(\mathbf{c}(t))$

This is a system of difference equations.

Recursive application of \mathbf{G} results in concentration-time functions with resolution Δt

number of variables of function \mathbf{G} = number of variables of the skeleton model

Fast calculations, because the integrated solution is stored.

269

Repromodel from detailed mechanisms

Presence of a slow manifold:

The trajectory quickly approaches a n_1 dimensional slow manifold

The location of the points of the n_1 -dimensional manifold in the n -dimensional space of concentrations can be parameterized by vector \mathbf{x} of n_1 elements:

function \mathbf{G}_2 : $\mathbf{c}(t) = \mathbf{G}_2(\mathbf{x}(t))$

Movement on the manifold during time Δt is characterized by function \mathbf{G}_1 :

$\mathbf{x}(t+\Delta t) = \mathbf{G}_1(\mathbf{x}(t))$

functions \mathbf{G}_1 and \mathbf{G}_2 can be determined by repro-modelling:

- Selection of Δt and n_1
- Building a database from the simulation results of the detailed mechanism:

$\mathbf{c}(t) \rightarrow \mathbf{c}(t+\Delta t)$

$\mathbf{c}(t+\Delta t) \rightarrow \mathbf{c}(t+2\Delta t)$

$\mathbf{c}(t+2\Delta t) \rightarrow \mathbf{c}(t+3\Delta t)$

- Fitting functions \mathbf{G}_1 and \mathbf{G}_2 to the data.

Original detailed mechanism: n variables; \mathbf{G}_2 repromodel: $n_1 < n$ variables

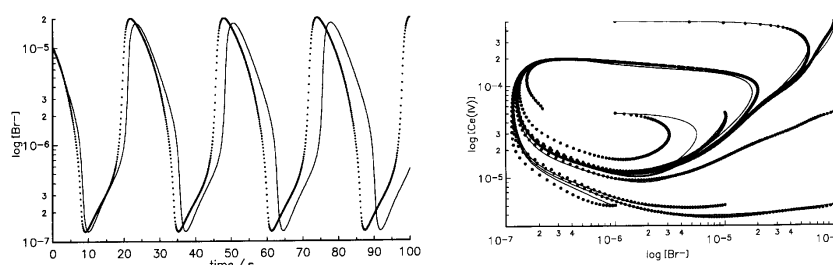
The calculation is much faster, because the repromodel has fewer variables AND because of the integrated results are fitted (e.g.: $n = 50$, $n_1 = 3$)

270

Example 1: the Oregonator model

3-variable skeleton model of the Belousov-Zhabotinskii reaction
 200 simulations started from the neighborhood of the limit cycle
 Result: 20 thousand $\mathbf{c}(t)$, $\mathbf{c}(t+\Delta t)$ datasets

Up to 8th order, 3-variate polynomials were fitted using the
 Gram-Schmidt orthonormalization process



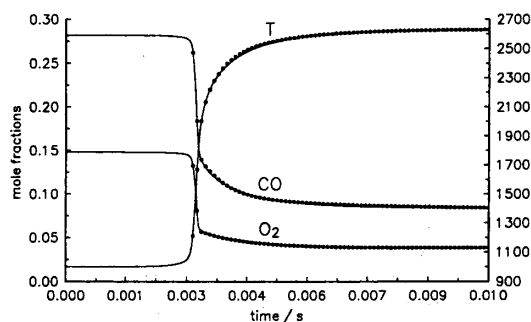
The repromodel can be calculated 60 times faster
 than the solution of the ODE of the Oregonator model

271

Example 2: ignition of CO/H₂/air mixtures

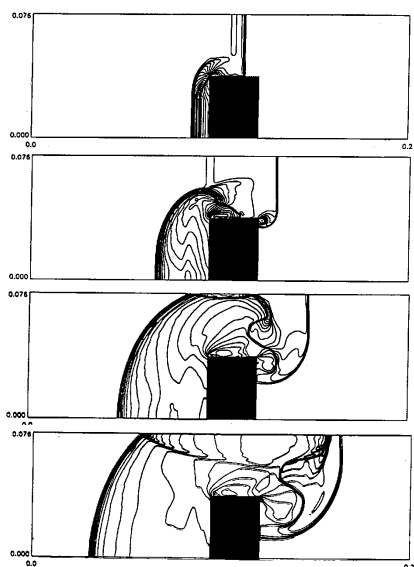
Detailed mechanism: 67 reactions of 13 species
 The ignition can be characterized by a 3-dimensional manifold (Maas and Pope (1992))
 $\phi=0.5-1.5$, H:C=1:10, $T=990-1010$ K; 300 random initial compositions
 $\Delta t = 10^{-4}$ s time step, $t_{\text{final}} = 0.01$ s
 The database contains 30000 entries.
 A 4th order polynomials were fitted to the change of
 temperature and the mole fractions of CO and O₂.

The repromodel calculated 11700 times faster
 the change of T , X_{CO} and X_{O_2} during the ignition of CO/H₂/air mixtures



272

Example 3: Spread of detonation wave in a $\text{H}_2/\text{O}_2/\text{Ar}$ mixture



273

Spread of detonation wave in $\text{H}_2/\text{O}_2/\text{Ar}$ mixture



Calculated density map based on a detailed
hydrogen combustion mechanism (9 variables)



Calculated density map based on a repromodel
(polynomial approximation with 3 variables)
100 times faster

274

Overview of mechanism reduction methods

I. without time scale analysis

1. determination of a skeleton mechanism (a part of the original one)
elimination of redundant species and reactions
⇒ smaller kinetic system of ODEs
2. species lumping and reaction lumping
⇒ smaller kinetic system of ODEs

II. using time scale analysis

1. classic methods: QSSA and partial equilibrium
⇒ smaller kinetic system of ODEs or
coupled differential/algebraic equations
2. slow manifolds
⇒ smaller kinetic system of ODEs
3. reparamodelling
⇒ difference equations

275

Topic 14: Similarity of sensitivity functions

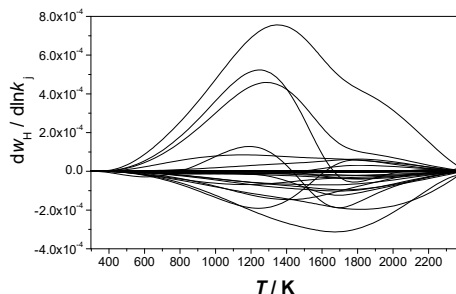
local similarity, scaling relationships, global similarity,

the origin of similarity,

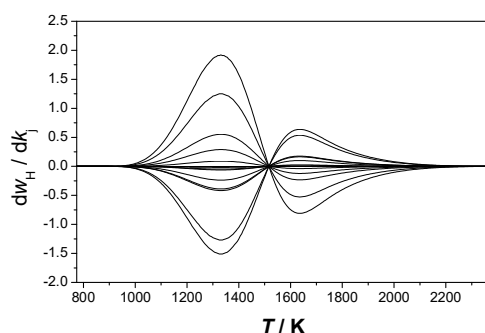
correlation of sensitivity vectors,

consequences of global similarity
on the interpretation of models

What is the similarity of sensitivity functions?



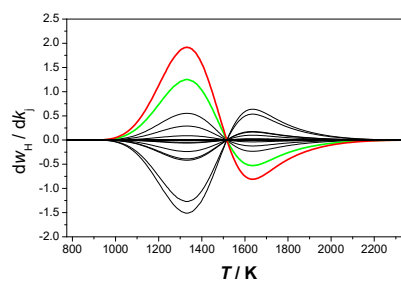
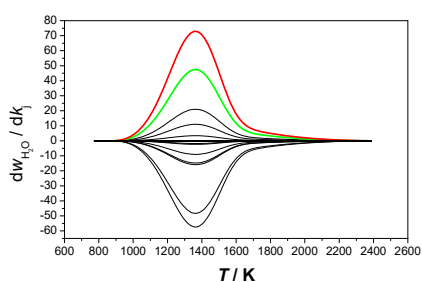
Generally, the sensitivity functions are not related, therefore they usually look scrabled.



Several researchers discovered that in some systems the sensitivity functions look very regularly.

277

Regularity 1: Local similarity of the sensitivity functions



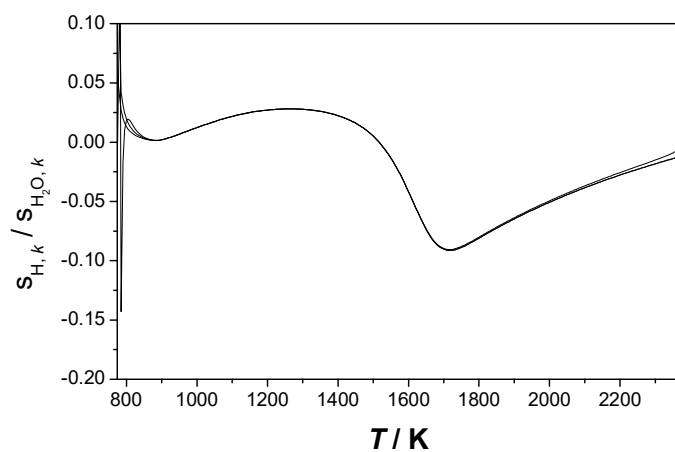
$$\lambda_{ij}(t) = \frac{s_{ik}(t)}{s_{jk}(t)}$$

[red is divided by red, green is divided by green]

278

Regularity 1: Local similarity of the sensitivity functions 2

$$\lambda_{ij}(t) = \frac{s_{ik}(t)}{s_{jk}(t)}$$



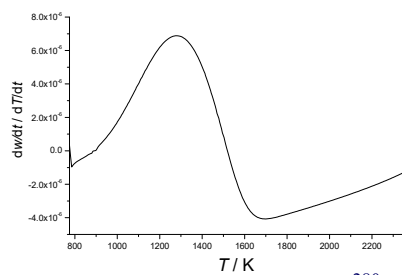
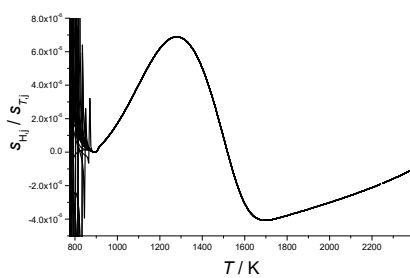
279

Regularity 2: Scaling relation

$$\lambda_{ij}(t) = \frac{s_{ik}(t)}{s_{jk}(t)}$$

$$\lambda'_{ij}(t) = \frac{\frac{dY_i(t)}{dt}}{\frac{dY_j(t)}{dt}}$$

$$\lambda_{ij}(t) = \lambda'_{ij}(t)$$

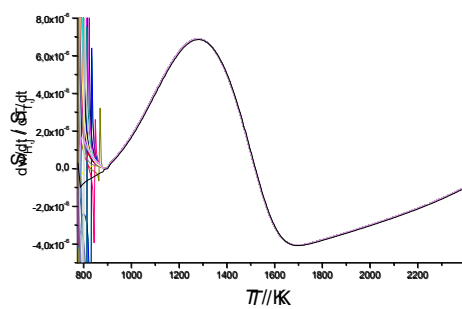


280

Regularity 2: Scaling relation 2

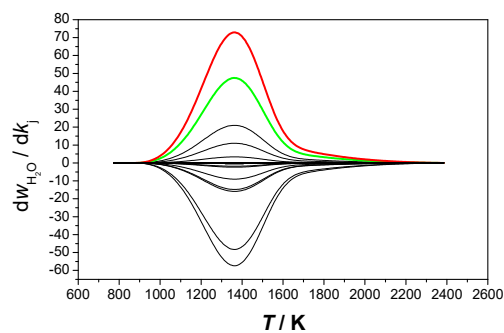
$$\lambda_{i,j}(t) = \frac{s_{i,k}(t)}{s_{j,k}(t)}$$

$$\lambda'_{i,j}(t) = \frac{\frac{dY_i(t)}{dt}}{\frac{dY_j(t)}{dt}}$$



281

Regularity 3: Global similarity of the sensitivity functions



$$\mu_{ikm}(t) = \frac{s_{ik}(t)}{s_{im}(t)}$$

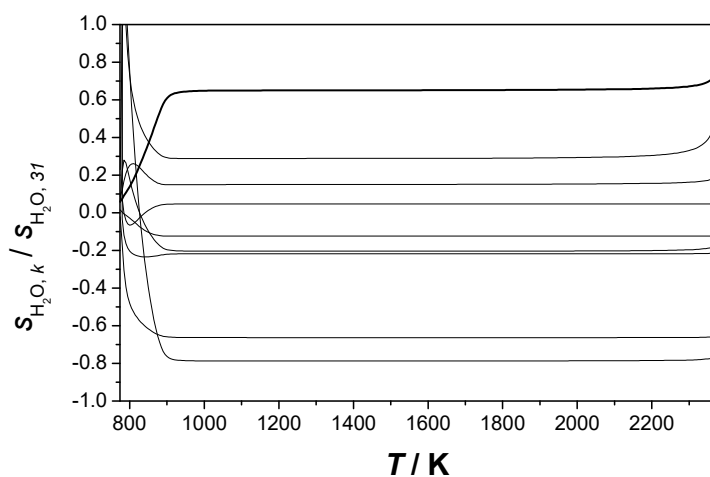
[red is divided by green]

282

Regularity 3: Global similarity of the sensitivity functions 2

$$\mu_{km} = \frac{s_{ik}(t)}{s_{im}(t)}$$

ratio is constant
in a wide range of the independent variable

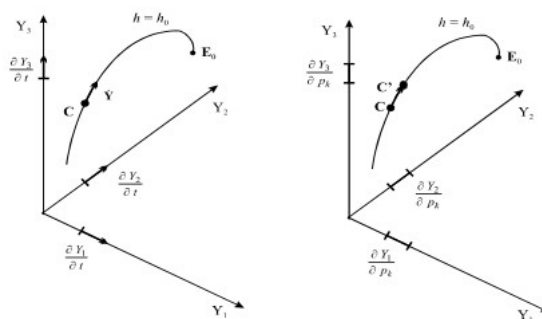


283

Origin of local similarity and scaling relation on a 1D manifold – geometry based reasoning

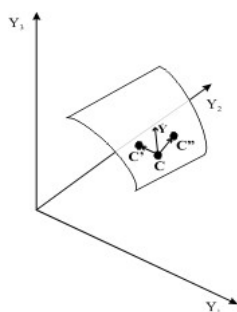
Necessary conditions:

1. The trajectory of the solution follows a 1D manifold
2. 1D manifold is not shifted due to parameter changes



284

Movement on a non-1D manifold



dimension of the manifold is larger than one ($n > 1$)

⇒ the sensitivity vectors are usually not parallel to the vector of production rates

⇒ local similarity and scaling relation will not emerge, but all these vectors are within an n -dimensional subspace

consequence:

dimension of the manifold \geq rank of the sensitivity matrix

285

Origin of local similarity and scaling relation on a 1D manifold – calculus based reasoning

equation of 1D manifold:

Y_i parameterising variable

F_i value of variable i

z independent variable (e.g. time)

$$Y_i(z, \mathbf{p}) = F_i(Y_1(z, \mathbf{p}))$$

Derivation with respect z

$$\frac{\partial Y_i(z, \mathbf{p})}{\partial z} = \frac{\partial F_i}{\partial Y_1} \frac{\partial Y_1(z, \mathbf{p})}{\partial z}$$

Derivation with respect p_j

$$\frac{\partial Y_i(z, \mathbf{p})}{\partial p_j} = \frac{\partial F_i}{\partial Y_1} \frac{\partial Y_1(z, \mathbf{p})}{\partial p_j}$$

Joining the two equations above:
(this is a general equation,
since the selection of y_1 is arbitrary)

$$\frac{\frac{\partial Y_i(z)}{\partial p_j}}{\frac{\partial Y_1(z)}{\partial p_j}} = \frac{\frac{\partial Y_i}{\partial z}}{\frac{\partial Y_1}{\partial z}}$$

286

Dimension of the manifold \geq rank of matrix **S** (calculus based reasoning)

equation on *n-dimensional manifold*

Y_1, Y_2, \dots, Y_n are the parameterizing variables

F_i value of variable i

z independent variable (e.g. time)

$$Y_i(z, \mathbf{p}) = F_i(Y_1(z, \mathbf{p}), Y_2(z, \mathbf{p}), \dots, Y_n(z, \mathbf{p}))$$

Derivative with
respect p_j

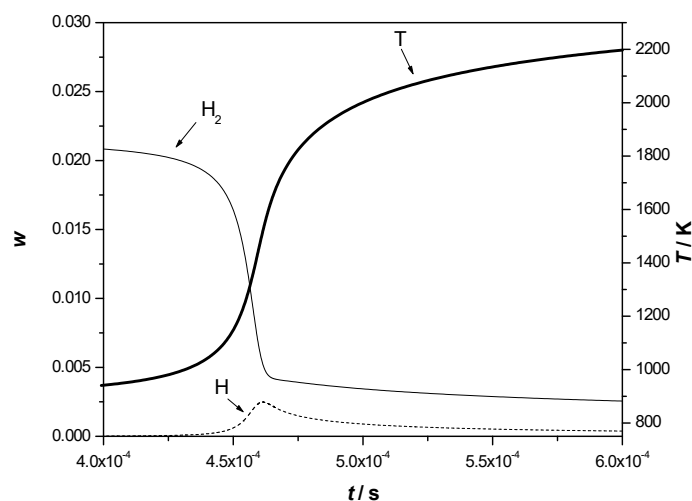
$$\frac{\partial Y_i}{\partial p_j} = \left(\frac{\partial F_i}{\partial Y_1} \right) \left(\frac{\partial Y_1}{\partial p_j} \right) + \left(\frac{\partial F_i}{\partial Y_2} \right) \left(\frac{\partial Y_2}{\partial p_j} \right) + \dots + \left(\frac{\partial F_i}{\partial Y_n} \right) \left(\frac{\partial Y_n}{\partial p_j} \right)$$

rank of matrix **S**
is at most n

$$\mathbf{s}_j^T = \lambda_{j1} \mathbf{s}_1^T + \lambda_{j2} \mathbf{s}_2^T + \dots + \lambda_{jn} \mathbf{s}_n^T$$

287

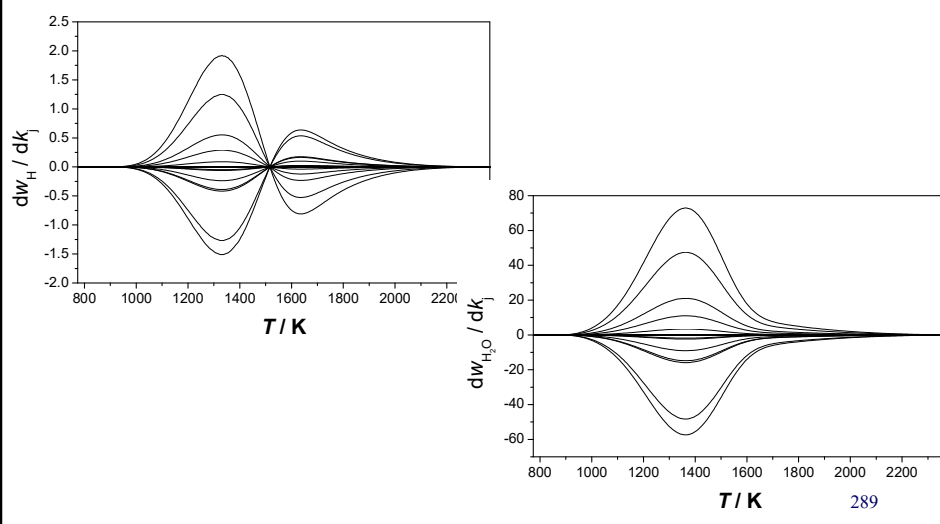
Adiabatic explosion of H_2 -air mixtures



288

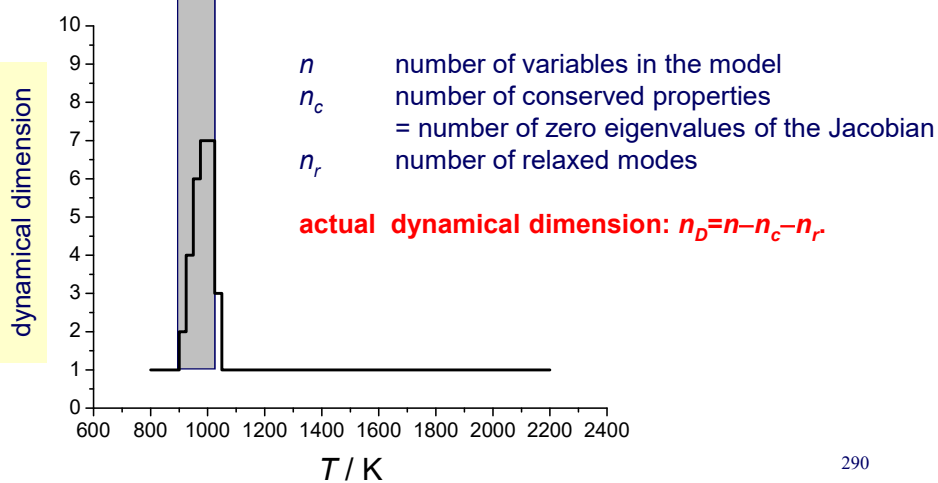
The sensitivity functions related to the adiabatic explosion of H₂–air mixtures...

... are very nice looking!



Change of dimension during adiabatic hydrogen/air explosion

grey region: here the largest eigenvalue is positive



Adiabatic hydrogen/air explosion

Local similarity:

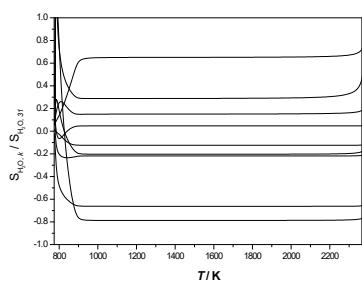
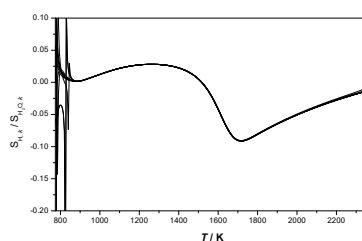
YES

Scaling relation:

YES

Global similarity:

YES



291

Why is global similarity important?

a very simple mechanism:



the corresponding ODE:

$$\dot{x} = k_1 - k_2 x$$

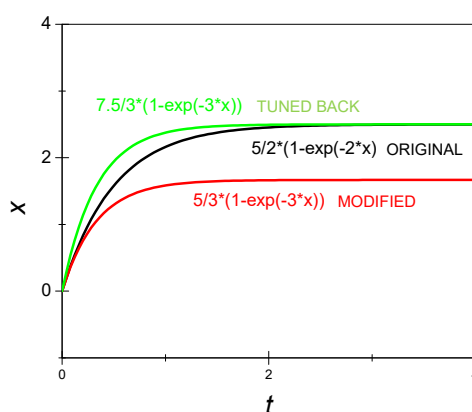
analytical solution:

$$x = \frac{k_1}{k_2} (1 - e^{-k_2 t})$$

In this model the sensitivity functions do not show global similarity.

If k_2 is changed,
it cannot be compensated
by changing k_1
The concentration curve of X
is not reproduced.

(Proper tuning of k_1 reproduces X at later times,
but not at early times.)

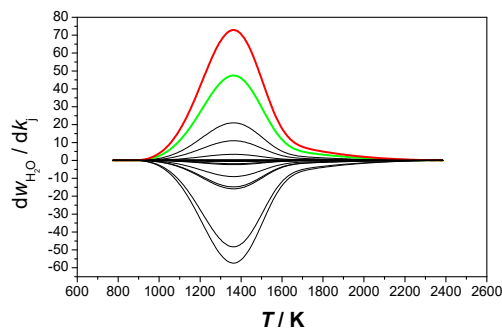


292

Regularity 3: Global similarity of the sensitivity functions

$$\mu_{ikm}(t) = \frac{s_{ik}(t)}{s_{im}(t)}$$

[red is divided by green]



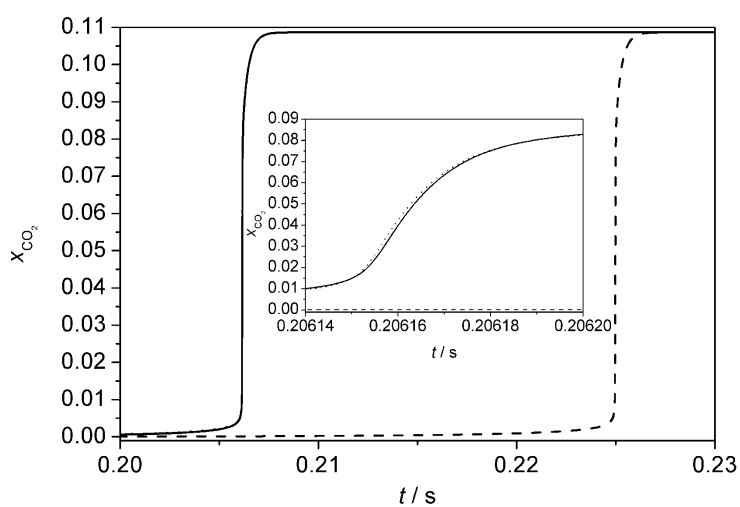
- 1 Global similarity means that a larger change of the green parameter may have identical effect to a smaller change of the red parameter at all times.
- 2 Global similarity means that a larger change of the green parameter can be fully compensated by a smaller negative change of the red parameter at all times.

293

Why is global similarity important?

calculated
mole fraction of CO₂

— methane explosion (calculated by the original mechanism)
 --- 4 important parameters are changed by 50%
 5th parameters is also changed by 9.875%



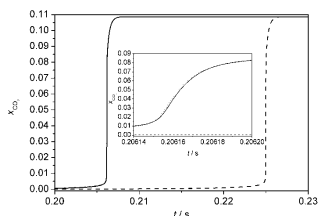
294

Why is global similarity important 2

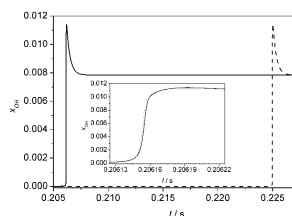
— methane explosion (calculated by the original mechanism)

--- 4 important parameters are changed by 50%

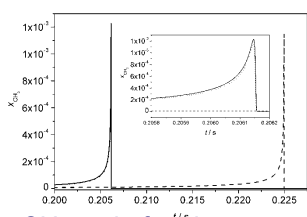
..... 5th parameters is **also** changed by 9.875%



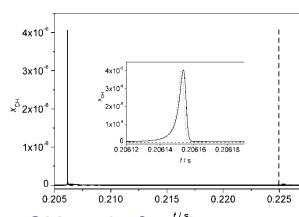
CO₂ mole fraction



OH mole fraction



CH₃ mole fraction



CH mole fraction

the original concentration curves are obtained back
for all variables and in the whole time interval

295

In the case of global similarity ...

Empirical models

These can be tuned with a single arbitrary but effective parameter

Physical models

The simulation results can be „validated” by indirect simulations,
BUT the fitted parameter values in general has no physical meaning.
(e.g. wrong k values can be obtained from flame measurements)

Self-regulation of cells

changing a single parameter may restore the optimal time profile
of all species.

New tool for the design of medical drugs

Current approach for the design of drugs: the wrong part is fixed.

Systems biology models of organs or cells allow

the identification of the group of globally similar parameters.

Tuning any parameter within this group may restore the original functioning.

296

Are the parameter sets of systems biology models unique?

We have investigated 8 models of systems biology
cell cycle – chemotaxis – HIV virus proliferation
(ODE models describing enzyme kinetic systems)

We have found the similarity of sensitivity functions in 7 models.

The required two features of the model

Presence of very different time scales

⇒ **low dimensional manifolds are present
in the variable (concentration) space**

Autocatalytic processes

⇒ pseudohomogeneity ⇒ **global similarity**

⇒ **infinite number of parameter sets
give exactly the same simulation results**

Significance of the similarity of sensitivity functions 1.

Information about the dynamic structure of the model

Similar sensitivity functions \Leftrightarrow

changing the corresponding parameters causes
qualitatively identical effect in different extent

⇒ **these parameters play similar role in the model**

Similarity of sensitivity functions is a new channel of information.

The usual wiring diagrams do not carry information on dynamics.

Significance of the similarity of sensitivity functions 2.

Robustness of living organisms

The environment of living organisms is continuously changing.
Changing temperature, salt content etc.

The automatic compensating mechanisms in living organisms maintain a near optimal operation in a changing environment
⇒ **ROBUSTNESS**

Robustness is an area of active research.

The similarity of sensitivity functions is one possible explanation to robustness.

Changing environment changes one or several parameters, but their effect can be fully compensated by changing another parameter having similar sensitivity function.

Significance of the similarity of sensitivity functions 3.

Correction of genetic errors

Most of the genetic errors are not lethal, but remove the organism from optimal operation.

Exact restoration of the original system by the same type of change in the DNA is very unlikely.

A situation of higher probability:

The genetic error changes a parameter in the biological system.
If a second genetic error appropriately changes another parameter and these two parameters have similar sensitivity function

⇒ **perfect correction of the first genetic change**

Significance of the similarity of sensitivity functions 4.

A new approach to design medical drugs

Assume, that human beings can be described by a multiparameter dynamic model. A part of the diseases (all?) can be related to wrong (tuned) parameters.

The healing effect of most of the current medical drugs is based on the restoration of the wrong function.

A possible alternative approach:

If the disease can be connected to a parameter that is related to effective parameters having similar sensitivity curves,

then the drug may tune these other parameters.

Is global similarity a general feature of dynamic models?

Most physical and chemical models describe interconnected fast and slow processes
 \Rightarrow existence of very different time scales
 \Rightarrow existence of attracting slow manifolds \Rightarrow **local similarity**

Dynamical systems close to the stationary (or equilibrium) point follow an attracting 1D manifold
 \Rightarrow 1D slow manifold \Rightarrow **scaling relation**

autocatalytic processes are widespread in chemical kinetics
 (e.g. explosions, runaways, molecular biology switches)

autocatalytic processes \Leftrightarrow pseudo homogeneity

local similarity & pseudo homogeneity of the ODE
 \Rightarrow **global similarity**

302

Topic 15: Computer codes for the study of complex reaction systems

general simulation codes in reaction kinetics,
simulation of gas kinetics systems,
analysis of reaction mechanisms,
investigation of biological reaction kinetic systems,
codes for global uncertainty analysis,
ReSpecTh information site

Reaction kinetics simulation codes

WINPP/XPP Windows simulation code

solving systems of ODEs, DAEs and PDEs.

The user has to provide the rate equations \Rightarrow applicable for small systems only

<http://www.math.pitt.edu/~bard/classes/wppdoc/readme.htm>

KPP: Kinetic Preprocessor <http://people.cs.vt.edu/~asandu/Software/Kpp/>

production of the kinetic ODE from the reaction mechanism

numerical solution of stiff ODEs; sparse matrix routines

V. Damian, A. Sandu, M. Damian, F. Potra, G. R. Carmichael:

The Kinetic PreProcessor KPP - A software environment for solving chemical kinetics.

Comp. Chem. Eng. **26**, 1567-1579 (2002)

SUNDIALS: SUite of Nonlinear and Differential/ALgebraic equation Solvers

<https://computation.llnl.gov/casc/sundials/main.html>

MATLAB interface to the following solvers:

CVODE solves initial value problems for ordinary differential equation (ODE) systems

CVODES solves ODE systems and includes sensitivity analysis capabilities

ARKODE solves initial value ODE problems with additive Runge-Kutta methods

IDA solves initial value problems for differential-algebraic equation (DAE) systems

IDAS solves DAE systems and includes sensitivity analysis capabilities

KINSOL solves nonlinear algebraic systems.

304

CHEMKIN

Developed at the SANDIA National Laboratories, Livermore, CA, USA

CHEMKIN-I (1975-1985)

CHEMKIN-II (1985-1995)

Simulation codes: SENKIN, PSR, PREMIX, SHOCK, EQLIB

+ utility programs, data bases

FORTTRAN codes, controlled by the input files

Kee R. J., Rupley F. M., Miller J. A.

CHEMKIN-II: A FORTRAN *Chemical Kinetics Package*

for the Analysis of Gas-Phase Chemical Kinetics

SANDIA report No. SAND79-8009B

Reaction Design www.reactiondesign.com (1995-)

Commercial codes; source code is not provided

Chemkin 3.x,

Graphical User Interface (GUI) to CHEMKIN-II

Chemkin 4.x

really new solvers, graphical interface, versatile

Chemkin Pro

Chemkin + additional utility codes (e.g. pathway plotting)

305

CHEMKIN simulation codes

www.reactiondesign.com

CHEMKIN → CHEMKIN -II → CHEMKIN 3 → CHEMKIN 4 → CHEMKIN PRO

CHEMKIN (1975–)

classified code

CHEMKIN-II (1986–)

classified code, then freeware

since CHEMKIN 3 (1996–)

commercial code

CHEMKIN-II simulation codes:

SENKIN

spatially homogeneous reactions

PREMIX

laminar premixed flames

SHOCK

shock tube simulations

PSR

perfectly stirred reactor simulations

Options of SENKIN:

adiabatic system, constant p pressure

adiabatic system, constant V volume

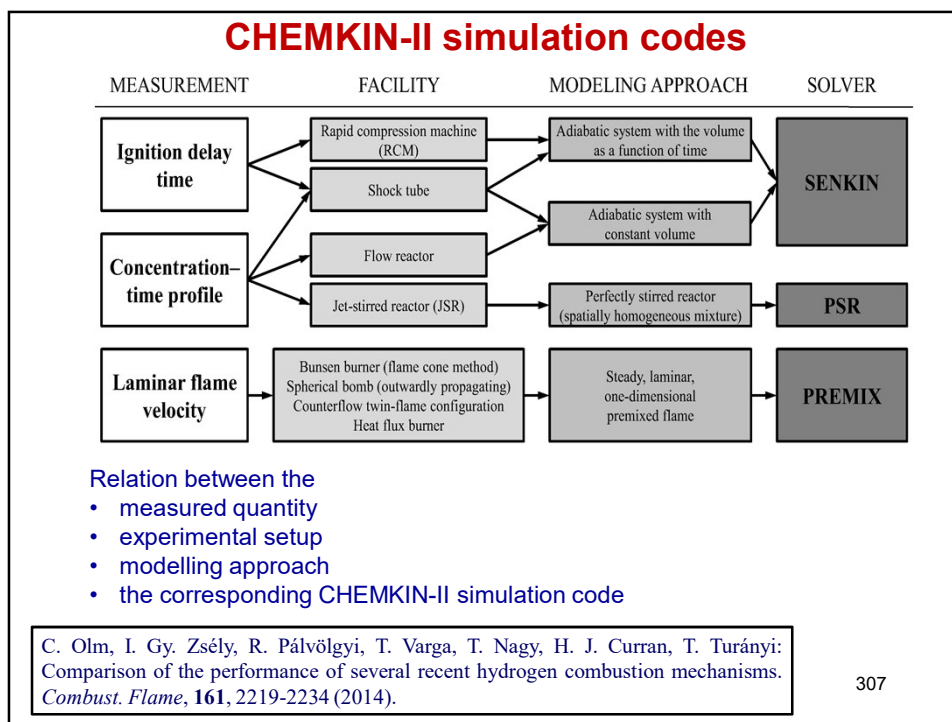
adiabatic system, $V(t)$ function

closed system, constant p , T

closed system, constant V , T

closed system, $p(t)$ and $T(t)$ function

306



KINALC: Kinetic Analysis of Combustion models

- uses CHEMKIN datafiles
- uses CHEMKIN-II subroutines for the calculation of rates
- uses the results of CHEMKIN simulation codes (concentrations and local sensitivity coefficients)

17 different methods for the analysis of reaction mechanisms
Compatible with codes CHEMKIN-II, Chemkin 3.x and 4.x

some keywords of KINALC:

| | |
|-----------------|---|
| UNC_ANAL | local uncertainty analysis |
| ROPAD | rate-of-production analysis – detailed results |
| ATOMFLOW | element fluxes ⇒ FluxViewer movie |
| CONNECT | connections among species (Jacobian analysis) → identification of redundant species |
| PCAF | principal component analysis of matrix F (PCAF) → identification of redundant reactions |
| PCAS | principal component analysis of matrix S (PCAS) |
| QSSAS | error of the application of the QSSA |
| ILDM | dynamical dimension of the system |

308

KINAL, MECHMOD, FluxViewer

KINAL: program for the analysis of any kinetic mechanism

Advantage:

- any mass action kinetic mechanism can be investigated
(may include negative and fractional stoichiometric coefficients)
- includes a simulation code

Disadvantage:

- isothermal simulations only
- fewer analysis methods compared to KINALC

MECHMOD: modification of reaction mechanisms

conversion of reversible reactions => pairs of irreversible reactions

conversion of physical units, automatic removal of species, modification of thermodynamic data

FluxViewer: visualization of reaction pathways (figures and movies)

KINALC, MECHMOD és FluxViewer

are available from the ReSpecTh web site:

<http://respecth.hu>

309

Alternatives to CHEMKIN

Cantera www.cantera.org

Open source code, available from SourceForge.net

chemical equilibrium, homogeneous and heterogeneous kinetics

reactor networks, 1D flames

Kintecus www.kintecus.com

Excel workbook; free for academic use

Simulation of combustion, atmospheric chemical and biological systems

COSILAB www.softpredict.com

commercial combustion simulation and mechanism analysis code

- visualization of reaction pathways
- reduction of kinetic mechanisms
- simulation of reactor networks
- two-dimensional reactors and flames
- spray and dust flames

310

Alternatives to CHEMKIN 2

OpenSmoke (Milano; <http://www.opensmoke.polimi.it/>)

freely available program

numerical modelling of laminar reacting flows

built on the OpenFOAM framework

homogeneous reactions, heterogeneous reactions on catalytic surfaces

FlameMaster (Aachen; <http://www.itv.rwthachen.de/downloads/flamemaster/>)

free for academic use

- homogeneous reactor and perfectly stirred reactor calculations
- freely propagating premixed flames
- steady counter-flow diffusion flames

Chem1D (Eindhoven; <https://www.tue.nl/>)

flame simulations with both detailed and few-step mechanisms

laminar flames:

adiabatic, burner stabilized, ceramic burner stabilized and counterflow flames

special effects in laminar flames:

simulation of stretch, curvature, gas radiation

311

SBML

SBML: Systems Biology Markup Language <http://sbml.org/>

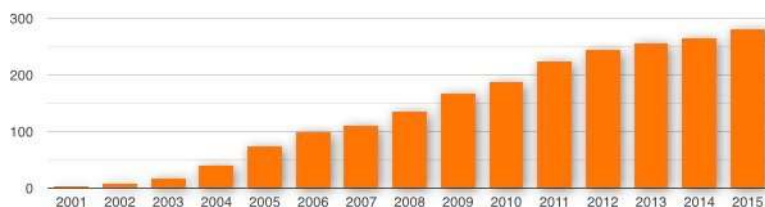
SBML model definition format was created

to promote the exchange of systems biology models

(similar to the role of CHEMKIN format in gas kinetics)

281 SBML-compatible software packages are available (January 2016)

The list of these simulation codes can be looked at <http://sbml.org/>



Increase of the number of SBML-based computer codes
(these include both academic and commercial codes)

312

Copasi

COPASI (COmplex PAthway Simulator)

<http://copasi.org/>

Simulation and **analysis** of biochemical network **models**.

Free, support, but source code is not provided.

Homogeneous kinetic systems in interacting compartments

Import and export of models in the SBML format (levels 1 to 3).

Export of models in many format (XPP, C code, Latex).

- ODE-based and stochastic simulations
- stoichiometric analysis of the reaction networks
- optimization of models; parameter estimation
- local sensitivity analysis.
- time scale separation analysis
- characterization of non-linear dynamics properties (oscillations and chaos)

S. Hoops, S. Sahle, R. Gauges, C. Lee, J. Pahle, N. Simus, M. Singhal, L. Xu, P. Mendes, U. Kummer:
COPASI — a COmplex PAthway Simulator. *Bioinformatics* **22**, 3067-3074 (2006)

Global uncertainty analysis codes

GUI-HDMR <http://www.gui-hdmr.de>

The GUI-HDMR software is based on the RS-HDMR approach, where all component functions are approximated by orthonormal polynomials using random (or quasi-random) samples. Calculation of up to second-order global sensitivity indices based on user supplied sets of input/output data. The component functions are approximated by up to 10th order orthonormal polynomials.

T. Ziehn, A. S. Tomlin: GUI-HDMR - A software tool for global sensitivity analysis of complex models
Environmental Modelling & Software, **24**, 775-785 (2009)

SimLab <https://ec.europa.eu/jrc/en/samo/simlab>

Developed at the EC Joint Research Centre (EC-JRC) in Ispra, Italy.

Versions up to 2.2: GUI based nice education tool

- (1) generation of random or quasi-random parameter sets
- (2) running the models (within SimLab or externally)
- (3) processing of the simulation results (FAST, Morris' and Sobol methods)
visualisation of the outcome of uncertainty/sensitivity analyses.

SimLab versions from 3.0:

subroutine can be called from Fortran, Python, C++, or Matlab

314

Respecth Collection



reaction kinetics



spectroscopy



thermochemistry

<http://respecth.hu>

- database of combustion and rate coefficient experimental data in XML format (in extended PRiMe format) for the hydrogen reactions
- code for reading and writing the XML files
- specification document of the XML data
- collection of Chemkin mechanisms (hydrogen and syngas)
- programs for the analysis of mechanisms including *u-Limits*, UBAC, JPDAP

NEW USERS ARE WELCOME !!!



*Thank you for
your attention!*

Supported by the Higher Education Restructuring Fund allocated to ELTE
by the Hungarian Government

316